



EUROPEAN
COMMISSION

Community research

STAR

(Contract Number: Fission-2010-3.5.1-269672)

DELIVERABLE (D-N°3.4)

Report on the feasibility of improving radioecological models using a process-oriented approach

Author(s): Laura Urso, Philipp Hartmann, Alexander Diener, Martin Steiner,
Jordi Vives i Batlle

Editor: Alexander Diener

Reporting period: [01/02/2014-31/07/2015](#)

Date of issue of this report: [31/07/2015](#)

Start date of project: [01/02/2011](#)

Duration: [54 Months](#)



[[STAR](#)]





EUROPEAN
COMMISSION

Community research



[STAR]



DISTRIBUTION LIST

Name	Number of copies	Comments
André Jouve, STAR EC Project Officer	1	Electronically (pdf file)
Laureline Février, STAR Co-ordinator (WP-1), IRSN	1	Electronically (pdf file)
Contributors Laura Urso, Philipp Hartmann, Alexander Diener, Martin Steiner, BfS Jordi Vives I Batlle, SCK•CEN	1 per contributor	Electronically (pdf file)
STAR Management Team members: WP-1: L. Février , IRSN WP-2: T. Ikäheimonen, STUK WP-3: A. Liland, NRPA WP-4: H. Vandenhove, SCK•CEN WP-5: F. Alonzo, IRSN WP-6: L. Skipperud, NMBU WP-7: B. Howard, NERC	1 per member	Electronically (pdf file)
STAR Steering Committee M. Steiner, BfS A. Real, CIEMAT J.-C. Gariel, IRSN T. Ikäheimonen, STUK H. Vandenhove, SCK•CEN C. Bradshaw, SU A. Liland, NRPA B. Howard, NERC B. Salbu, NMBU N. Fischer, SUNY J. Nishikawa, Tokai University	1 per member	Electronically (pdf file)
STAR Members Wiki site		Electronically (pdf file)
STAR's External Advisory Board	1 per member	Electronically (pdf file)
ALLIANCE members	1 per member	Electronically (pdf file)

Project co-funded by the European Commission under the Seventh Euratom Framework Programme for Nuclear Research & Training Activities (2007-2011)		
Dissemination Level		
PU	Public	PU
RE	Restricted to a group specified by the partners of the [STAR] project	
CO	Confidential, only for partners of the [STAR] project	

List of Acronyms and Abbreviations

ARTM:	Atmospheric Radionuclide Transport Model
C _{org} :	Organic carbon
CDE:	Convection-dispersion equation
CEC:	Cation exchange capacity
CF:	Concentration factor
CR:	Concentration ratio
DOM:	Dissolved organic matter
dw:	Dry weight
ECOSYS-87:	Dynamic model for assessing radiological consequences of nuclear accidents
ERICA Tool:	Software tool for assessing environmental risks
FA:	Fulvic acid
FARMLAND:	Dynamic model for terrestrial food chains
FeOX:	Iron oxides
fw:	Fresh weight
HA:	Humic acid
HOTSPOT:	Atmospheric dispersion models
HTO:	Tritiated water
HYDRUS:	Hydrogeological code for transport modelling
K _d :	Distribution coefficient
MINEQL ⁺ :	Equilibrium speciation model
MINTEQA2:	Equilibrium speciation model
MOIRA:	Software for assessing the effectiveness of countermeasures in complex aquatic systems
NORM:	Naturally Occurring Radioactive Materials
NPP:	Nuclear power plant
OBT:	Organically bound tritium
ODE:	Ordinary differential equation
OM:	Organic matter
PDE:	Partial differential equation
PHREEQC:	Hydrogeochemical software based on mass balance equations
POM ¹⁴ C:	Model of C-14 cycling in the terrestrial biosphere

REFESOL:	Reference soils (for Germany)
RIP:	Radiocaesium interception potential
SDE:	Stochastic differential equation
SLT:	Solute transport model for unsaturated soil
SOLEMI:	German service for providing high-quality irradiance data for the solar energy community
SSA:	Specific surface area
STAR:	Strategy for Allied Radioecology
SWP:	Soil-water-plant hydrological model
T _{agg} :	Aggregated transfer factor
T _{bio} :	Biological half-life
T _{eco} :	Ecological half-life
TF:	Transfer factor
TIC:	Total inorganic carbon
TOCATTA:	Dynamic model for the transfer of ¹⁴ C from the atmosphere to soil-plant systems
VS2DT:	2-D code to simulate water flow and contaminant transport
WHAM:	Geochemical speciation code

Table of Contents

1	Executive Summary	9
2	Introduction	11
3	Radioecological models: definition, purpose and requirements	12
3.1	Comparison of empirical models and process-oriented approach.....	15
3.2	Bibliography	16
4	Mathematical structures in radioecological modelling	17
4.1	Empirical parameters	17
4.1.1	Transfer from freshwater to aquatic biota	18
4.1.2	Transfer from prey-to-predator in freshwater	19
4.1.3	Transfer from soil solution to soil: the distribution coefficient	20
4.1.4	Transfer from atmospheric layer to surface: the deposition velocity.....	20
4.1.5	Aggregated transfer factor T_{agg}	21
4.1.6	Transfer to edible parts of plant: the translocation coefficient.....	22
4.2	Empirical parametric equations	22
4.2.1	Parametric model for K_d of radium	23
4.2.2	Parametric model for calculating radon concentration at the emission site of radon from mining industrial sites.....	23
4.2.3	Ecological half-life	23
4.2.4	Biological half-life	24
4.3	Ordinary differential equations (ODE).....	25
4.3.1	Double compartment model: sorption process.....	25
4.3.2	Double compartment model: intake and release of radionuclide in fish.....	26
4.3.3	Double compartment model: root-uptake of radionuclides.....	26
4.3.4	Triple compartment model: exchange of radionuclides between the medium and a two-component biota compartment	27
4.4	Systems of partial differential equations (PDE)	28
4.5	Stochastic differential equations (SDE)	28
4.6	Bibliography	30
5	Feasibility studies for process-oriented modelling.....	33
6	Estimating K_d values via geochemical speciation modelling.....	34
6.1	Introduction	34

6.2	State of research and theoretical background	35
6.2.1	The geochemical reaction code PHREEQC	36
6.2.2	The Hormann and Fischer approach for modelling K_d	37
6.3	Sorption properties of radium	38
6.3.1	Aqueous speciation of radium	39
6.3.2	Dissolution/precipitation/co-precipitation of radium	39
6.3.3	Sorption/Desorption of radium	39
6.4	Radium K_d values in literature	40
6.5	Extension of Hormann and Fischer model for radium	42
6.5.1	Model parameters	42
6.5.2	Thermodynamic constants for radium	44
6.6	REFESOL soils compared to Vandenhove and Van Hees' soils	45
6.7	Discussion	50
6.8	Bibliography	53
7	Migration of radionuclides in soil: convection-dispersion equation with initial realistic deposition profile	56
7.1	Introduction	56
7.2	Review context of Cs migration in soils	57
7.2.1	Relevant processes	57
7.2.2	Water flow	58
7.2.3	Solute transport: the convection-dispersion equation (CDE)	59
7.3	Geo-hydrological code HYDRUS-1D	60
7.4	Available experimental data	61
7.5	HYDRUS simulation with Norwegian data	63
7.6	Discussion	67
7.7	Bibliography	69
8	A process-oriented model for C-14 uptake of C3 crops near nuclear power plants	72
8.1	Introduction	72
8.2	Material and Methods	73
8.2.1	Model formulation	73
8.2.2	Environmental conditions	76
8.2.3	Parameterisation	77
8.2.4	Atmospheric dispersion model	77
8.2.5	Modelling of C-14 uptake	77

8.3	Results	78
8.4	Parameters influencing the content of C-14 in <i>Triticum aestivum</i>	80
8.5	Discussion.....	81
8.6	Bibliography	83
9	Contamination of wild boar meat.....	84
9.1	Introduction	84
9.2	Basic information about wild boars.....	84
9.2.1	Contamination levels of wild boar	85
9.2.2	Food of wild boar	86
9.3	Stochastic modelling of Cs-137 contamination of wild boar	87
9.3.1	Mathematical framework	87
9.3.2	Model parameters	89
9.3.3	Results	90
9.4	Discussion.....	91
9.5	Bibliography	93
10	Conclusion.....	94

1 Executive Summary

Radioecological models are used to quantitatively describe and predict the behaviour of radionuclides in the environment. They have been developed to perform research regarding the biogeochemical cycling of radionuclides since the beginning of radioecology. Radioecological models are also the basis for human and environmental risk assessments, when activity levels in environmental media are not available and/or cannot be obtained with reasonable effort. Examples are licensing procedures, for which the radiological consequences of future discharges have to be predicted.

Radioecological models are often based on greatly simplifying concepts, use uncertain empirical parameters and therefore provide only rough estimates. Whether the predictive uncertainty is acceptable or not, depends on the research question and/or the assessment purpose. For some fields of applications, e.g. if the dose to humans is close to a dose limit or if the degree of conservatism would lead to unwarranted restrictions, there is a need to improve the quality of radioecological predictions. This report deals with the question whether process orientation in radioecological modelling is a promising strategy to reduce the predictive uncertainty while keeping the models as simple as possible. The idea is to identify key processes that determine the (dynamic) behaviour of radionuclides in the environment, improve the mechanistic understanding and translate this knowledge into a robust process-oriented submodel. The restriction to key processes is expected to keep the overall complexity of the radioecological model and the total number of model parameters reasonably low.

A broad range of mathematical structures is commonly used for radioecological modelling. Empirical models rely mostly on ratio equations or parametrical equations with experimentally derived parameters. These types of models are easy to apply but do not account for dynamic processes, e.g. after an accidental release of radionuclides. In addition, parameter values might be site-specific and often vary over several orders of magnitude. Time-dependent empirical relations, such as ecological and biological half-lives, and compartment models provide the opportunity to model dynamic processes but are still based on empirical parameters. Compartment models subdivide the system to be modelled into homogeneously contaminated 'black boxes' and are described by a set of ordinary differential equations. Continuous transport processes, e.g. advection and dispersion in unsaturated soil, are described by partial differential equations. Some processes, however, exhibit a distinct stochastic nature and stochastic differential equations are a suitable mathematical description. The appropriate complexity of a model strongly depends on the assessment purpose or the research question to be answered.

Four examples demonstrate that process-oriented modelling might help to reduce the uncertainty of empirical parameters and/or remove conceptual deficiencies:

- The first example showed that highly uncertain empirical parameters can successfully be replaced by submodels. The hydrogeochemical speciation model PHREEQC was used to predict the distribution coefficient K_d for radium. Experimentally determined values vary up to seven orders of magnitude. Although several thermodynamic constants for radium were lacking and had to be replaced by the corresponding values for the chemically similar elements barium and strontium, the predictive uncertainty could be reduced to only one or two orders of magnitude.

- The second example investigated the consequences of simplistic assumptions for the migration of radionuclides in soil. During heavy rain showers radionuclide infiltrate with water in soil and lead to an ‘initial’ depth profile. This first phase was modelled neglecting sorption processes. After the deposition event, the long-term migration of radionuclides accounts for sorption processes in a simplified way by using K_d values. This approach realistically describes the key processes infiltration and sorption.
- The third example demonstrates that equilibrium approaches are not necessarily conservative. It deals with the assimilation of C-14 originating from nuclear power plants by C3 plants. Model calculations confirm the correlation of the diurnal variations of turbulent atmospheric mixing and photosynthetic activity. Since elevated activity levels in the lower atmospheric layer coincide with high photosynthetic activity, established equilibrium approaches underestimate the C-14 contamination of plants.
- The last example is a stochastic modelling approach to describe the Cs-137 contamination of wild boars due to the irregular uptake of highly contaminated deer truffles. The stochastic modelling approach successfully predicted the median of the activity levels in wild boars from first principles. The predicted and experimental values for the 5th and 95th percentiles were within one order of magnitude. The differences between measured data and model prediction can partially be explained by a lack of knowledge regarding the mass of the wild boars. This example shows that stochastic modelling allows to predict the variability of radioecological parameters.

2 Introduction

Radioecological models are required to quantitatively describe and predict the behaviour of radionuclides in the environment. They have been developed to perform research regarding the biogeochemical cycling of radionuclides since the beginning of radioecology. Radioecological models are also the basis for human and environmental risk assessments, when activity levels in environmental media are not available and/or cannot be obtained with reasonable effort. Examples are licensing procedures, for which the radiological consequences of future discharges have to be predicted.

Radioecological models are often based on greatly simplifying concepts, use uncertain empirical parameters and therefore provide only rough estimates. Whether the predictive uncertainty is acceptable or not, depends on the research question and/or the assessment purpose. For some fields of applications, e.g. if the dose to humans is close to a dose limit or if the degree of conservatism would lead to unwarranted restrictions, there is a need to improve the quality of radioecological predictions. This report deals with the question whether process orientation in radioecological modelling is a promising strategy to reduce the predictive uncertainty while keeping the models as simple as possible. The idea is to identify key processes that determine the (dynamic) behaviour of radionuclides in the environment, improve the mechanistic understanding and translate this knowledge into a robust process-oriented submodel. The restriction to key processes is expected to keep the overall complexity of the radioecological model and the total number of model parameters reasonably low.

3 Radioecological models: definition, purpose and requirements

A radioecological model is a mathematical description of a process or an ensemble of processes which are responsible for the transfer of radionuclides in the environment. It aims at quantifying a radiological entity (e.g. radionuclide concentration) needed for the determination of key factors as well as for radiation exposure to humans, biota or the abiotic environment. A radioecological model can be a stand-alone object or can contain different sub-models, each of which quantifies a different radiological entity.

Since the beginning of radioecological research (mid 1950s) many different models have been developed to perform fundamental research regarding the biogeochemical cycling of radionuclides and to quantify the radiation exposure to man and more recently also to biota within assessment models. Furthermore, radioecological models provide the basis for the assessment of radiation exposure in many situations. In fact, they are necessary supporting tools for decision making in case of nuclear emergencies, for the selection of remedial actions for existing exposure situations, and for epidemiological studies relating radiation exposure to health effects. They also serve to quantify radionuclide concentrations in case values are too small to be directly measured or measurements are not feasible because of costs or other constraints.

Depending on the purpose, the entered values in radioecological models for use in assessments can be conservative or realistic assumptions. A conservative assessment may be sufficient, if radiation exposure estimates are expected to be well below the maximum permissible values. A realistic estimate is needed in case radiation exposure is above or close to the maximum permissible value. Parallel to the distinction between conservative and realistic approach, models are also distinguished between those in equilibrium and dynamic ones. For example, in many environmental processes, the transfer of radionuclides takes place under equilibrium conditions, e.g. the interaction of natural U or Th-232 containing host rock with groundwater. This means that the activity concentrations in a certain media are on average more or less constant because releases are continuous or quasi-continuous. On the opposite, in case of a radiological emergency, the transfer of radionuclides may be a highly dynamical process and activity concentration can vary drastically with time. However, also in this case, sometimes equilibrium models are applied as the uncertainty in the quantification of the source term dominates over the uncertainty with which other model parameters can be estimated. When developing a model for radioecological purposes, all the aspects mentioned above need to be considered in a well-integrated way.

Radioecology is a discipline on which decision-makers rely to deal with very different situations which range from planned exposure situations (e.g. licensing procedures) to emergency exposure situations (e.g. radiological incidents). Therefore, when radioecological models are intended for assessment purposes, they need to be fit for a large variety of specific purposes. At the same time they need to be as simple as possible but efficient, since often decision-making needs to be as quick as possible. Therefore, before developing an assessment model, it is not only necessary to clearly outline the purpose of the model but also the mathematical complexity required for this scope and what type of analysis on uncertainty is needed for the output results. In fact, if the uncertainty is too large, the model may not be adequate for robust predictions.

The necessary steps for developing a radioecological model and the related criteria are namely:

1. The determination of the model purpose
 - Degree of conservatism
2. The development of a conceptual model
 - Development of interaction matrices
 - Selection of the dominant mechanisms
3. The design of the model algorithm and the model structure (coding)
 - Possibility of obtaining model parameters
 - Mathematical complexity of the model
4. The analysis of output results (verification and validation)
 - Overall uncertainty

The degree of conservatism determines to large extent the type of model to be chosen. In radioecology, there are cases for which a conservative estimate or at least a rough estimate can be sufficient. On the opposite, there are also cases for which a realistic estimate is necessary, i.e. when doses are expected to be close to maximum permissible levels, epidemiological studies, and emergency exposure situations. In addition, the choice between a conservative or realistic approach may also depend on legislative regulations. For example, the European Council Directive 96/29/Euratom is laying down basic safety standards for the protection of the health of workers and the general public against the dangers arising from ionizing radiation, in form of the Euratom Basic Safety Standards from 1996. The radiation exposure requires as much a realistic determination as possible for the population as a whole and for reference groups of the population. Nevertheless, sometimes a role of thumb prediction is the only possibility in case limited information on the event to be analysed is available. However, a role of thumb prediction does not necessarily coincide with a conservative prediction: for example, in the early phase of an accidental release, the source term estimates may vary over more than one order of magnitude. In addition, meteorological conditions may change and the deposition may vary over more than three orders of magnitude, depending on aerosols' size. In this case, the radiation exposure assessment may be rather rough but not necessarily conservative.

Once the purpose of the model has been clearly defined, the conceptual model and the mathematical structure of the model have to be developed. For the link between different media, interaction matrices may be used and the dominant mechanisms need to be distinguished. When determining the model structure, it is necessary to know, what kind of time-dependence needs to be allowed in the model since, as mentioned above, some processes take place under equilibrium conditions, whereas others are highly dynamical. In addition, only model parameters should be included, which are quantifiable, i.e. quantities which can be either measured, derived from measurements or derived from theoretical principles. A further aspect are the mathematical complexity and the software code of the model: if the mechanisms to be modelled take place under equilibrium conditions, and time-dependence does not need to be included, then simpler mathematical structures can be used, like empirical ratios, namely transfer factor and distribution coefficient approaches. On the opposite, if processes take place under dynamic conditions, then dynamic equations are necessary, the time variable needs to be explicitly included and ordinary (ODE) or partial differential equations (PDEs) may be used. Between simple empirical ratios and complex PDEs, however, a range of 'intermediately-

complex' structures can be considered. An exhaustive review of the mathematical structures for radioecological modelling is given in section 4. Model development also benefits from the knowledge of what kind of uncertainty budget can be expected and what kind of analysis on output results can be carried out. In this respect, the determination of overall uncertainty is an important factor of the assessment procedure, as it quantifies the robustness of the predictions. In accordance to Barthel and Thierfeldt (2012), the uncertainties that contribute to the overall uncertainty are:

1. Scenario uncertainty:

This refers to missing knowledge or incomplete information of the exposure scenario as, for example in case of predictive exposure assessments for natural or anthropogenic contaminations, in case of unknown living conditions of potentially exposed persons or incomplete analysis of exposure pathways.

2. Model uncertainty:

The aspect refers to missing knowledge, incomplete information or simplifying assumptions used to model an exposure path. Such a type of uncertainty arises also, when models are extrapolated from their context of validity, i.e. they are validated on a certain dataset but applied to much different data. Also neglecting the correlation among model parameters refer to this type of uncertainty as well as the effects of assuming an idealised statistical distribution for model parameters. For example, often the assumption of a log-normal distribution is implicitly assumed, not knowing, whether it is representative for the real data.

3. Parameter uncertainty:

This point is related to missing knowledge of the real value of the model parameter or its real statistic distribution. Such uncertainty is for example due to uncertainty of measurements. In addition, qualitative aspects can contribute to this type of uncertainty, like the assignment of data measured in the past and applied to actual situations or rough estimates suggested by experts. This type of uncertainty can be reduced by improving measurement techniques or the methodology.

As far as parameter uncertainty is concerned, for simple models, classical statistics can be used to obtain ranges of variation of the output values. Eventually, when large amounts of output values are obtained, statistical distribution probabilities can be matched to the obtained data. This has been often done for large databases, e.g. IAEA (2009, 2010), etc. In case of more complex models, probabilistic and stochastic approaches to analyse uncertainties can be undertaken. In particular, a probabilistic description of model parameters can be introduced, to quantify separately aleatory (statistical) and epistemic (systematic) uncertainties. In addition, sensitivity studies can be carried out and the parameters' dependency among input variables can be investigated.

The community applying radioecological models varies from scientific experts, who show readiness for using sophisticated models and computational programs, to administrative staff, who need simpler and ready-to-use tools. For all of them, the developed model has to be an efficient compromise between the amount of information needed and obtainable (site-specific data collection) as input, the kind of output desired, and the type of effort (computing time, costs) to run it.

3.1 *Comparison of empirical models and process-oriented approach*

Based on the stages and criteria resumed above, a distinction can be made between an empirical and a process-oriented modelling approach. The first one is used, whenever a rule of thumb or a conservative assessment is sufficient or when only limited knowledge of the processes involved is available. Physical, chemical and biological mechanisms are not distinguished and are quantified with macroscopic quantities. Furthermore, comparatively simple mathematical structures are adequate for the model formation. However, model predictions can only be given with a large overall uncertainty. Consequently, a process-oriented model becomes necessary in order to obtain robust model components and maybe even a smaller overall uncertainty. A process-oriented model can be considered as the next step upwards to the empirical modelling approach. The key factors of an environmental process are accounted for in a more detailed way.

Generally, more complex mathematical structures are required for process-oriented models. This is not necessarily the case, as was shown with the carbon specific activity model (Wirth, 1982). Under equilibrium conditions, the specific activity of carbon is constant along the food chain and can be directly applied to humans. Hence, there is no need to model the transfer of carbon through the whole food chain, thus even lowering the mathematic effort required. Indeed, the major challenge and at the same time, the major requirement is to develop a process-oriented model as simple as possible but fit for purpose. To achieve this, the following criteria need to apply (Kirchner and Steiner, 2008):

1. Key processes involved in radionuclide transfer need to be taken into account with a minimum amount of complexity. This means, removing the finer level of detail (secondary processes) that play only a minor quantitatively role in the model output
2. The number of model parameters, for which values have to be specified, needs to be small, eliminating any parameters that are dependent on (derived from) combinations of others
3. Model parameters need to be reliable (moderately uncertain)
4. The model parameters need to be constant in time and devoid of hidden dynamics (dynamic parameters must be treated accordingly avoiding an oversimplification of the problem)

This report focuses on the analysis of some transfer processes via a process-oriented modelling in order to test their practical feasibility. The goal is to improve the quality of the predictions by covering the most important environmental processes and factors, which determine the fate of a radionuclide present in nature.

3.2 Bibliography

Barthel, R. and Thierfeldt, S. (2012): Vergleichende Betrachtung der probabilistischen/stochastischen und deterministischen Modellierung von Expositionen im Hinblick auf die Belastbarkeit des Modellergebnisses und die Anforderungen an die Qualität der Eingangsdaten. Final report of the project 3609S50002 (in German).

IAEA (2009): Quantification of radionuclide transfer in terrestrial and freshwater environments for radiological assessments. IAEA-TECDOC-1616. Vienna, International Atomic Energy Agency.

IAEA (2010): Handbook of parameter values for the prediction of radionuclide transfer in terrestrial and freshwater environments. Technical Reports Series No. 472. Vienna, International Atomic Energy Agency.

Kirchner, G. and Steiner, M. (2008): Uncertainties in radioecological assessment models – Their nature and approaches to reduce them. *Applied Radiation and Isotopes* 66: 1750-1753.

Wirth, E. (1982): The applicability of the C-14 specific activity model. *Health Physics* 43: 919-922.

4 Mathematical structures in radioecological modelling

In this review chapter, different types of mathematical structures used for radioecological modelling are identified, based on the type of assumptions adopted and on the frequency with which they are found in literature:

1. Constant factors, which are the basis for empirical ratio concepts like transfer factors, concentration ratios, aggregated transfer factors
2. Time-dependent empirical relations like for ecological half-lives, biological half-lives
3. Constant empirical parametric equations like parametric expressions for sorption K_d for different radionuclides
4. Systems of ordinary differential equations which are the basis of compartment models
5. Partial differential equations which are related to a detailed description of the mechanisms involved in the behaviour of radionuclides like the advection-diffusion or the transport equations for migration of radionuclides
6. Stochastic differential equations

In general, 1) and 3) are used to describe mechanisms under equilibrium or quasi-equilibrium conditions whereas 2), 4), 5) and 6) are mostly applied under dynamic conditions.

4.1 Empirical parameters

Multiplicands

Multiplicands are empirical ‘ratio concepts’ (ER), which relate the radionuclide content X in one medium (M1) to that (Y) of another one (M2) in the form:

$$ER = \frac{X_{M1}}{Y_{M2}} \quad (\text{Eq. 4.1})$$

Applications of this concept can be found in all ecosystems (e.g. grassland, agricultural, forest, marine, freshwater) and are commonly used as database in risk assessment tools for radiation exposure like the ERICA Tool (Brown et al., 2008), ECOSYS-87 (Müller and Pröhl, 1993), FARMLAND (Brown and Simmonds, 1995), MOIRA (Monte et al., 1997) and in many more. They are obtained empirically by field or laboratory measurements, while an equilibrium situation as precondition is assumed. The empirical ratios implicitly account for all processes involved. The use of multiplicands is the simplest and most reductionist approach, when describing the distribution of radionuclides between media, and is most often found in literature. These ratios are assumed time-independent and consistent with site-specific characteristics. Most often, they express a linear relationship between radionuclide content in media. However, non-linear empirical ratios exist. Main examples are transfer factors, concentration ratios, aggregated transfer factors as well as distribution coefficient K_d and deposition velocity v_d .

Some problems are associated with the use of the empirical ratio concept:

- Often, there is no sure way of knowing that the medium of interest is in equilibrium with the reference medium (especially in cases for which the time-scale of radionuclide transfer is not clearly ascertainable).

- Field measurements may show significant variations (e.g. among different soil types) and laboratory measurements' conditions can differ from field measurements, because e.g. field measurements may be strongly affected by mycorrhizal symbiosis or some marine K_d experiments are carried out with artificial seawater or the use of extractants can change the chemical conditions of the system under study, etc.
- For many radionuclide-organism combinations, there are only few to none measured values for concentration ratios or maybe stable element data on a higher concentration range than the trace levels prevailing for radionuclides are used.
- It can oversimplify the system's description and therefore its values can vary with the time at which measurements are taken.

It is well acknowledged that the applicability of the empirical ratios should be restricted to specific and well documented environmental conditions. Indeed, there are various scientific papers, which critically review the concept of empirical transfer ratios, their range of validity and uncertainty (McGee et al., 1996; Shepperd and Evenden, 1998; Ward and Johnson, 1986).

Nevertheless, it is often claimed that the application of empirical ratios is the only possible way for predicting radionuclide distribution in cases with poor data availability or the limited knowledge about the physicochemical and biological processes. Even if the relevant processes are known and models do exist which explicitly describe them, it is possible that uncertainties of these models are sometimes larger than those associated with empirical ratios. They are used to quantify the following transfer processes for various radionuclides and ecosystems. Typical empirical models are the transfer from:

1. Freshwater to aquatic biota (as concentration ratio CR ($L\ kg^{-1}$))
2. Prey-to-predator in freshwater (as CR ($L\ kg^{-1}$))
3. Diet to animal derived food products (as concentration factors ($d\ kg^{-1}$)) or transfer factors ($d\ L^{-1}$)
4. Soil to water (as distribution coefficient K_d ($L\ kg^{-1}$))
5. Atmospheric layer to soil (as deposition velocity v_d ($m\ s^{-1}$))
6. Soil to fungi, animals and plants (as aggregated transfer factor T_{agg} ($m^2\ kg^{-1}\ dw$))
7. Transfer to edible parts of plant (as translocation coefficient ($m^2\ kg^{-1}$))
8. Freshwater to plant (as CR ($L\ kg^{-1}$))

4.1.1 Transfer from freshwater to aquatic biota

The concentration ratio between freshwater and aquatic biota is defined as:

$$CR = \frac{\text{Activity concentration in biota (whole body; Bq kg}^{-1}\ \text{fresh weight)}}{\text{Activity concentration in filtered water (Bq L}^{-1}\text{)}} \quad (\text{Eq. 4.2})$$

In general, mainly two mechanisms are responsible for radionuclide accumulation by an organism. The first one is the active bioaccumulation in form of incorporation of the radionuclides into the tissue. This is a slow process. Secondly, on external and internal surfaces of organism, the passive adsorption leads to contamination, being a fast process. Both mechanisms will affect the transfer of radionuclides from water to aquatic biota.

The ERICA Tool (Brown et al., 2008) includes i.a. a list of default values for CRs for different aquatic species in the transfer database, providing a value for each element and reference organism. For numerous cases, however, no empirical data are available, resulting in the derivation of values from taxonomic or biogeochemical analogues, a fact that enhances the uncertainty in the values. In addition, not always in literature it is clearly mentioned, whether water for measurements is filtered or not and this generates further uncertainty. A further problem is that transfer from freshwater to aquatic biota is sometimes not linear, e.g. in case of caesium, there is evidence (Tuovinen et al., 2003).

The equilibrium modelling approach is only appropriate for cases, in which the radionuclide activity concentration in fish can be assumed to be in equilibrium with that in water. This can be true several years after radionuclide contamination or for continuous releases of radionuclides on long-time scale.

4.1.2 Transfer from prey-to-predator in freshwater

The radionuclide accumulation by aquatic organisms is estimated from the radionuclide concentration in water, using the radionuclide concentration factor CF (Sazykina, 2003):

$$CF = \frac{\text{Activity concentration in predator (Bq kg}^{-1}\text{)}}{\text{Activity concentration in prey (Bq kg}^{-1}\text{)}} \quad (\text{Eq. 4.3})$$

In general, it is expected that:

1. Radionuclides accumulating due to adsorption have CFs which decrease in aquatic food chains. In fact, larger organisms have lower surface/volume ratio compared to smaller organisms.
2. The transfer of a radionuclide through the aquatic food chain is tracing the transfer of stable analogous element as no distinction can be made between the two.
3. Radionuclides transformed into insoluble forms, like Sr-90 and Ca-45, have CFs generally decreasing from lower trophic levels to fish and aquatic mammals. These, in fact, either are excreted or, for example in case of Sr-90, are located in the hard portions of the fish.
4. Radionuclides, which are accumulated in soft tissues as analogues of major bioelements like Cs-137, K-40, P-32, are easily transferred, and CFs may increase from lower to higher trophic levels.

However, Tuovinen et al. (2003) determined that in the freshwater food chain, prey-to-predator CFs for Cs-137 are constant as function of Cs-137 concentration in water, whereas point 4 suggests the opposite. Plots of prey-to-predator concentration ratios as a function of Cs-137 concentration in prey, look rather scattered and range between factors 2 and 6 (mean values with 95% confidence level). In general, the transfer of radionuclides from prey-to-predator in water seems very difficult to quantify with mechanistic approaches and little literature about this topic is found. In addition, the difference in the biological half-life for each species may play an important role.

4.1.3 Transfer from soil solution to soil: the distribution coefficient

The degree of radionuclide sorption on the solid phase is quantified by using the solid-liquid distribution coefficient, K_d , defined as:

$$K_d = \frac{\text{Activity concentration in solid phase (Bq kg}^{-1}\text{)}}{\text{Activity concentration in liquid phase (Bq L}^{-1}\text{)}} \quad (\text{Eq. 4.4})$$

The water-soil distribution coefficient (K_d) of elements or compounds quantifies as sum parameter the effect of numerous geochemical parameters and sorption processes like adsorption, absorption, desorption, dissolution, precipitation. The number of significant influencing parameters, their variability in the field, and differences in experimental methods result in up to seven orders of magnitude variability in measured metal K_d values reported in the literature (e.g. IAEA, 2010). This variability is even higher for metals (including radionuclides) than for organics and makes it generally difficult to derive generic K_d values.

The partition coefficient is an empirical transfer ratio, when considering the measured distribution of radionuclide from soil to soil solutions. Such distribution can also be parameterised via empirically derived relationships with aqueous and solid phase independent parameters. In the ERICA Tool, distribution coefficients are also used to derive activity concentrations in sediment from water and vice versa. K_d values are usually grouped based on soil types, soil texture and organic matter and, when possible, on co-factors affecting sorption. The IAEA technical report (IAEA, 2010) shows tabulated values for K_d . If e.g. K_d for caesium is taken, based on soil type, one would get a span between $2.7 \cdot 10^2 - 5.3 \cdot 10^2$ from organic (organic matter content $\geq 20\%$) to sandy soils (sand fraction $\geq 65\%$). If one considers the grouping based on co-factors like radiocaesium interception potential (RIP), the values range between $7.4 \cdot 10^1$ for low RIP < 150 , and $7.2 \cdot 10^3$ for high RIP > 2500 , respectively, which spans over three orders of magnitude. Given the large range of variation, it is often recommended to critically consider any value for K_d presented in tabulated form from literature. The underlying publications should be considered and the characteristics of soil and soil solution taken into account. Additionally, it has to be figured out, if the K_d are conditional values, meaning only valid for the present conditions of the experiment, or if they are standardised to an ionic strength of 0 and standard conditions (25°C , 1 bar pressure). This is useful for a direct comparison of the distribution coefficients from different study areas (Merkel et al., 2005).

4.1.4 Transfer from atmospheric layer to surface: the deposition velocity

Another example of empirical transfer parameter is the interaction between atmosphere and soil, water or canopy in absence of rain events, so-called dry deposition. In this case, the deposition flux D ($\text{Bq m}^{-3} \text{ s}^{-1}$) of the radionuclide r from the atmosphere to the medium is quantified by multiplying the deposition velocity v_d (m s^{-1}) with the surface of interest C (Bq m^{-2}):

$$D = v_d \cdot C \quad (\text{Eq. 4.5})$$

The process of dry deposition is highly dynamic and depends on particle size, the characteristics of roughness layer, meteorological conditions and chemical composition of the deposit. For large particles ($> 20 \mu\text{m}$), gravitational settling and aerodynamic drag force interact to determine the deposition velocity (Whicker and Schulz, 1982). For particles with small size ($< 20 \mu\text{m}$) account other mechanisms that determine the deposition velocity, namely surface

impaction, electrostatic attraction, turbulent diffusion, adsorption, and chemical interaction. The last two mechanisms are also dependent on the chemical properties of the radionuclide.

The deposition velocity is an example of empirical transfer parameters with very large uncertainties, for which barely any alternative in literature can be found. Often, tabulated values of the deposition velocity are used to quantify the amount of activity deposited in case of a radiological incident (HOTSPOT, 2013). The deposited activity is directly proportional to the deposition velocity. Therefore, for risk assessment purposes, a large uncertainty in the deposition velocity does directly affect the predicting capability of the model. An alternative to the empirical determination of this quantity is the use of a resistance model, where aerodynamic, surface layer and transfer effects are considered. This formulation, however, is not very practical, as many necessary parameters, like e.g. the friction velocity u^* , are difficult to handle:

$$u^* = \sqrt{\tau \rho^{-1}} \quad (\text{Eq. 4.6})$$

Where τ is the shear stress (Pa) and ρ is the fluid density (kg m^{-3}). In Underwood (2001), a review about deposition velocities based on physicochemical properties of the pollutant, surface type and weather conditions is carried out. Pröhl (2003) mentions that for deposition velocity on grass for particles' sizes between $0.1 \mu\text{m}$ and $10 \mu\text{m}$, the uncertainty factor is estimated to be about 5 – 10.

4.1.5 Aggregated transfer factor T_{agg}

In some situations, the concept of T_{agg} rather than TF or CR is preferred. T_{agg} is defined as:

$$T_{\text{agg}} = \frac{\text{Activity concentration in fungal fruit body or plant or animal (Bq kg}^{-1} \text{ dw or fw)}}{\text{Inventory in soil (Bq m}^{-2})} \quad (\text{Eq. 4.7})$$

The used denominator is the inventory rather than the concentration in soil. This is convenient for processes in the environment, which show a high variability, like seasonality effects, small-scale heterogeneity in soil and climate parameters, specific habits of free ranging animals. For example, for forests and semi-natural ecosystems, T_{agg} is an empirical measurement to normalize radionuclide accumulation, regardless of variations in the vertical radionuclide distribution and availability in the soil profile.

In addition, T_{agg} is applied for quantifying the transfer from soil to plants and animals by aggregating the ecological characteristics of an ecosystem and hence, there is no requirement to estimate parameters such as herbage, intake, etc. For example, $T_{\text{agg,milk}}$ ($\text{m}^2 \text{ L}^{-1}$) for the transfer into cow's milk is defined as:

$$T_{\text{agg,milk}} = \frac{\text{Activity concentration in milk (Bq L}^{-1})}{\text{Inventory in soil (Bq m}^{-2})} \quad (\text{Eq. 4.8})$$

In addition, if activity levels need to be estimated very quickly, for example after an accidental release of radionuclides, the aggregated transfer factors may assess the order of magnitude contamination levels, e.g. in fungi and plants, shortly after a deposition event. In fact, in this initial period, the activity per unit area is likely to be amongst the first calculations available. However, a transfer factor that averages over the total inventory in soil, can exhibit a strong time-dependence and oversimplify the conceptual model of the ecosystem. Some observations, in fact, report on the time-dependence of the migration in soil and movement of radionuclides between the various environmental components. For example $T_{\text{agg,fungi}}$ values peak when the maximum of the vertical radionuclide distribution reaches the rooting zone. Therefore, $T_{\text{agg,fungi}}$

range over about 4 orders of magnitude, mainly because of the non-uniform vertical distribution of radionuclides in soil. Alternatively, transfer factors related to specific soil horizons are much more robust as they directly relate the behaviour of radionuclides to a distinct soil layer with mycelia (Steiner et al., 2002).

An example that shows how the use of aggregated transfer factors can oversimplify the description of the process, is the use of $T_{\text{agg, fungi}}$ for quantifying intake of Cs-137 of the wild boar. Over the first 18 years after the accident in Chernobyl, wild boars have exhibited the highest Cs-137 contamination of any type of game in Bavaria, Germany. During the years 1986 to 1999, the median activity concentration in wild boar from Bavaria decreased for each year, with $T_{\text{eco}} = 10.5 \pm 1.6$ years. Nevertheless, the variability within the year increased to about four orders of magnitude, e.g. in 1998, and the values varied between 80 kBq kg^{-1} fresh meat and 2 Bq kg^{-1} . This variability can be explained by the fact that the wild boar has the habit to consume the fungus deer truffle, *Elaphomyces granulatus* Fr., which substantially accumulates Cs-137. As a consequence, the irregular intake of the truffle, together with the short biological half-life (20 days), have led to an increase of meat contamination. On the opposite, the location of these mycelia in the forest soil have led to an averaged constant contamination of the wild boar meat (Fielitz, 2005). Such a process can only be properly understood with a process-oriented approach.

4.1.6 Transfer to edible parts of plant: the translocation coefficient

The translocation coefficient ($\text{m}^2 \text{ kg}^{-1}$) is quantified as the ratio of the activity concentration in the edible part (Bq kg^{-1}) to the total activity retained by the plant canopy per unit ground area (Bq m^{-2}). Although translocation has little influence on the long-term fate of radioactivity in the environment, it is an important quantity for the estimate of radionuclides in foods. The most important factors influencing translocation are the physiological behaviour of the radionuclides in the plant and the time at which deposition occurs during the growth phase (Pröhl, 2003). In this regard, radionuclides can be differentiated according to their mobility in the plants and to whether they are transported via the xylem or the phloem.

4.2 *Empirical parametric equations*

Another type of empirical relation is obtained by parametric models (EPA, 1999). Parametric equations are polynomial or algebraic expressions that express a set of quantities as explicit functions of a number of independent variables. In this case, the value of the quantity of interest varies as a function of empirically derived relationships. To obtain such equations, one can, for example, vary simultaneously several parameters and determine the systematic change resulting from varying the independent variables. Generic algorithm models can also be used to derive such equations. They can be applied in case of equilibrium or quasi-equilibrium conditions since no time-dependence is included. Alternatively, time-dependent parametric functions can arise in case if, for example, one or more independent variables are time-dependent. Many attempts for different radionuclides exist to obtain K_d in form of a parametric equation with independent variables being the soil properties, e.g. cation exchange capacity (CEC), organic matter content (OM), etc. Another example of parametric equation can be found in atmospheric dispersion modelling to relate the averaged concentration to the distance r from the source location. Compared to empirical ratios, such a modelling approach has the advantage of being

more robust and removes the burden of determining new values for different environmental conditions. On the opposite, such statistical relationships are devoid of causality and sometimes deliver neither certain information about the mechanism involved in the process under analysis nor about identification of the relevant processes.

4.2.1 Parametric model for K_d of radium

To determine the soil and plant factors ruling radium availability in plants, a soil experiment with ryegrass and clover has been carried out (Vandenhove and Van Hees, 2007). A selection of nine soils was made, such that it covered a wide range of parameters hypothesised to be important in determining radium availability (e.g. cation exchange capacity, organic matter, clay content, Ca content, pH). These soils have been spiked with Ra-226 and the solid liquid-partitioning coefficient K_d was determined. K_d was found to be linearly related to cation exchange capacity (CEC) and organic matter content (OM) in the form:

$$K_d = 0.71 \cdot (\text{CEC}) - 0.64 \quad (\text{Eq. 4.9})$$

and

$$K_d = 27 \cdot (\text{OM}) - 27 \quad (\text{Eq. 4.10})$$

4.2.2 Parametric model for calculating radon concentration at the emission site of radon from mining industrial sites

For an average emission rate Q (kBq s^{-1}) of Rn-222 placed on the ground, the averaged Rn-222 concentration (Bq m^{-3}) at distance r from the source location can be calculated with the following empirical equation which relates the averaged Rn-222 concentration (Bq m^{-3}) to the distance r from the source location (BfS, 2010):

$$C_{\text{Rn},s}(r) = 377 \cdot Q \cdot r^{-1.58} \quad (\text{Eq. 4.11})$$

This dependency on r resumes the influence on parameters like wind velocity, meteorological class and wind direction.

4.2.3 Ecological half-life

In the previous section, the ecological half-life has been introduced as an example of the use of empirical functions to quantify the transfer of radionuclides in the environment. The ecological half-life integrates all processes that cause a decrease of activity in a given medium, taking into account the interactions with the external environment. It is mainly related to long-term behaviour of the radionuclides and the processes involved are specific to the medium considered (Pröhl et al., 2006). For example, in terrestrial ecosystems, it can aggregate processes like the reduction of activity in game, losses of radionuclides from the root layer of the soil, fixation to soil particles and uptake by plants, leaching, fixation and erosion.

It corresponds to the one-compartment model with a time-independent rate coefficient $\lambda_{eco} = \ln 2 / T_{eco}$, where T_{eco} is the ecological half-life of the radionuclide considered. Therefore, all the properties of a single-compartment model apply, like the typical exponential decrease. The radionuclide concentration in the specific medium $C(t)$ can be written as:

$$C(t) = A \cdot \exp\left(-\frac{\ln 2}{T_{eco}+T_{phy}} t\right) \quad (\text{Eq. 4.12})$$

where A is the peak concentration present (Bq kg^{-1}), and T_{phy} is the physical half-life of the radionuclide. This model implies that a single process with first-order kinetics dominates. Later, though, other secondary processes may become substantial so that more than one ecological half-life needs to be considered. For example, indication of the existence of a second ecological half-life was obtained from analysis of measurements in German forests after the Chernobyl accident. In this case, the ecological half-life for Cs-137 in roe deer appeared to increase with the length of the observation period. It is suggested that, later on, processes like redissolution determined the availability of Cs-137 more than processes like fixation or migration into the rooting zone, which instead dominated immediately after deposition. A sinusoidal function in the form $[1 - b \cdot \sin(\omega t + \varphi)]$ can be added, when describing possible occurring seasonal effects. Considering both seasonal variation and multiple N ecological half-lives, the concentration $C(t)$ in the medium is quantified as:

$$C(t) = A \cdot \exp\left(-\frac{\ln 2}{T_{phy}} t\right) \cdot [1 - b \cdot \sin(\omega t + \varphi)] \cdot \sum_{i=1}^N \frac{a_i}{A} \cdot \exp\left(-\frac{\ln 2}{T_{eco,i}} t\right) \quad (\text{Eq. 4.13})$$

with $A = \sum_{i=1}^N a_i$

Ecological half-life values can span from days to years, depending on the radionuclide and medium considered. The concept of the ecological half-life is questionable, when it is applied to situations where the distribution of radionuclides is non-uniform and/or mixing and transport-processes are important. For example, in forest ecosystems, a systematic increase of the ecological half-life with increasing soil layer thickness is observed. Here, low migration velocity and slow transport of radiocaesium within the soil layer and the smoothing out of the concentration gradients become more important as the layer thickness increases, whereas the fraction of activity which is transported out becomes smaller.

4.2.4 Biological half-life

Another example of empirical relation often used is the biological half-life T_{bio} , which quantifies the time it takes for an organism to eliminate half of the amount of radionuclide activity retained. It accounts for different processes, which take place within an organism to control radionuclide concentration. Such mechanisms can be rates of bioaccumulation, proportional sequestration and distribution among various tissue types, excretion, etc. The biological half-life depends on both, the chemical characteristics of the radionuclide and on its chemical form. One chemical form of the radionuclide might be rapidly eliminated from the organism, whereas other chemical forms may be eliminated slowly. In general, to measure the biological half-life of a particular chemical form of a radionuclide, this chemical form needs to be studied in animals and humans. Since the biological processes of different animals vary considerably, an accurate determination of the biological half-life requires that each chemical form of the radionuclide has to be studied in each organism of interest. For example, for tritium intakes as tritiated water (HTO), T_{bio} for humans is about 10 days, whereas tritiated foodstuffs contain organically bound forms of tritium (OBT) with longer biological half-lives. These half-lives are variable and may extend to several years (ICRP, 1979). However, metabolism of OBT is not well understood yet.

4.3 Ordinary differential equations (ODE)

Systems of ordinary differential equations are the mathematical representation of choice for many radioecological dynamical models. Many of these models can be classified as compartment models. A compartment of a system is an individual, homogeneous sub-section of a system, e.g. a soil layer. The radionuclide dynamics in a compartment are described by a mass-balance equation. Each addend in the mass-balance represents a flux of matter between compartments or between the system and the environment. For long-term processes (i.e. annual or longer time-scale), linear models have been often applied, though not always. In a linear model, the kinetic rate is considered proportional to the radionuclide content in the medium of reference. The kinetic rate is constant and accounts for chemical, biological and physical mechanisms that cause the transfer of radionuclides from one compartment to the other.

Compartment models can have different degrees of complexity, going from single compartment to multi-compartments in series, in parallel or with feedback processes. They are used to describe many processes like root-uptake of radionuclides, migration of radionuclides in soil, transfer of radionuclide through food chains, etc. Such models do not only provide time-dependent evolution but eventually also equilibrium of activity levels in the compartments. In addition, by using distributions of stable/unstable isotopes, one can apply these models to obtain long-term predictions.

The ODE systems for multi-compartment models describing mass balances typically have a structure, which allows for the application of standard numerical and analytical procedures. Regarding the application of multi-compartment models, it can be said that the main hurdles are of conceptual nature, because the partitioning of an ecosystem into compartments is not always straightforward. In addition, compartments are assumed to be homogeneously contaminated, which is not always the case. In addition, it is often difficult to derive the rate constants robustly via measurements and even to identify their physical meaning.

4.3.1 Double compartment model: sorption process

An example for a dynamical compartment model is the closed double compartment model with interchange, governed by the following differential equations:

$$\frac{dq_1(t)}{dt} = k_2 q_2(t) - k_1 q_1(t) \quad \frac{dq_2(t)}{dt} = k_1 q_1(t) - k_2 q_2(t) \quad (\text{Eq. 4.14})$$

Concentration q_2 increases proportionally to the amount of concentration in q_1 with a rate k_1 . The parameter k_2 is a coefficient of backward transfer proportional to q_1 . Both rates are assumed constant. The analytical solution of the system of differential equations listed above is given by

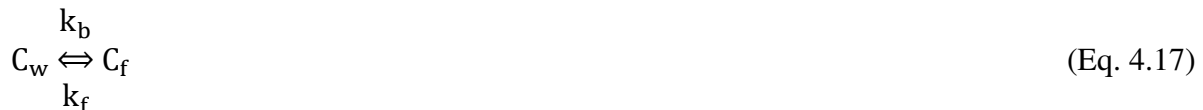
$$q_1(t) = \frac{k_2(q_1(0) + q_2(0))}{k_1 + k_2} [1 - e^{-(k_1 + k_2)t}] + q_1(0)e^{-(k_1 + k_2)t} \quad (\text{Eq. 4.15})$$

$$q_2(t) = \frac{k_1(q_1(0) + q_2(0))}{k_1 + k_2} [1 - e^{-(k_1 + k_2)t}] + q_2(0)e^{-(k_1 + k_2)t} \quad (\text{Eq. 4.16})$$

Such a compartment model can be used to describe the dynamic transfer of radionuclide from one environmental medium to another, involving sorption as a transfer of material between a solution phase (typically water) and a solid phase (e.g. soil). With respect to the example chosen, this is under assumption that a transfer occurs proportionally to the amount of radionuclide in liquid and soil phase respectively.

4.3.2 Double compartment model: intake and release of radionuclide in fish

Such a double compartment model is also used to describe the uptake and release of radionuclides in fish (Smith et al., 2002). In this case, the reaction scheme is:



Whereas C_w (Bq l^{-1}) is the concentration of the radionuclide in water, C_f (Bq l^{-1}) in fish and k_b ($\text{l kg}^{-1} \text{d}^{-1}$) and k_f (d^{-1}) are the rate constants describing transfers of Cs-137 to fish through the food chain and the backward rate constant describing excretion of radioactivity from the fish respectively. The ratio of these rates gives the concentration factor $CF = k_f k_b^{-1}$ of Cs-137 in fish relative to water.

4.3.3 Double compartment model: root-uptake of radionuclides

Root-uptake can also be modelled using a double-compartment model. This is used to describe the Michaelis-Menten kinetics for enzymatic reactions. The manner in which ions seemingly compete for a carrier suggests a situation analogous to an enzyme-substrate complex. In fact, from the analysis of different experiments for ion uptake by roots (Epstein, 1966; Shaw et al., 1992), it was observed that in different plants, concentrations of ions as a function of concentrations in soil generally exhibit a steep increase at low concentrations towards a plateau at high concentrations (hyperbolic function). Hence, it follows a so-called ‘accumulator’ relationship (Shaw and Bell, 1989). This relationship indicates that the uptake from soil to plant is limited at some point, when the amount of ion substrate concentration reaches a certain value, by metabolic processes. In addition, if a variety of similar ions is presented to the cells, the uptake of any ion in the group is slower than when the ion is alone (dilution effect). At some point though, clear metabolic distinction is made between chemical analogous elements (concurrence effect), and the element relevant for physiological reactions is preferred. For example, in experiments for root uptake, where increasing concentrations of Cs^+ , NH_4^+ and K^+ were added, it was observed that, although lower ion concentrations in the substrate were present, no difference between the uptake rates of the three cations was found. At much larger concentrations of the ions in the substrate, clear preference to K^+ was observed. The Michaelis-Menten reaction scheme for uptake of caesium in roots of winter wheat (Shaw and Bell, 1989) is a model for the following reaction:



Cs_{ext} is the amount of ion concentration present in substrate (soil), Cs_{root} is the ion concentration absorbed by the root, R is a metabolically-produced carrier, undergoing a conformational change R’.

CsR is a dissociable carrier-ion complex and the k values are rate constants. The Michaelis-Menten formulation provides the following formula for the uptake of caesium by roots:

$$v = \frac{V_{\max} [Cs_{\text{ext}}]}{K_m + [Cs_{\text{ext}}]} \quad (\text{Eq. 4.19})$$

V_{\max} is a numerical constant representing the maximum velocity obtained when the carrier-ion complex S is formed. K_m is the Michaelis constant defined as the ratio:

$$K_m = \frac{k_{-1} + k_2}{k_1 + k_{-2}} \quad (\text{Eq. 4.20})$$

K_m quantifies the dissociation rate of the CsR complex with respect to the reaction. In addition, in Shaw and Bell (1989), at low concentrations of Cs_{ext} , i.e. between 1 μM and 10 μM , uptake of roots was almost linear. Up to 50 mM (Cs_{ext}), a high affinity for Cs^+ was found and no increase of Cs concentration in the root system was observed. However, at even larger concentrations, i.e. > 1 mM, a negative power function of the form $v S^{-1} = k S^{-n}$ was observed, with k and n being two constants. A similar behaviour was found for ions and compounds like potassium, rubidium, ammonium, sodium, magnesium, strontium, chloride, bromide and sulphate. Especially in semi-natural ecosystems, in addition to the carrier-mediated ion uptake, also effects like co-precipitation of elements, rhizosphere effects, effects due to mycorrhizae are responsible for root uptake and translocations of trace elements (Ehlken and Kirchner, 2002). However, some unsolved problems of this approach are that:

1. The K_m constant needs to be robustly estimated and this is possible only if many measurements of different concentrations at different times during uptake are available. A clear understanding of what mechanisms this constant represents is not available. Shaw et al. (1992) suggest that K_m represents the degree of affinity of the ion. Aksnes and Egge (1991) indicate that V_{\max} reflects the cellular morphology and intracellular process, while K_m reflects the hydrodynamic processes, cellular morphology, mobility and intracellular processes.
2. The reaction scheme for active uptake of caesium is dominant but no information about passive uptake as pure diffusive process can be obtained from such a model.

4.3.4 Triple compartment model: exchange of radionuclides between the medium and a two-component biota compartment

For the transfer to and from biota, a dual biological half-life ($T_{B1/2}$) approach can be applied. This is, in essence, a 3-compartment model (seawater, slow and fast biological compartments), reflecting the fact that in the most general case, organisms depurate much of the radionuclide activity from seawater in their bodies via a short-term fast process, followed by a longer-term slow process with short- and long-term biological half-lives $T_{B1/2}^a$ and $T_{B1/2}^b$, respectively, as well as radioactive decay (Vives i Batlle et al., 2004). The general solution is of the form:

$$q_i(t) = \frac{f_i}{\gamma\delta} + \frac{(q_i\gamma^2 - d_i\gamma + f_i)}{\gamma(\gamma - \delta)} e^{-\gamma t} + \frac{(q_i\delta^2 - d_i\delta + f_i)}{\delta(\delta - \gamma)} e^{-\delta t}, \quad i=1,2,3 \quad (\text{Eq. 4.21})$$

Where q_1 is the activity in seawater (Bq m^{-3}), q_2 and q_3 represent the activity retained by the organism (Bq kg^{-1} , fresh mass) and the remaining coefficients are complex functions of the

inter-compartmental exchange rates. The full details are given elsewhere (Vives i Batlle et al., 2008). For the case of a single component biological have-life, the governing equations of the model reduce to a simple two-compartment model with two rate constants; k_w for uptake and k_o for elimination:

$$\frac{dA_o}{dt} = k_w A_w \frac{V}{M} - (k_o + \lambda)A_o; \frac{dA_w}{dt} = -(k_w + \lambda)A_w + k_o \frac{M}{V} A_o \quad (\text{Eq. 4.22})$$

Where CF is the concentration factor, $k_o = \frac{\ln 2}{T_{B1/2}}$, $k_w = (k_o + \lambda) \frac{M}{V} CF$, λ is the radionuclide decay constant, M is the mass of the organism and V is the volume of the water compartment (Vives i Batlle, 2012).

4.4 Systems of partial differential equations (PDE)

Partial differential equations are differential equations that involve rates of change with respect to several continuous variables, expressed with partial derivatives. Such equations are used for modelling of physico-chemical and biological processes, fluid dynamics and water/solute transport in porous media, to mention a few. PDEs can be linear or nonlinear, homogeneous or inhomogeneous equations. Furthermore, they can be either equilibrium equations, that is involve only space variables and describe unchanging physical systems or dynamical equations, which model time-varying processes. For example, the advection-diffusion equation is applied in radioecology for quantifying the migration of radionuclides in soil or in modelling the atmospheric dispersion. Other examples in radioecology mainly relate to hydrodynamic processes, like the Richards' equation and Saint-Venant equations.

For the vast majority of PDEs, the easiest way to produce general solutions is through numerical schemes such as finite differences and finite elements and therefore the handling can be more difficult than with other mathematical structures. In addition, for modelling dynamical processes, in which time is an independent variable, the solution is to be specified by one or more initial conditions. Also on bounded domains, one must also impose suitable boundary conditions in order to uniquely characterize the solution, and hence the dynamical behaviour of the system. Therefore, determining appropriate and consistent initial-boundary conditions becomes a key point of the modelling problem.

4.5 Stochastic differential equations (SDE)

Stochastic differential equations can be used to describe systems which are characterised by a random perturbation (Walsh, 1986). They describe in detail the physical, chemical and biological processes of a system and account for stochastic variations in the model description. In radioecology, the use of such mathematical structure is often recommended for model improvement, since some dominant mechanisms, such as contaminated food ingestion, have an intrinsic stochastic nature. On the opposite, this is a rather new approach, on which no one has ever focused in radioecology before.

A possible application of SDE in radioecology has been the introduction of a stochastic term in the advection-dispersion equation for describing the (stochastic) spatial variations of the soil properties and systematic changes of these with depth (Kirchner et al., 2009) or the variations

of radon concentration in a room being sometimes exposed to air draught (Barthel and Thierfeldt, 2012). In addition, SDE can be applied for accounting random intake of contaminated food by animals, e.g. wild boar's random intake of contaminated deer truffles.

4.6 Bibliography

- Aksnes, D. L. and Egge, J. K. (1991): A theoretical model for nutrient uptake in phytoplankton. *Marine Ecology Progress Series* 70: 65-72.
- Barthel, R. and Thierfeldt, S. (2012): Vergleichende Betrachtung der probabilistischen/stochastischen und deterministischen Modellierung von Expositionen im Hinblick auf die Belastbarkeit des Modellergebnisses und die Anforderungen an die Qualität der Eingangsdaten. Final report of the project 3609S50002 (in German).
- BfS (2010): Berechnungsgrundlagen zur Ermittlung der Strahlenexposition infolge bergbaubedingter Umweltradioaktivität, BfS-SW-07/10.
- Brown, J. E., Alfonso, B., Avila, R., Beresford, N. A., Copplestone, D., Pröhl, G. and Ulanovsky, A. (2008): The ERICA Tool. *Journal of Environmental Radioactivity* 99: 1371-1383.
- Brown, J. E. and Simmonds, J. R. (1995): FARMLAND: A dynamic model for the transfer of radionuclides through terrestrial food chains. Report NRPB-R273. National Radiological Protection Board, Chilton, Didcot, Oxon, UK.
- Crout, N., Beresford, N., Sanchez, A. and Scott, E. M. (2003): Predicting transfer of radionuclides: soil-plant-animal. Modelling radioactivity in the environment. E. M. Scott (Ed.). Elsevier Science Ltd.
- Ehlken, S. and Kirchner, G. (2002): Environmental processes affecting plant root uptake of radioactive trace elements and variability of transfer factor data: a review. *Journal of Environmental Radioactivity* 58: 97-112.
- EPA (1999): Understanding variation in partition coefficient, K_d , values. United States Environmental Protection Agency: EPA 402-R-99-004A.
- Epstein, E. (1966): Dual pattern of ion absorption by plant cells and by plants, *Nature* 212: 1324.
- Fielitz, U. (2005): Untersuchungen zum Verhalten von Radiocäsium in Wildschweinen und anderen Biomedien des Waldes, Abschlussbericht Forschungsvorhaben StSch 4324 im Auftrag des BMU.
- HOTSPOT (2013): Health Physics Code. National Atmospheric Release Advisory Center Lawrence Livermore National Laboratory.
- IAEA (2010): Handbook of parameter values for the prediction of radionuclide transfer in terrestrial and freshwater environments. Technical Reports Series No. 472. Vienna, International Atomic Energy Agency.
- Vives i Batlle, J., Wilson, R. C., McDonald, P. & Parker, T. G. (2004): Uptake and depuration of ^{131}I by the edible periwinkle *Littorina littorea*: uptake from seawater. *Journal of environmental radioactivity*, 78: 51-67.
- Vives i Batlle, J., Wilson, R. C., Watts, S. J., Jones, S. R., McDonald, P. & Vives-Lynch, S. (2008): Dynamic model for the assessment of radiological exposure to marine biota. *Journal of environmental radioactivity*, 99: 1711-1730.

Vives i Batlle, J. (2012): Radioactivity in the marine environment. In *Encyclopedia of Sustainability Science and Technology*, 8387 -8425. Springer.

ICRP (1979): Limits for intakes of radionuclides by workers. ICRP Publication 30 (Part 1) Ann. ICRP 2 (3-4).

Kirchner, G., Strebl, F., Bossew, P., Ehlken, S. and Gerzabek, M. H. (2009): Vertical migration of radionuclides in undisturbed grassland soils. *Journal of Environmental Radioactivity* 100: 716-720.

McGee, E. J., Johanson, K. J., Keatinge, M. J., Synnott, H. J. and Colgan, P. A. (1996): An evaluation of ratio systems in radioecological studies. *Health Physics* 70(2): 215-221.

Merkel, B. J., Planer-Friedrich, B. & Nordstrom, D. (2005): Groundwater geochemistry. A Practical Guide to Modeling of Natural and Contaminated Aquatic Systems. Springer

Mertz, W. (1986): Trace elements in human and animal nutrition, fifth ed., Vol. 2, Academic Press Inc., London.

Monte, L., Hakanson, L., Brittain, J. (1997): Prototype models for the MOIRA computerised system. 90 p. ENEA, Rome (Italy). Dipartimento Ambiente. ISSN/1120-5555

Müller, H. and Pröhl, G. (1993): ECOSYS-87: A dynamic model for assessing radiological consequences of nuclear accidents. *Health Physics*, 64(3).

Pröhl, G. (2003): Radioactivity in the terrestrial environment. Modelling radioactivity in the environment. Scott, E. M. (Ed.). Elsevier Ltd.

Pröhl, G., Ehlken, S., Fiedler, I., Kirchner, G., Klemm, E. and Zibold, G. (2006): Ecological half-lives of ⁹⁰Sr and ¹³⁷Cs in terrestrial and aquatic ecosystems. *Journal of Environmental Radioactivity* 91: 41-72.

Sazykina, T. G. (2003): Radioactivity in aquatic biota. Modelling Radioactivity in the Environment. E. Marian Scott (Editor). Elsevier Science Ltd.

Shaw, G. and Bell, J. N. B. (1989): The kinetics of caesium absorption by roots of winter wheat and the possible consequences for the derivation of soil-to-plant transfer factors for radiocaesium. *Journal of Environmental Radioactivity* 10: 213-231.

Shaw G., Hewamanna, R., Lillywhite, J., Bell, J. N. B. (1992): Radiocaesium uptake and translocation in wheat with reference to the transfer factor concept and ion competition effects. *Journal of Environmental Radioactivity* 16: 167-180.

Shepperd, S. C. and Evenden, W. G. (1988): The assumption of linearity in soil and plant concentration ratios: An experimental evaluation. *Journal of Environmental Radioactivity* 7: 221-247.

Smith, J. T., Kudelsky, A. V., Ryabov, I. N., Daire, S. E., Boyer, L., Blust, R. J., Fernandez, J. A., Haddingh, R. H. and Voitsekhovitch, O. V. (2002): Uptake and elimination of radiocaesium in fish and the “size effect”. *Journal of Environmental Radioactivity* 62: 145-164.

Steiner, M., Linkov, I. and Yoshida, S. (2002): The role of fungi in the transfer and cycling of radionuclides in forest ecosystems. *Journal of Environmental radioactivity* 58: 217-241.

Tuovinen, T. S., Saengkul, C., Ylipietti, J., Solatie, D. and Juutilainen, J. (2003): Transfer of Cs-137 from water to fish is not linear in two northern lakes. *Hydrobiologia* 700: 131-139.

Underwood, B. Y. (2001): Review of deposition velocity and washout coefficient. In Atmospheric dispersion modelling liaison committee. Annual Report 1998-1999 (Annex A). Chilton: NRPB-R322.

Vandenhove, H. and Van Hees, M., (2007): Predicting radium availability and uptake from soil properties. *Chemosphere* 69: 664-674.

Walsh, J. B. (1986): An introduction to stochastic partial differential equations, In: Lecture notes in mathematics 1180: 265-439, Springer, Berlin.

Ward, G. M. and Johnson, J. E (1986): The validity of the term transfer coefficient. *Health Physics* 50 (3): 411-414.

Whicker, F. W. and Schultz, V. (1982): Radioecology: nuclear energy and the environment Vol. II, CRC Press.

5 Feasibility studies for process-oriented modelling

Radioecological models are often based on greatly simplifying concepts, use uncertain empirical parameters and therefore provide only rough estimates. Whether the predictive uncertainty is acceptable or not, depends on the assessment purpose. For some fields of applications, e.g. if the dose to humans is close to a dose limit or if the degree of conservatism would lead to unwarranted restrictions, there is a need to improve the quality of radioecological predictions. Oversimplified approaches are often based on misconceptions:

- Using static models to describe non-equilibrated dynamic systems
- Describing complex processes by a single empirical parameter
- Neglecting the stochastic nature of a process
- Assuming homogeneity in case of heterogeneous media

In these cases, process-oriented approaches might be a promising way to replace over-simplified radioecological models. Process-oriented approaches should be fit-for-purpose but as simple as possible. A model of optimum complexity requires a minimum number of parameters necessary for meeting the requirements of the research question and/or the assessment purpose. These parameters have to be constant in time. Time dependent parameters are an indicator of hidden processes, which are not adequately described in the model. Highly sensitive parameters should show a low uncertainty. The necessary data must be available or easily obtainable.

In the following chapters, the question whether process orientation in radioecological modelling is a promising strategy to reduce the predictive uncertainty while keeping the models as simple as possible is addressed. The selected examples are motivated by various deficiencies of common radioecological approaches, such as a systematic underestimation of contamination levels or a high uncertainty caused by an aggregating empirical parameter. The idea is to identify key processes that determine the (dynamic) behaviour of radionuclides in the environment, improve the mechanistic understanding and translate this knowledge into a robust process-oriented submodel. The restriction to key processes is expected to keep the overall complexity of the radioecological model and the total number of model parameters reasonably low.

6 Estimating K_d values via geochemical speciation modelling

Empirically derived distribution values K_d of the solid/aqueous ratio of a present contaminant often vary in the range of six to seven orders of magnitude. Modelling the K_d for a specific investigation area on the basis of literature values is difficult due to its sensitivity on several environmental factors. A recently published approach about the determination of the K_d by modelling the most important factors with thermodynamic calculations showed encouraging results with the outcome that it is well possible to simulate the retention of radionuclides by sorption on the local soil matrix. Based on the same model, the calculation of radium sorption was performed in this study. The further difficulty was that essential thermodynamic values as input parameters were lacking. For the missing values, the thermodynamic constants of other earth-alkali elements were taken. This approach showed clearly, to which extent the adoption of such constants is useful or not.

6.1 Introduction

Partition coefficients (K_d) are used to quantify the distribution of the dissolved species between solid and liquid phase in soils and to estimate its migration behaviour. It combines the processes of sorption, colloidal formation, mineral precipitation and -dissolution next to solid solution formation and assumes instantaneous equilibrium and reversibility. The distribution coefficient can be applied to model the retardation of a species during groundwater transport or it is used more specifically to describe a single process of retardation, like in Henry or Freundlich-sorption isotherms. In these empirical models, the apparent concentration of a dissolved element is multiplied with the site-specific K_d -value to determine its amount being sorbed on the solid matter (in mg kg^{-1}).

In case of radionuclides, the adsorption, meaning the accumulation of atoms or molecules on the surface of a solid matter, is the dominating part in the retardation of a species. It occurs due to the mostly reversible physical bonding forces (Van-der-Waals, physisorption) or hardly reversible chemical bonding (Coulomb forces, hydrogen bridge bond or chemisorption). The adsorption is enabled by free valences of specific surface sites (isomorphic substitution) and/or the strongly pH-dependent protonation of functional groups like $-\text{OH}$, $-\text{SH}$, $-\text{COOH}$ (Merkel and Planer-Friedrich, 2008; Sigg and Stumm, 2011).

The problem with empirical models (e.g. regression equations basing on distribution coefficients) is that the determined K_d values are often site-specific and cannot be adopted for other investigation areas without a careful comparison of the composition of solid matter and solution chemistry (Vandenhove et al., 2009). Neither the complex processes on the surfaces are projected, nor the boundary conditions of pH, Eh, ionic strength, nor competition for bonding places. To account for such mechanisms in a quantifiable way, it is necessary to use a mechanistic approach to describe the surface complexation, which can be implemented in geochemical speciation codes (e.g. PHREEQC (Parkhurst and Appelo, 1999), MINTEQA2 (Allison et al., 1990), MINEQL⁺ (Schecher and McAvoy, 1992), WHAM (Lofts and Tipping, 2000; Tipping et al., 1998). These codes need input information such as pH, redox potential, the aqueous temperature in soil, concentration of dissolved elements and mineral composition of the solid matter, next to thermodynamic data (Gibb's energy, Helmholtz energy and entropy, equilibrium constants, dissociation constants, type and number of binding sites) for the calculation at equilibrium conditions for each reaction and element considered. Necessary soil

information for model description, like soil texture, mineral composition, organic matter content, pH, temperature, cation exchange capacity (CEC), etc., is usually available from literature.

Previous studies showed, if the distribution coefficient of long-lasting radionuclides can be reasonably modelled for reference biospheres (Hormann and Fischer, 2012, 2013). After the successful validation of the model by comparison of the calculated distribution coefficient with the experimentally determined K_d -value, the K_d -values of Cs-135, Ni-63, U-238 and Se-79 were calculated with PHREEQC for six different reference soils. The results are encouraging and look reasonable. Next to the obtained partition coefficients does this method allow the determination of the radionuclide distribution on the solid matter (Fe- and Al-hydroxides, clay, organic matter), the speciation of the residual radionuclide in solution, the application of scenarios (e.g. effect of a strong raining event or a long-lasting dry phase) and sensitivity tests by varying different parameters (e.g. rising clay content, soil acidification, etc.). All these calculations can only be performed based on reliable and robust thermodynamic data. What can one do if these data are partially lacking or not fully consistent?

One of the naturally occurring radionuclides is radium. Since it is located in rocks (e.g. alpha emitter Ra-226 as decay product in U-ores) and soils, Ra is of environmental concern (Loveland et al., 2005). Radium is known as highly reactive element, which always exhibits the oxidation state +II. Furthermore, Ra is of interest for NORM industries (e.g. Gäfvert et al., 2006) and regarding the long-term safety assessments for nuclear waste disposals.

The main goal of this study is to calculate the K_d of radium with the process-oriented model by Hormann and Fischer (2012, 2013), though some of the necessary thermodynamic data are not available. Therefore, the approach is to use published values of other elements originating from the same main group of the periodic system of elements, being the alkaline earth metals. Thus, the empirically based model is replaced by mathematical equations that describe the key physical and chemical processes that govern radium transfer from soil solution to solid matter. In summary, the steps to calculate the Ra-distribution coefficients with PHREEQC are:

- Outlining the sorption properties of radium
- Presenting the range of variation of K_d values for radium originating from literature
- Extending the Hormann and Fischer model regarding radium and implement the necessary thermodynamic data in PHREEQC
- Calculating K_d for radium for two REFESOL soils and a fictitious soil solution. For one of the soils, a sensitivity analysis is performed. Experiments carried out by Vandenhove and Van Hees (2007) are also considered and their obtained K_d values are compared to simulated ones.
- Results are discussed and conclusions are drawn regarding the link between input parameters of PHREEQC and soil parameters obtained from typical available experimental information

6.2 *State of research and theoretical background*

In radioecology and radiation protection, the assessment of environmental impact and risks associated with radioactive contamination is still most often derived from total concentrations of radionuclides, e.g. in form of the distribution coefficient K_d or the soil-to-plant transfer factor TF. These parameters are in great part the result of different sorption mechanisms in soil,

frequently leading to a wide range of values for a specific radionuclide, since these values are depending on the hydrochemical and the soil conditions. However, the main factors affecting the value of K_d are the contaminant concentration, competing ion concentration, variable/fixed surface charge on the absorbent and solution species distribution. With respect to sorption, processes such as complexation, ion exchange and precipitation/dissolution reactions as well as the formation of colloids or bacterial activities are key factors (EPA, 1999; Mahoney, 1998; Salbu, 2009). Precipitation and dissolution are highly dependent on mineralogical composition of the soil and the hydrochemical composition of the pore water. If the solution is undersaturated with respect to dissolved elements, dissolution occurs. If the solution is oversaturated, precipitation is likely though the rate of formation is depending on the kinetics. Furthermore, co-precipitation or even the formation of solid solutions, meaning the incorporation of an atom as crystal defect or as substitution of a ligand, does often happen after sorption. This process is coupled to further crystal growth and sometimes accompanied with recrystallization. Though all the processes of sorption and co-precipitation are efficient retention mechanisms and of course depending on the geological situation, sorption/desorption will likely be the key process controlling radionuclide retardation in areas (especially in case of clay stone but less important in halite formations), which contain a nuclear waste repository.

6.2.1 The geochemical reaction code PHREEQC

The software PHREEQC is a useful tool for modelling hydrochemical reactions for equilibrium conditions, given that the thermodynamic constants for specific reactions and reactants are available. It allows calculations of e.g. aqueous speciation and degree of saturation of aqueous solutions, the simulation of mass transfer due to mineral precipitation/dissolution or sorption as a function of reaction progress. Furthermore, it is possible to include models for surface complexation on clays, on aluminium-ferric hydroxides and humic substances, which are relevant for sorption of many radionuclides. For all these types of calculations, mathematical formulae based on the mass action law are performed (Parkhurst and Appelo, 1999).

PHREEQC solves numerically a set of balance equations for chemical reactions, specified by the user. In principle, the calculations are based on two steps, i.e. the calculation of species composition next to their thermodynamic activities of the initial soil solution, followed by the subsequent equilibration of the initial soil solution with the exchange assemblage, mineral phase, etc. The code has different databases containing thermodynamic constants but no reaction kinetics are included. These can only manually be integrated into the model. It is in general possible to add manually further thermodynamic constants into PHREEQC. With respect to the intended study, important commands used in PHREEQC are SOLUTION, EQUILIBRIUM PHASES, EXCHANGE and SURFACE. Below the command SOLUTION, the aqueous water composition is listed next to initial values for pH, pe and water temperature in °C. EQUILIBRIUM PHASES is the command to equilibrate the defined solution with the host rock. The result can be modifications in the modelled solution due to mineral precipitation or dissolution reactions. For both, EXCHANGE and SURFACE, the number of exchange sites and complexation sites need to be provided in number of moles per solid mass per liter water (referred to as kgw). This is obtained by multiplying the number of surface sites (moles kg⁻¹ dry mass) by the factor ρ/θ (kg L⁻¹), where ρ is the soil bulk density (kg dm⁻³) and θ is the soil porosity (Parkhurst and Appelo, 1999).

6.2.2 The Hormann and Fischer approach for modelling K_d

The distribution of various radionuclides (Cs-135, Ni-63, U-238 and Se-79) is quantified by Hormann and Fischer (2012, 2013) between the solid and liquid phase for two different soil types and an average soil solution. Their approach is to implement different state-of-the-art models into PHREEQC, dealing with sorption processes on various soil components namely clay silicates, the oxalate extractable amorphous iron-, and aluminium hydroxide and organic matter. Then, they calculate the amount of radionuclides being sorbed to each of these components. The investigated soils are chosen from REFESOL database (Kördel et al., 2009), whereas the fictitious soil solution is taken from Scheffer and Schachtschabel (2010). Hormann and Fischer (2012, 2013) have used the NAGRA thermodynamic database (Hummel et al., 2002), which turns out to be the most reliable one for the radionuclides they have considered. Some reactions are not available in the database, but they are included in the input file directly. The sorption models consider various soil components:

- The model of Bradbury and Baeyens is about the interaction between cations and clay materials (Bradbury and Baeyens, 2000; 2009a, b). The clay fraction with particle size $< 2 \mu\text{m}$ has the largest active surface area and is considered to be the dominant component.
- The Tipping model VI deals with the interaction of the dissolved species with humic and fulvic substances
- The model of Dzombak and Morel (1990) takes into account the interaction with oxalate extractable iron and aluminium.

The model that describes the surface complexation of metal ions on hydrous ferric oxide (namely ferrihydrite) is provided by Dzombak and Morel (1990). Ferrihydrite binds the metal ions and protons on strong and weak sites. The model considers complexation reactions for two sites, a strong site (Hfo_s) and a weak site (Hfo_w). The strong sites are estimated to be in the amount of $0.005 \text{ mol mol}^{-1} \text{ Fe}$, whereas the weak sites are $0.2 \text{ mol mol}^{-1} \text{ Fe}$. The surface area of ferrihydrite is estimated to be $600 \text{ m}^2 \text{ g}^{-1}$ and the electrostatic contribution to surface complexation is considered by including the two-layer model in form of the Gouy-Chapman equation (Appelo and Postma, 2005).

Sorption of cations on organic matter is considered via the Tipping Model VI, which is a discrete site electrostatic model. It takes into account both, specific and non-localised (diffuse-layer) types of binding. The model considers humic and fulvic acids to be homogeneous materials, with molecular dimensions corresponding to the average mass of real materials. Model VI assumes that two classes of sites are present. Type A sites correspond approximately to the COOH content of the humic (or fulvic) material, while type B sites correspond to weaker acid moieties, e.g. phenolic-OH. The basic underlying principle is that dissociation of protons from humic matter enables the replacement by metal ions. Model VI uses a structured formulation of discrete binding sites for protons to allow the creation of regular arrays of monodentate, bidentate and tridentate binding sites for metals. The electrostatic interaction is considered with the inclusion of the Donnan model for counterion accumulation (Tipping, 2002).

One of the major premises in Hormann and Fischer (2013) is that sorption is dominated by the illite mineral component as main representative material for clay in arable soils in Europe. In addition, surface complexation of metals on clay materials is described in detail for illite and monovalent cations K^+ , Cs^+ , Rb^+ by Bradbury and Baeyens (2000, 2009a). The authors consider sorption in terms of the uptake on sets of different sorption sites. These can be planar sites (I_{pa}

with concentration being 0.16 eq kg⁻¹ illite), frayed edge sites FES (I_{fes} : 0.5 eq kg⁻¹ illite), exchange sites type II (I_{pb} : 0.04 eq kg⁻¹ illite), strong and weak sorption site types (I_s : 0.002 eq kg⁻¹ illite, I_{wa} , I_{wb} : 0.04 eq kg⁻¹ illite). In fact, in case of illite, an experimental study coupled to adsorption model showed that binding coefficients for formation of neutral complexes on illite surfaces almost follow the typical dependency of CEC on valence and atomic size of the dissolved species (Polubesova and Nir, 1999). To summarize, the most important features of Hormann and Fischer approach are the following:

- Illite is assumed the most important clay fraction in soils of our climate and hence, all the ion exchange and complexation reactions are those taking place over illite. This is possibly an oversimplification, because the clay composition in soils is highly variable and depending on the host rock, climate and degree of weathering.
- If the required parameters for the models considered are not available, some ‘standard’ values are considered. This is the case for the concentrations of present dissolved organic matter, the partial CO₂ pressure in soil, the amount of organic carbon in soil, and the composition of soil solution.
- The experimental data available do not include analysis of the present soil mineral phases, which could have further effect on the soil-pore water interactions.
- Neither uncertainty in thermodynamic constants is considered nor their temperature dependence.
- A pre-equilibration scheme of the mineral phases with contaminated soil solution is carried out before exchange and surface calculations. This is necessary, because the soil solution is fictively assumed.

6.3 Sorption properties of radium

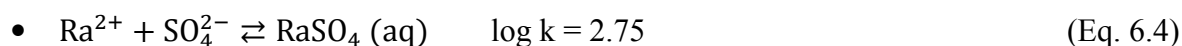
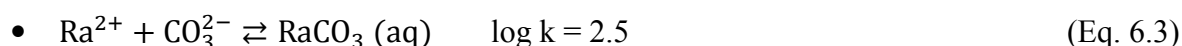
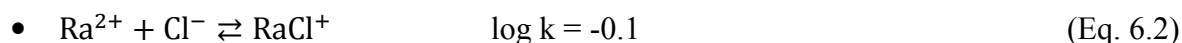
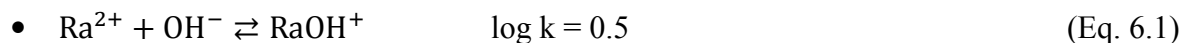
Radium is an alkaline earth element and can be in a dissociated or colloidal aqueous state or being adsorbed. Since there is no change in oxidation level of +II, redox reactions are not relevant for radium sorption and do not need to be considered (Shoesmith, 1984). If present in soils, radium adsorption behaviour is highly pH-dependent, because Ra adsorbs well to clays, metal hydroxides and humic substances especially at near neutral to alkaline pH conditions (Bordelet et al., 2013; Sajih et al., 2014). It also seems that sorption of radium on organic matter is about 10 times stronger than on clay (Simon and Ibrahim, 1990). In this regard, the clay composition should have been clarified, since the CEC depends highly on the type of clay mineral (Scheffer and Schachtschabel, 2010). Furthermore, the sorption of Ra depends strongly on the concentration of other competing ions (Nathwani and Philips, 1979a, 1979b). In case of dissolved sulphate and/or carbonate presence, precipitation of radium takes place as RaSO₄ or RaCO₃. If dissolved barium is also part of the solution, precipitation of a solid solution in form of (Ba, Ra)SO₄ is likely (Brandt et al., 2015).

In general, the concentration of radium in soil depends mainly on the abundance of parent radioactivity in local rocks. However, in case of areas where mining industry is exploited, much higher levels of Ra can be found in soils, most probably due to the so-called alpha recoil effect. This process describes the mobilization of a radioactive daughter atom to the opposite direction of the emitted He-particle during alpha decay (Sun and Semkow, 1997). Co-precipitation is often used in NORM industry, to remove high amounts of Ra from mine waters (Chalupnik and Wysocka, 2008). In addition, fine-textured soils generally have a higher CEC than medium and coarse-textured soils, resulting in a higher sorption capacity of radium. Evidence for this

circumstance is presented in Ebbers (2011), Nathwani and Philipps (1979a, 1979b), Vandenhove and Van Hees (2007).

6.3.1 Aqueous speciation of radium

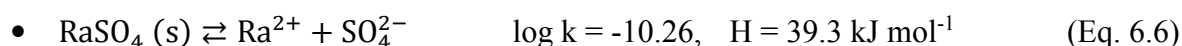
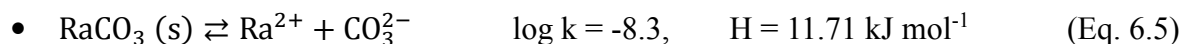
In the pH range of 3 to 10, the non-complexed ion Ra^{2+} is the dominant aqueous species for dissolved radium in natural waters (Vandenhove and Van Hees, 2007). Dissolved Ra shows little tendency to form aqueous complexes, although the following reactions are also possible:



The noted thermodynamic constants $\log k$ for these equilibrium reactions are valid for equilibrium and standard conditions, 25° C and 1 bar atmospheric pressure (Langmuir and Riese, 1985). The values of the thermodynamic constants indicate, when positive that the reaction favours the products, when negative that the reaction favours the reactants or educts.

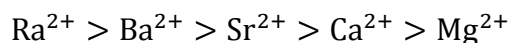
6.3.2 Dissolution/precipitation/co-precipitation of radium

When sulphate is present, precipitation and re-dissolution of Ca, Sr, Ba could control the concentrations of dissolved radium in the soil environment. Precipitation of radium is possible as solid-solutions $(\text{Ba}, \text{Ra})\text{SO}_4$ and $(\text{metal}, \text{Ra})\text{CO}_3$ in water, where the concentrations of dissolved sulphate and/or carbonate are sufficiently high. Nevertheless, in literature, there were no relevant thermodynamic values available for these reactions. The precipitation/dissolution reactions for radium, which are considered in Langmuir and Riese (1985) are these:



6.3.3 Sorption/Desorption of radium

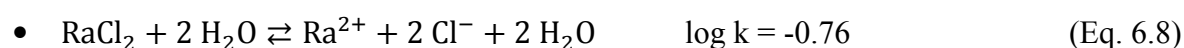
Next to the charge of a dissolved ion, the relative affinity for ion exchange on clay minerals is as well coupled to the atomic size. Thus, in accordance to Sposito (1989) and Shoosmith (1984), the affinity of the alkaline earth elements is:



Hence, the adsorption of radium is expected to be greater than that of all other alkaline earth elements. Furthermore, radium does compete with other cations for sorption sites in soil pore water, especially the typical main and minor elements like Na, K, Ca, Mg, Fe, Al, Mn. However, specifically for radium and illite, no exchange constants are found in literature. Only one comprehensive study of radium sorption on clay in form of kaolinite has been performed. It is two-layered clay, which have almost no permanent negative surface charge. As consequence, the CEC (30 – 150 meq kg^{-1}) of kaolinite is low due to its structure and small specific surface

area (SSA: 10 – 150 m² g⁻¹), whereas illite is a three-layered one with comparably higher sorption capabilities (CEC: 200 – 400 meq kg⁻¹, SSA: 50 – 200 m² g⁻¹). In general, the CEC of illite is only ordinary compared to other clays like vermiculite or smectite (800 – 1500 meq kg⁻¹, because the interlayers cannot be flared (Meunier and Velde, 2013; Scheffer and Schachtschabel, 2010). Therefore, when considering Bradbury and Baeyens model for Ra, only the exchange reaction at the binding site I_{pa} is considered; and for surface complexation, only reaction at I_{wb} is taken into account. In both cases, the log k constants are equal for all earth-alkali metals and their validity is extended to radium.

Other reactions considered and included in the database for radium are:



6.4 Radium K_d values in literature

For many different radionuclides as well as for radium, it is valid that the range of variation for K_d is extremely high. Thibault et al. (1990), for example, compile data, which spans over several orders of magnitude (table 6.1).

Table 6.1: K_d values for several types of soil (Thibault et al., 1990)

K _d Values (L kg ⁻¹)			
Soil type	Geometric mean	No. of observations	Range (L kg ⁻¹)
Sand	500	3	57 – 21,000
Silt/Loam	36,000	3	1262 – 530,000
Clay	9100	8	696 – 56,000
Organic	2400	1	N.A.

Looney et al. (1987) present data for environmental assessment of waste sites at US department of Energy (DOE), originating from Savannah River Plant in South Carolina. They recommend a K_d of 100 L kg⁻¹, and publish a range from 10 to 1000,000 L kg⁻¹.

Table 6.2: K_d values of IAEA (2010)

K_d values ($L\ Kg^{-1}$)			
Soil type	Arithmetic mean	No. of observations	Range ($L\ kg^{-1}$)
All soils	2500	51	12 – 950,000
Sand	1900	39	12 – 120,000
Loam + clay	38,000	6	700 – 950,000
Organic	1300	2	200 – 2400

Vandenhove and Van Hees (2007) list measured K_d values over a range from 38 $L\ kg^{-1}$ to 446 $L\ kg^{-1}$. Meier et al. (1994) consider site-specific waters and crushed sedimentary rocks from strata that overlay the Gorleben salt dome in Germany. For these samples, they obtain at pH values ranging between 4 and 9, K_d values spanning between 7 – 40 $L\ kg^{-1}$. Natwhani and Philips (1979b) have measured the sorption of Ra-226 on different types of soils and have found that sorption of radium in all soils decreases with increasing concentrations of dissolved calcium. These authors obtain some of the highest K_d values in literature, ranging between 7100 $L\ kg^{-1}$ and 950,000 $L\ kg^{-1}$. Serne (1974) measured K_d values of radium on sandy, arid soil samples, originating from Utah, by using a simulated river water solution. The pH of water/soil ranged between 7.6 and 8. The soil consisted of quartz and feldspar with 2 – 5 percent calcite and minor amounts of muscovite and smectite. Belonging K_d values ranged between 214 and 467 $L\ kg^{-1}$.

The data presented in the tables 6.1 and 6.2 has been collected among various authors and each of the observation highly depends on geochemical conditions and soil compositions. The geometric means do not represent any particular environmental system or geochemical condition. Whenever very large K_d ($\sim 10^4 - 10^5$) values are listed, measurements may have included precipitated components (EPA, 2004). These values are also included in IAEA (2010; table 6.2), which is mainly used for exposure assessments. The texture/OM criterion for grouping soils, which are noted in table 6.2, is the following:

- Sand, if sand fraction > 65%, clay fraction < 18%
- Clay, if clay fraction > 35%
- Loam for all other mineral soils
- Organic, if the organic matter content was > 20%

However, in Sheppard et al. (2006), the authors revised the K_d mean values from table 6.1 to 40, 30, 30 and 200 $L\ kg^{-1}$ for sand, loam, clay and organic, respectively. In this work, it was further recommended to use an average value of 47 $L\ kg^{-1}$ (geometric mean value with geometric standard deviation of 4.9), irrespective of soil type. In figure 6.1, the probability distribution considered in Sheppard et al. (2006) is shown.

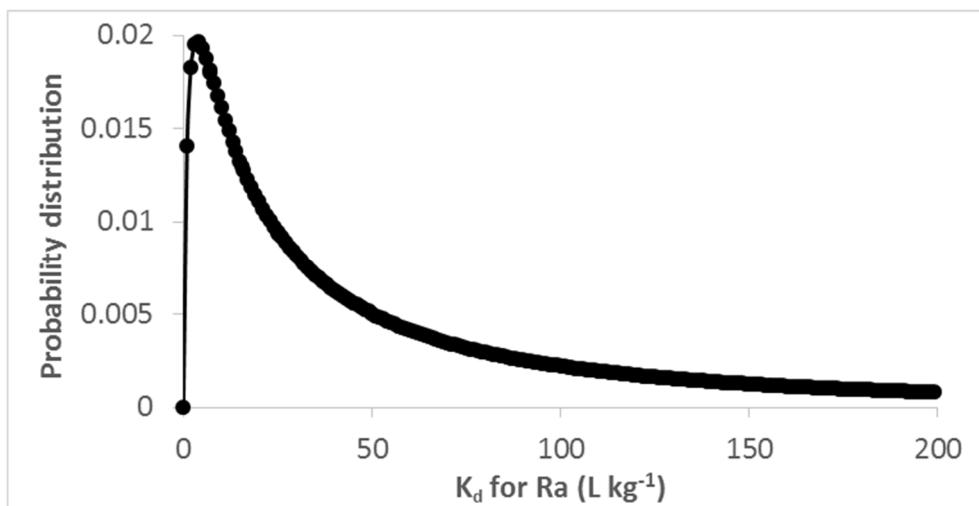


Figure 6.1: Log-normal probability distribution. The function is related to the range of K_d values recommended for Ra in Sheppard et al. (2006)

An experimental determination of partition coefficients under field conditions can be achieved by in-situ batch methods (e.g. Jackson and Inch, 1989). Here, a core sample containing both, the solid and aqueous phase, is removed directly from an aquifer or soil layer. The aqueous phase is separated from the solid phase by centrifugation or filtration and then analysed regarding the solute concentration. The solid is analysed for the radionuclide concentration, associated with a characterization of the solid phase. This type of investigation has been seldom applied. The data listed above, however, is partly obtained from field measurements (e.g. Jackson and Inch, 1989), partly from laboratory batch experiments (e.g. Vandenhove and Van Hees, 2007). The difference in the methodology for determining sorption K_d should also be accounted for, when considering the large range of variation in the K_d values.

6.5 Extension of Hormann and Fischer model for radium

The Hormann and Fischer approach, outlined in section 6.2.2, is applied also in case of sorption of radium in soil. The NAGRA database is considered and the chemical reactions and thermodynamic constants applicable for radium are included in the PHREEQC input file, if the value is not already available in the database. The data on which simulations are based is taken from Hormann and Fischer (2013) and Vandenhove and Van Hees (2007).

6.5.1 Model parameters

With the command SOLUTION, the input parameters for soil solution, cations and anions concentrations are written in the unit desired, e.g. in mmol l^{-1} or mg l^{-1} . Water temperature is set to 15°C . It is assumed that the carbon content present in soil solution is in equilibrium with the partial CO_2 pressure of soil. This value is written in log scale and entered as $\text{pCO}_2 = -3.5$. This value is similar to what Hormann and Fischer (2013) propose for the data in Vandenhove and Van Hees (2007). When modelling the K_d of radium for REFESOL soils, the pCO_2 is set to -2.

With EQUILIBRIUM_PHASES, it is possible to calculate the new solution composition after the reaction of a host rock matrix and an initial solution content for equilibrium conditions. Furthermore, it is possible to determine the amount of precipitated new phases or dissolved minerals. The mineral phases gibbsite and hydrous ferric oxide are included in order to calculate by equilibration the aluminium and iron concentrations in solution, which are not available for both sets of data.

In EXCHANGE, the amount of I_{pa} sites (eq kgw⁻¹) is entered. The value can be calculated following Hormann and Fischer (2013):

$$I_{pa} = c_i \cdot \frac{\rho}{\theta} \cdot (CEC - C_{org} - 0.001 \cdot (510 \cdot pH - 590)) \quad (\text{Eq. 6.10})$$

The equation above requires the measured CEC (meq kg⁻¹) and amount of C_{org} (g kg⁻¹) in soil. For soil B, the CEC amounts to 438 meq kg⁻¹, whereas C_{org} is assumed to be half of the organic matter content (soil B contains 12.3 % OM). In this equation, pH of pore water is necessary. However, it is not mentioned in the study of Vandenhove and Van Hees (2007) and therefore, pH in soil is assumed the pH under circumneutral conditions. I_{pa} sites are 80 % of the sites available for exchange on clay silicates. Hence, their abundance in equation is set to $c_i = 0.8$. Exchange reactions involving the other types of binding sites I_{fes} and I_s are not relevant for divalent cations like radium and therefore are not considered.

In SURFACE, the amount of weak complexation sites of illite I_{wb} (eq kgw⁻¹) need to be included together with the complexation sites on hydrous ferric oxides Hf_{os} and Hf_{ow} . In addition, strong complexing sites I_s and weak complexing sites I_{wa} are not relevant for radium and other earth-alkali metals. Hence, they are not considered in this study. The I_{wb} are calculated as in Hormann and Fischer (2013):

$$I_{wb} = \left(\frac{\rho}{\theta}\right) \cdot v_j \cdot (m_c - m_{ox} - 0.5 \cdot C_{org}) \quad (\text{Eq. 6.11})$$

where v_j (0.04 eq g⁻¹) is the number of binding sites I_{wb} per gram illite, m_c is the mass of clay (g kg⁻¹), and m_{ox} is the mass of oxalate extractable Fe-oxide.

$$Hf_{os,w} = \left(\frac{\rho}{\theta}\right) \cdot \mu_k \cdot 1000 \cdot (m_{Fe,ox}/M_{Fe}) \quad (\text{Eq. 6.12})$$

where μ_k is 0.005 mol mol⁻¹ Fe for Hf_{os} and 0.2 mol mol⁻¹ Fe for Hf_{ow} respectively and M_{Fe} is the molar mass of Fe.

The Bradbury and Baeyens model is non-electrostatic. In this case, the required input parameters surface area and mass of soil component are set to a high value (10⁸), in order to neglect the Coulomb potential at the surface. In case of complexation on oxalate Fe-oxide surfaces instead, the surface area is set to 600 m² g⁻¹, whereas the m_{ox} is given in g kgw⁻¹. Hence, the m_{ox} in g kg⁻¹ is multiplied by the factor ρ/θ . To resume, for soil B, the obtained values are $I_{wb} = 0.045$ eq kgw⁻¹, $Hf_{os} = 0.42$ eq kgw⁻¹, $Hf_{ow} = 0.0105$ eq kgw⁻¹

The calculation of the amount of complexation sites on organic matter is done for radium as in Hormann and Fischer (2013). The abundances f_i of the various monodentate, bidentate and tridentate sites are found in table 9.10 of Tipping (2002). The number of binding sites $(n_{HA})_i$ is then given by:

$$(n_{HA})_i = 0.6 \cdot v_{HA} \cdot f_i \cdot C_{org} \left(\frac{\rho}{\theta}\right) \quad (\text{Eq. 6.13})$$

It is assumed that 30 % of the OM can bind cations and that $OM = 2 \cdot C_{org}$. It is also suggested that immobile organic matter, on which surface complexation occurs, consists of humic acids (HA). In case of sorption on organic matter, it is not only necessary to calculate the number of binding sites for the different monodentate, bidentate and tridentate options but it is also necessary to consider that there are strong, moderate and weak sites appearing 0.9 %, 9.1 %, and 90 % of the times. In addition, it is necessary to provide the equilibrium constants for the sorption reactions on each monodentate, bidentate and tridentate site. They are calculated as:

$$\log k(i) = \log k_{MA} + \frac{2i-5}{6} \Delta K_1 \quad (\text{Eq. 6.14})$$

$$\log k(i) = \log k_{MA} + \frac{2i-13}{6} \Delta K_1 \quad (\text{Eq. 6.15})$$

$$\log k(j, k) = \log k(j) + \log k(k) + x \Delta LK_2 \quad (\text{Eq. 6.16})$$

$$\log k(l, m, n) = \log k(l) + \log k(m) + \log k(n) + y \Delta LK_2 \quad (\text{Eq. 6.17})$$

Here, $\log k_{MA}$ is a parameter obtained by fitting Model VI to respective data for metal binding. Its value varies for each cation considered (see table 10.5 in Tipping, 2002). For earth-alkali metals, the equilibrium constants $\log k$ do not differ for the weak, moderate and strong sites, because in the formula considered for calculating the $\log k$ constants for bidentate and tridentate sites, the ΔLK_2 parameter is zero (Tipping, 2002). In case of the dissolved organic matter (DOM), the chemical elements are assumed to interact with fulvic acid (FA). In this case, the $\log k$ constants are calculated similarly to the HA case, but with $\log k_{MA}$ relevant for fulvic acids.

6.5.2 Thermodynamic constants for radium

The thermodynamic constants are usually evaluated from empirical data or estimated based on extrapolation of the thermodynamic properties of Ca, Sr and Ba complexes and solids, plotted against cationic radii and charge to radius functions (Langmuir and Riese, 1985). However, such evaluations do not exist for the equilibrium constants required in the sub-models for surface complexation and ion exchange of radium on various soil components. Thus, they need to be determined. In this case, the approach adopted is, in analogy to Langmuir and Riese (1985), to assume that behaviour of radium is similar to that of the other earth-alkali metals and that their equilibrium constants cannot differ greatly, especially when considering those earth-alkali metals to be similar in ionic size (i.e. Ra, Ba and Sr). Nevertheless, for surface complexation and exchange constants, no linear regression is applied based on cationic radii, since no reasonable linear trend has been proven yet (table 6.3).

Table 6.3: Log k constants, measured for analogous elements and assumed valid for radium regarding various exchange and complexation processes

Type of binding site	Analogous element	Log k
I_{pa}	Mg, Ca, Sr, Al	1.04
Hfo_s	Ba	5.46
Hfo_w	Ba	-7.2
I_{wb}	Ca, Sr, Mg	-5
Fulvic acid $\log k_{MA}, \Delta LK_2$	Sr or Ba	1.2, 0 – 0.6, 0
Humic acid $\log k_{MA}, \Delta LK_2$	Sr or Ba	1.1, 0 – -0.2, 0

Table 6.3 lists all the thermodynamic constants assumed for radium for applying the Hormann and Fischer approach. In case of the exchange constant for I_{pa} and the complexation constant for I_{wb} , one common value is published for the elements Mg, Ca, Sr and therefore applied to Ra as well. Regarding the Dzombak and Morel constants Hfo_s and Hfo_w , the value for Ba was considered valid for Ra. With respect to the constants related to the organic matter component, namely $\log k_{MA}$ for fulvic acid and humic acid, the constants for Ba and Sr have been considered alternatively. In this case, the available constants for Ba are -0.2 for HA and 0.6 for FA, indicating the weakest binding among all earth-alkali metals. This is in contrast to the theoretical assumption that due to its bonding size, radium is possibly the element which binds most to organic matter among earth alkali metals. In addition, experimental observations have shown that radium binds very strongly to OM. Hence, the model implemented in PHREEQC was run twice: once assuming the thermodynamic constants of barium being valid for radium reactions on OM, and once assuming the thermodynamic constants for strontium. The impact of such assumptions on the estimate of K_d values will be discussed in the next section.

6.6 REFESOL soils compared to Vandenhove and Van Hees' soils

In this work, sorption K_d are simulated for different soil types and soil solutions taken from Hormann and Fischer (2013) and Vandenhove and Van Hees (2007). Hormann and Fischer considered two REFESOL soils, namely 02-A (loam) of stagnic, luvisol type and 04-A (sand) of gleyic, luvisol type, with characteristics shown in table 6.4. The soil solution considered is a fictitious one, taken from the median values of the solution, presented in Scheffer and Schachtschabel (2010). It is assumed representative for agricultural (unfertilized) soils in Europe. The amount of Ra-226 considered is 1 Bq kg⁻¹ dry weight as applied in Hormann and Fischer (2013).

Table 6.4: REFESOL soils used for K_d estimates of radium

REFESOL	Sand %	Silt %	Clay %	pH	C_{org} %	CEC meq kg^{-1}	Fe_{ox} $g\ kg^{-1}$	Al_{ox} $g\ kg^{-1}$	Bulk soil density $g\ cm^{-3}$	Porosity -
02-A (loam)	2	83	15	6.6	1.3	133.2	3.54	0.69	1.37	0.48
04-A (sand)	85	11	4	5.1	2.9	85.7	0.63	1.51	1.7	0.35

In figure 6.2, the calculated K_d values are shown for two cases, the use of thermodynamic constants of barium or instead those of strontium. In the first case, K_d values are $7.14\ L\ kg^{-1}$ and $15.6\ L\ kg^{-1}$ for podsol and luvisol, respectively. When assuming thermodynamic constants for strontium, K_d values increase to $25.5\ L\ kg^{-1}$ and $25.2\ L\ kg^{-1}$. The latter two values are well in the range of the probability distribution function proposed for radium K_d values by Sheppard et al. (2006). In accordance to figure 6.3, radium is predominantly bound to clay.

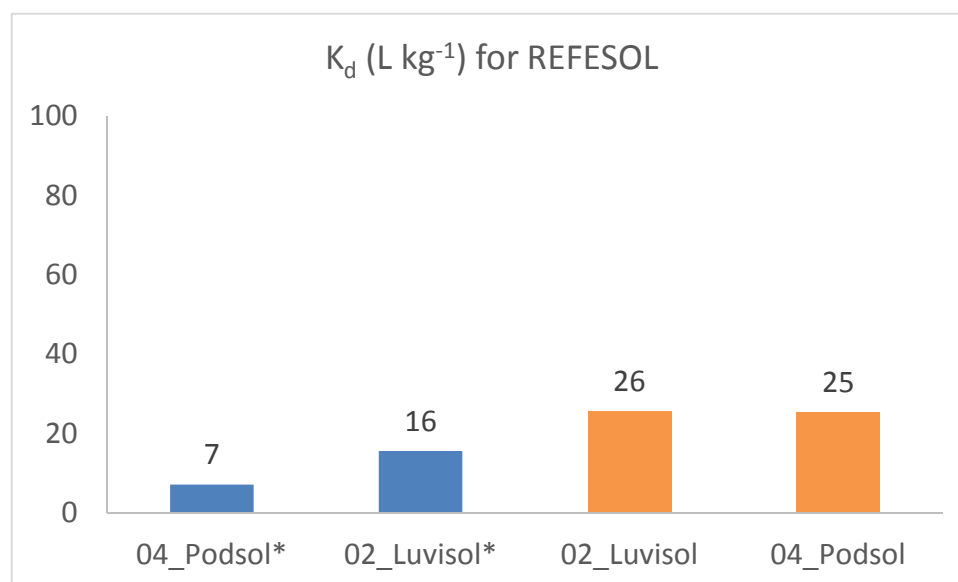


Figure 6.2: K_d values obtained for REFESOL soils. The asterisk refers to calculations with Ba constants for sorption on OM

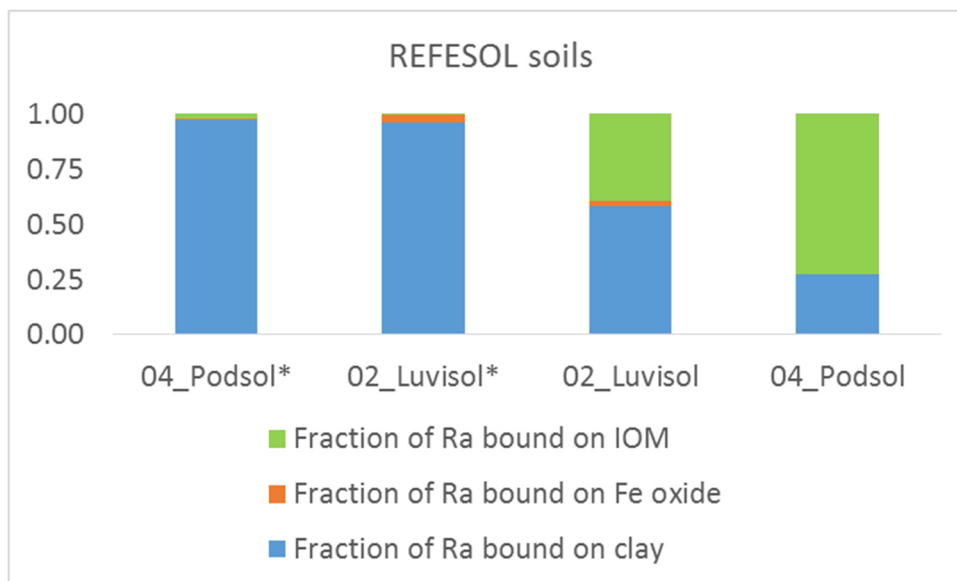


Figure 6.3: Fraction of radium bound to various soil components of REFESOL soils. The asterisk refers to calculations with Sr constants for sorption on OM

Regarding the thermodynamic constants for sorption on organic matter in the Tipping model VI, the K_d values for REFESOL soils are obtained by considering the thermodynamic constants for strontium to apply for radium. Those of barium were largely negative and the result of the calculations made no sense. Indeed, the K_d values increase to $K_d \sim 25$ for both soil types. The similar K_d value for the two different soil types is explained by the fact that Podsol Nord soil contains double the amount of C_{org} compared to Luvisol Süd soil. For REFESOL 02-A, a sensitivity study is carried out to quantify the impact on the most important parameters on the K_d estimate.

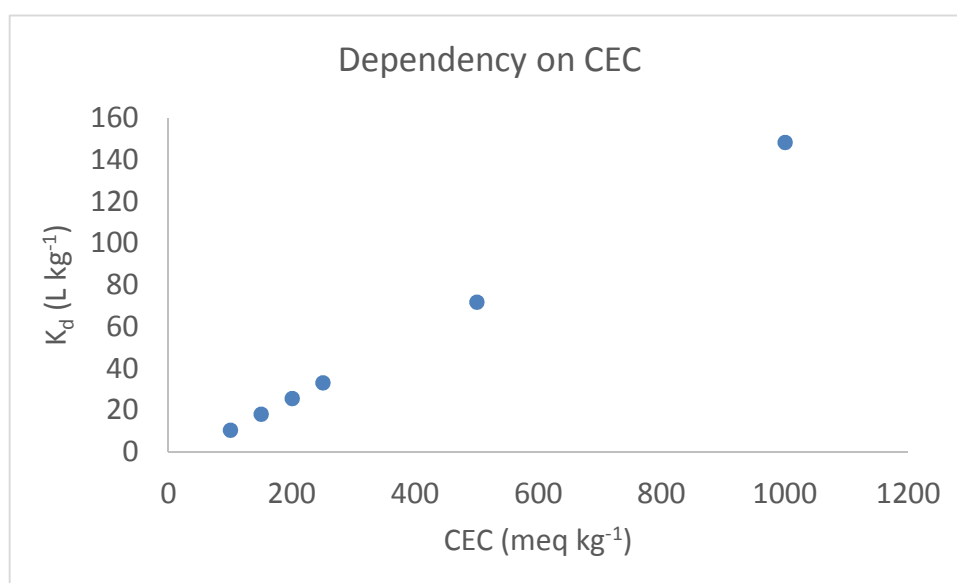


Figure 6.4: Sensitivity of K_d on CEC

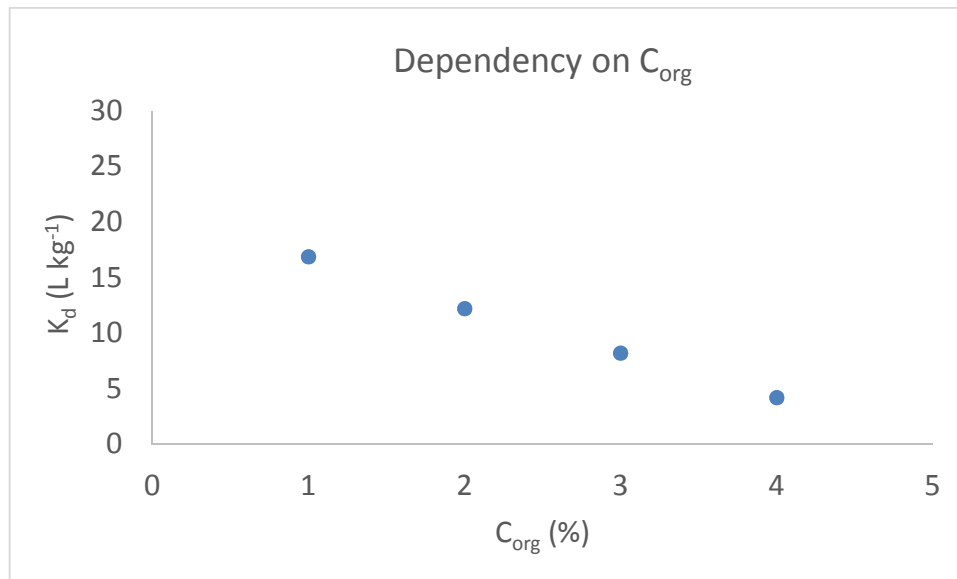


Figure 6.5: Sensitivity of K_d on C_{org}

The dependency of sorption on CEC and OM is partly confirmed by a sensitivity test, in which CEC and C_{org} have been varied and K_d value has been calculated. The results can be seen in figures 6.4 and 6.5. However, such sensitivity analysis, which was extended also to other parameters like pCO_2 , pH, clay, FeOX and OM, cannot be considered fully consistent. In fact, when varying the single parameters, only the relations for the calculation of the binding sites were changed accordingly. Quite surprisingly, by increasing the amount of C_{org} in soil, the K_d values decrease and this is not expected. If considering higher thermodynamic constants (i.e. strontium), however, the dependency reverses and C_{org} and K_d are positively related (figure 6.6).

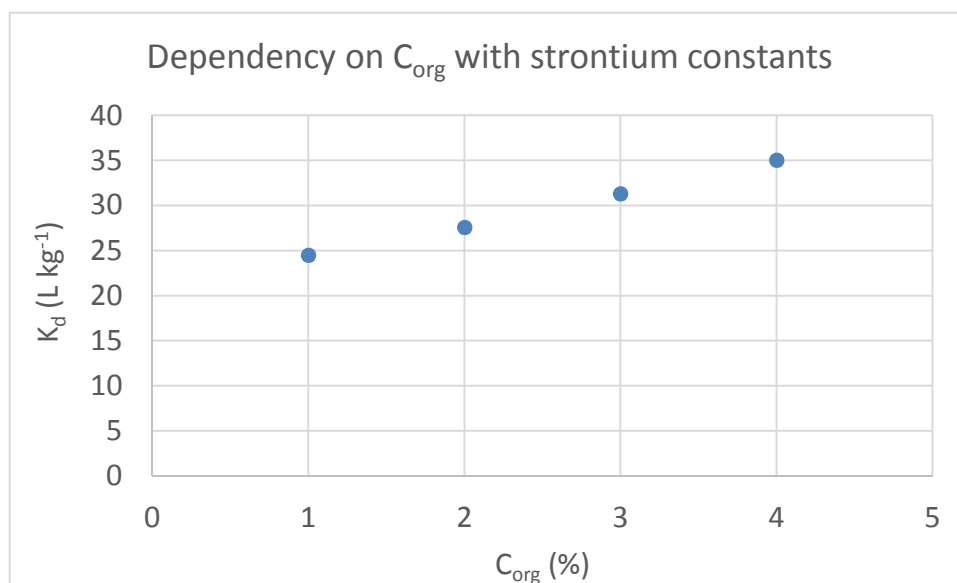


Figure 6.6: Sensitivity of K_d on C_{org} assuming strontium constants for Tipping Model

On the opposite, when varying the amount of DOM in soil solution, the K_d values increase as DOM increases, even though this is a smaller effect. In this case, even when considering thermodynamic constants of strontium, the trend shows an unexpected slow rising of K_d values. The dependency on the other parameters does not much affect the K_d values, they remain almost unchanged. In particular, a high correlation is expected by varying the amount of clay. This is not the case.

Vandenhove and Van Hees (2007) determined the K_d experimentally for 9 different soils. Each soil sample, about 3800 g dry weight, was spiked with 50,000 Bq kg^{-1} dry weight of Ra-226 and was left to equilibrate for about 4 weeks. In soil solution, Ca, Mg, K, Cl, NO_3 , SO_4 , total inorganic carbon (TIC) and HPO_4 were measured as well as pH. Furthermore, the soil CEC, soil field capacity, soil density, particle size (i.e. soil texture), amount of organic matter (OM), and total iron content (Fe), iron in amorphous form (FeOX) as well as total phosphorus (P) content were measured. The soil solutions had the pH ranging between 4.6 and 7.5, whereas the amount of clay amounted to 10% – 30%, CEC between 51 and 517 meq kg^{-1} , OM between 3 % and 15 %, FeOX between 887 mg kg^{-1} and 20,367 mg kg^{-1} , P with values of 680 – 1178 mg kg^{-1} and soil density ranging between 1.12 and 1.60 g cm^{-3} . Unfortunately, information on soil porosity was not available and therefore the nominal value of $\theta = 0.35$ was taken. The experimental K_d values obtained ranged between 38 and 446 L kg^{-1} and were found to be linearly, positively related to CEC and organic matter content.

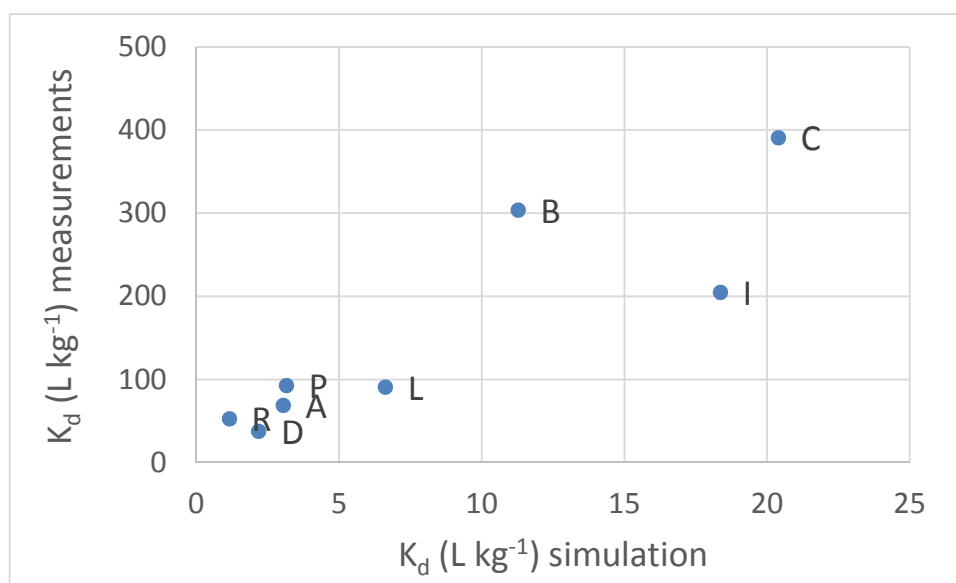


Figure 6.7: Comparison between experimental K_d values from Vandenhove and Van Hees (2007) and simulated ones calculated with PHREEQC: the same trend applies, although the simulated ones are about a factor 20 – 30 smaller, while soil R is about 46 times smaller. The simulations in this case are carried out using strontium constants for the OM component.

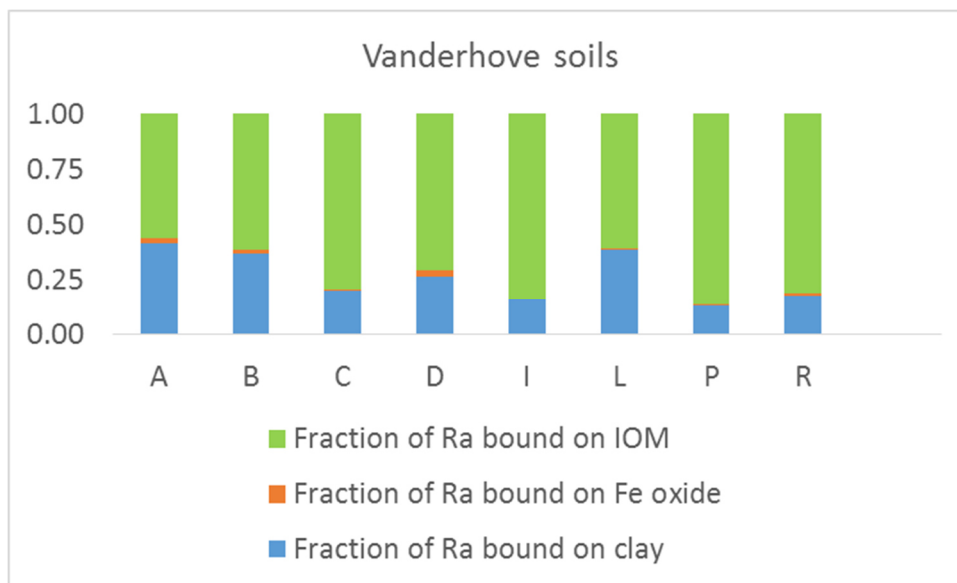


Figure 6.8: Fraction of Ra bound to various components for Vandenhove and Van Hees (2007) soils.

For Vandenhove and Van Hees (2007) soils, large discrepancies are detected, when comparing experimental K_d with simulated ones (figure 6.7). Better results are obtained, when thermodynamic constants for strontium instead of barium were taken. The simulated K_d values, despite being a factor 20 – 30 smaller, followed the same trend as the experimental findings. This may be an indication that the thermodynamic constants are in general of low quality and play the major role in determining the uncertainty. At least, the model describes the correct geochemistry. With respect to the types of fraction Ra is bound to, the organic matter is by far the most important part, amounting to 56 – 86 % for the soils considered (figure 6.8).

6.7 Discussion

The successful approach developed by Hormann and Fischer (2012, 2013) was performed for modelling sorption of radionuclides in soil with the geochemical speciation code PHREEQC. The authors considered sorption on clay (Bradbury and Baeyens model) under assumption the dominant clay component in soil being illite as well as sorption on organic matter (Tipping Model VI) and on hydrous ferric oxide (Dzombak and Morel model) as the dominant mechanisms for sorption of radionuclides in soils. Their model included a fictitious average soil solution. The outcome showed similar results to experimentally determined K_d -values, indicating that the modelling of partition coefficients is well possible. The local K_d -value of an investigation area depends on many environmental factors and the published distribution coefficients cover several orders of magnitude, which complicates the modellers' decision to choose a 'realistic' one. This circumstance justifies the time-consuming work on such a complex model with plenty of input parameters, because this process-oriented approach offers the possibility to calculate the migration behaviour of a contaminant within the soil system.

Based on the attempt of Hormann and Fischer (2012, 2013), a model for radium sorption was developed, including the most relevant chemical reactions for Ra in soil. Already known from

publications regarding its chemical behaviour, radium is expected to be sorbed on organic matter and clay material and to compete with other dissolved cations for the same binding sites. In solution, it is mostly present in form of Ra^{2+} . In case of high sulphate or carbonate content, it can precipitate as RaSO_4 or RaCO_3 or as solid solution $(\text{Ba,Ra})\text{SO}_4$. The latter was frequently found and indicates that radium occurrence in nature can be accompanied by barium. Obviously, both show similar chemical behaviour. Reliable partition coefficients of Ra show rather low values compared to other radionuclides, amounting to 10 – 100 L kg^{-1} , with geometric mean value of 47 (Sheppard et al., 2006).

The described process-oriented approach via geochemical speciation modelling has the disadvantage that it requires a high number of parameters, which are not always experimentally available. For example, very often, soil solution is not known, and organic matter is rarely distinguished between fulvic acid and humic acid. The thermodynamic constants are moderately uncertain and for some radionuclides, as in the case of radium, not fully determined. Intend of this work is the examination of the outcome in case of such incomplete datasets.

In this study, the K_d values of radium were calculated using PHREEQC by considering the REFESOL soils Luvisol Süd 02-A (loam) and Podsol Nord 04-A (sand) together with experimental data obtained from Vandenhove and Van Hees (2007). The thermodynamic constants required for balancing the radium sorption reactions are rather limited. Therefore, the missing thermodynamic constants are taken from other earth-alkali elements, strontium and barium. Values of K_d obtained using REFESOL data and fictitious soil solution are compared to the recommended values from Sheppard et al. (2006), whereas the K_d values calculated with Vandenhove data are compared directly to their experimental results.

In general, low radium K_d values are the result of model calculations. The outcome by using thermodynamic values of barium was too low to be realistic, indicating that further investigation regarding barium parameterization should be undertaken. With thermodynamic constants of Sr under consideration and depending on the literature considered, the calculated distribution coefficients are in the range of what was proposed in the literature (Sheppard et al., 2006) or factor 20 – 30 lower (Vandenhove and Van Hees, 2007). The performed sensitivity study shows that the model reflects radium sorption behaviour. Sorption on organic matter is the most dominant contributor to overall distribution coefficient, while the one on hydrous ferric oxide does not play an important role, which is expected for this component. Partially, the amount of radium sorbing on clay is lower than expected. This could indicate that the thermodynamic constants used in Bradbury and Baeyens model may be too low. At the same time, it is possible that sorption of radium on clay may not be at best described by assuming that illite is main contributor of radium sorption, which has furthermore a comparatively low cationic exchange capacity. In soils, the clay composition is quite heterogeneous and mainly depending on the host rock, climate conditions and the degree of weathering. Since other clays like smectite, vermiculite, chlorite, mica and so on, can be relevant fractions, the model could probably be enhanced by considering other clays, being typically present in the local soil types of a certain study area.

The functionality of the described complex, process-oriented model to calculate partition coefficients has been proven in Hormann and Fischer (2012, 2013). The approach undertaken in this study about the adoption of missing thermodynamic constants from elements with similar chemical behaviour shows clearly that the outcome depends on the quality of the input parameters. Since barium has been found accompanied with radium in natural samples, it is expected that Ba reflects radium sorption behaviour better than strontium, but the opposite is

the case. However, as long as better models to calculate the distribution coefficient are lacking, it is still worth to perform this effort, because the uncertainty regarding the apparent retention potential of an investigation site can be significantly reduced. The narrowing of the K_d -value to an order of magnitude in the range of 1 – 2 is much better than picking the distribution coefficient based on literature, with varying numbers in the order of magnitude of 6 – 7. Important to note that the distribution coefficient, which is a condensed variable resulting from many complex hydrogeochemical processes, can be properly calculated with thermodynamic data from chemical analogues.

6.8 Bibliography

- Allison, J. D., Brown, D. S. and Novo-Gradac, K. J. (1990): MINTEQA2\ PRODEFA2. A geochemical model for environmental systems: Version 3.0 User's Manual. US Environmental Protection Agency. Environmental Research Laboratory, Athens, Georgia.
- Appelo, C. A. J. and Postma, D. (2005): Geochemistry, groundwater and pollution. CRC Press.
- Bordelet, G., Beaucaire, C., Phrommavanh, V. and Descostes, M. (2013): Sorption Properties of Peat for U (VI) and 226 Ra in U Mining Areas. *Procedia Earth and Planetary Science*, 7, 85-88.
- Bradbury, M. H. and Baeyens B. (2000): A generalised sorption model for the concentration dependent uptake of caesium by argillaceous rocks. *Journal of Contaminant Hydrology* 42: 141-163.
- Bradbury, M. H. and Baeyens, B. (2009a): Sorption modelling on illite Part I: Titration measurements and the sorption of Ni, Co, Eu and Sn. *Geochimica et Cosmochimica Acta* 73: 99-1003.
- Bradbury, M. H. and Baeyens, B. (2009b): Sorption modelling on illite Part II: Actinide sorption and linear free energy relationships. *Geochimica et Cosmochimica Acta* 73: 1004-1013.
- Brandt, F., Curti, E., Klinkenberg, M., Rozov, K. and Bosbach, D. (2015): Replacement of barite by a (Ba, Ra) SO₄ solid solution at close-to-equilibrium conditions: A combined experimental and theoretical study. *Geochimica et Cosmochimica Acta*, 155, 1-15.
- Chalupnik, S. and Wysocka, M. (2008): Radium removal from mine waters in underground treatment installations. *Journal of Environmental Radioactivity* 99: 1548-1552.
- Dzombak, D. A. and Morel, F. M. M. (1990): Surface complexation modeling: hydrous ferric oxide, Wiley-Interscience, New York.
- Ebbers, B. (2011): Multicomponent transport of contaminants released into the environment following the application of phosphogypsum. Master Thesis, Utrecht University.
- EPA (1999): Understanding variation in partition coefficient, K_d , values. United States Environmental Protection Agency EPA 402-R-99-004A.
- EPA (2004): Understanding variation in partition coefficient, K_d , values. Volume III: Review of geochemistry and available K_d values for americium, arsenic, curium, iodine, neptunium, radium, and technetium. United States Environmental Protection Agency EPA 402-R-04-002C
- Gäfvvert, T., Færevik, I. and Rudjord, A. L. (2006): Assessment of the discharge of NORM to the North Sea from produced water by the Norwegian oil and gas industry. *Radioactivity in the Environment*, 8, 193-205.
- Hormann, V. and Kirchner, G. (2002): Prediction of the effects of soil-based countermeasures on soil solution chemistry of soils contaminated with radiocesium using the hydrogeochemical code PHREEQC. *Science of the Total Environment* 289: 83-95.
- Hormann, V. and Fischer, H. W. (2012): Fachliche Interstützung des BfS bei der Erstellung von Referenzbiosphärenmodellen für den radiologischen Langzeitsicherheitsnachweis von Endlagern – Modellierung des Radionuklidtransports in Biosphärenobjekten (FKZ 3609S50005). Endbericht des Teilprojekts Boden. Februar 2012.

- Hormann, V. and Fischer, H. W. (2013): Estimating the distribution of radionuclides in agricultural soils – Dependence on soil parameters. *Journal of Environmental Radioactivity* 124: 278-286.
- Hummel, W., Berner, U., Curti, E., Pearson, F. J. and Thoenen, T. (2002): NAGRA/PSI chemical thermodynamic data base 01/01. Technical Report 02-16. National cooperative for the disposal of radioactive waste (NAGRA). Switzerland.
- IAEA (2010): Handbook of parameter values for the prediction of radionuclide transfer in Terrestrial and freshwater environments. Technical Reports Series No. 472. International Atomic Energy Agency, Vienna, Austria.
- Jackson, R. E. and Inch, K. J. (1989): The in-situ adsorption of ⁹⁰Sr in a sand aquifer at the Chalk River Nuclear Laboratories. *Journal of contaminant hydrology*, 4(1), 27-50.
- Kördel, W., Peijnenburg, W., Klein, C. L., Kuhnt, G., Bussian, B. M. and Gawlik, B. M. (2009): The reference-matrix concept applied to chemical testing of soils. *Trends in Analytical Chemistry* 28 (1): 51-63.
- Langmuir, D and Riese, A. C. (1985): The thermodynamic properties of radium. *Geochimica et Cosmochimica Acta* Vol 49: 1593-1601.
- Lofts, S. and Tipping, E. (2000): Solid-solution metal partitioning in the Humber rivers: application of WHAM and SCAMP. *Science of the total environment*, 251, 381-399.
- Looney, B. B., Grant, M. W. and King, C. (1987): Estimating of geochemical parameters for assessing subsurface transport of the Savannah river plant. DPST-85-904, Environmental Information Document, E. I. du pont de Nemours and Company, Savannah River Laboratory, Aiken, South Carolina.
- Loveland, W. D., Morrissey, D. J. and Seaborg, G. T. (2005): Modern nuclear chemistry. John Wiley & Sons.
- Mahoney, J. (1998): Incorporation of coprecipitation reactions in predictive geochemical models. Tailings and Mine Waste '98. 1998 Balkema, Rotterdam, ISBN 90 54 10 922 X.
- Meier, H., Zimmerhacki, E., Menge, P. (1994): Parameter studies of radionuclide sorption in site-specific sediment/ groundwater systems. *Radiochimica Acta* 66/67: 277-284.
- Merkel, B. J. and Planer-Friedrich, B. (2008): Grundwasserchemie: praxisorientierter Leitfaden zur numerischen Modellierung von Beschaffenheit, Kontamination und Sanierung aquatischer Systeme. 2nd Ed., Springer-Verlag.
- Meunier, A. and Velde, B. D. (2013): Illite: Origins, evolution and metamorphism. Springer Science & Business Media.
- Nathwani, J. S. and Phillips, C. R. (1979a): Adsorption of Ra-226 by soils (I). *Chemosphere* 5: 285-291.
- Nathwani, J. S. and Phillips, C. R. (1979b): Adsorption of Ra-226 by soils (II). *Chemosphere* 5: 293-299.
- Parkhurst, D. L., and Appelo, C. A. J. (1999): User's Guide to PHREEQC (Version 2). Water Resources Investigations Report 99-4295. U. S. geological Survey, Denver, Colorado.
- Polubesova, T. and Nir, S. (1999): Modeling of organic and inorganic cation sorption by illite. *Clays and clay minerals*, 47(3), 366-374.

Sajih, M., Bryan, N. D., Livens, F. R., Vaughan, D. J., Descostes, M., Phrommavanh, V., Nos, J. and Morris, K. (2014): Adsorption of radium and barium on goethite and ferrihydrite: A kinetic and surface complexation modelling study. *Geochimica et Cosmochimica Acta*, 146, 150-163.

Salbu, B. (2009): Fractionation of radionuclide species in the environment. *Journal of Environmental Radioactivity* 100: 283-289.

Schecher, W. D. and McAvoy, D. C. (1992): MINEQL+: a software environment for chemical equilibrium modeling. *Computers, Environment and Urban Systems*, 16(1), 65-76.

Scheffer, F. and Schachtschabel, P. (2010): Lehrbuch der Bodenkunde. 16. ed., 570 p. Springer-Verlag.

Serne, R. J. (1974): Waste Isolation Safety Assessment Program Task 4. Contractor Information Meeting Proceedings. PNL-SA-6957, Pacific Northwest Laboratory, Richland, Washington.

Sheppard, S. C., Sheppard, M. I., Tait, J. C. and Sanipelli, B. L. (2006): Revision and meta-analysis of selected biosphere parameter values for chlorine, iodine, neptunium, radium, radon and uranium. *Journal of Environmental Radioactivity* 89: 115-137.

Shoesmith, D. W. (1984): The behaviour of radium in soil and in uranium mine-tailings, AECL-7818, Atomic Energy of Canada Limited, September 1984.

Simon, S.L., Ibrahim, S.A., 1990. Biological uptake of radium by terrestrial plants. In: The environmental behaviour of radium. IAEA. Technical report series No. 310, 545–599.

Sigg, L. and Stumm, W. (2011): Aquatische Chemie: Einführung in die Chemie natürlicher Gewässer (Vol. 8463). UTB, Switzerland.

Sposito, G. (1989): The chemistry of soils. Oxford University Press, New York.

Sun, H. and Semkow, T.M. (1998): Mobilization of thorium, radium and radon radionuclides in ground water by successive alpha-recoils. *Journal of Hydrology*, 205(1), 126-136.

Tipping, E. (1993): Modeling the Competition between Alkaline Earth Cations and Trace Metal Species for Binding by Humic Substances. *Environmental Science and Technology* 27: 520-529.

Tipping, E., Lofts, S. and Lawlor, A. J. (1998): Modelling the chemical speciation of trace metals in the surface waters of the Humber system. *Science of the Total Environment*, 210, 63-77.

Tipping, E. (2002): Cation binding by humic substances. Cambridge environmental chemistry series 12. Cambridge University Press.

Thibault, D. H., Sheppard, M. I. and Smith, P. A. (1990): A critical compilation and review of default soil/solid/liquid partition coefficients, K_d , for use in environmental assessments. AECL-10125, Whiteshell Nuclear Research establishment, Atomic Energy of Canada Limited, Pinawa, Canada.

Vandenhove, H. and Van Hees, M. (2007): Predicting radium availability and uptake from soil properties. *Chemosphere* 69: 664-674.

Vandenhove, H., Gil-García, C., Rigol, A. and Vidal, M. (2009): New best estimates for radionuclide solid–liquid distribution coefficients in soils. Part 2. Naturally occurring radionuclides. *Journal of Environmental Radioactivity*, 100(9), 697-703.

7 Migration of radionuclides in soil: convection-dispersion equation with initial realistic deposition profile

In case of an atmospheric fall-out of radioactive matter via wet deposition, e.g. after accidents in nuclear power plants like Chernobyl and Fukushima or experiments with nuclear weapons, the further movement of the contaminant from the surface into the soil and maybe even into the groundwater is of high concern. The understanding of the migration behaviour is fundamental to assess the resulting risk. The goal of this work is to use successively an exponential function to describe the initial short-term deposition, followed by the model to describe the long-term Cs-migration under sorption conditions. This new approach covers the most relevant processes regarding the time-dependent contaminant transport. The outcome of the calculations is finally compared with experimental observations of migrated caesium in Norway from fall-out of the Chernobyl accident.

7.1 Introduction

The migration of radionuclides in soil is an important mechanism since it controls the long-term behaviour of radionuclides in the environment, their uptake by flora and fauna including human food chains, but also their potential as a groundwater contaminant. The basic processes controlling the mobility of radionuclides in undisturbed soil include convective transport by flowing water, dispersion and diffusive movement within the fluid and physico-chemical interaction with the soil matrix. An approach for modelling the migration of radionuclides in soil is the use of a one-dimensional convection-dispersion equation (CDE), which has been often applied for Cs-137 (Bossey and Kirchner, 2004; Bunzl, 1978; Elshamy et al., 2007). In these studies, the analytical or numerical solution of the CDE has always been obtained assuming a pulse-like input at $t = 0$. The models predicted a slower migration in soil than experimentally observed. In addition, several studies (Isaksson and Erlandsson, 1995; Poiarkov et al., 1995) imply that for experimental profiles directly after deposition, the vertical distribution of Cs-137 could be fairly well described by an exponential function. Such a wet deposition leads to a certain contaminant transport into soils, which occurs initially independently of sorption processes. Thus, the initial profile has the form:

$$C(x, 0) = J_0 \cdot m e^{-mx} \quad (\text{Eq. 7.1})$$

where the constant m (cm^{-1}) is set in a way that the integral over the soil column equals the input J_0 (Bq cm^{-2}). During the initial phase, a CDE with the retardation factor $R = 1$ and hence, $K_d = 0$ is applied. The initial deposition profile may only depend on hydraulic properties of soil, such as soil conductivity and soil water content and to climatic conditions like temperature and the temporal rainfall pattern. This described function only depicts the deposition condition. With rising time, mainly sorption leads to the retention and the deceleration of the vertical contaminant transport within soil matrix. Hence, this period can be calculated with equation 7.1 under consideration of the distribution coefficient K_d .

In order to model the initial deposition profile numerically, the hydrogeological code HYDRUS-1D is used, which is a program for modelling the movement of water, heat, and multiple solutes in variably saturated media. With this tool, the CDE is solved in two steps. First, by calculating the initial fast migration following the deposition of radionuclides under assumption that no retardation of the radionuclide movement occurs (i.e. adsorption). Secondly,

the long-term migration profile is calculated, taking into account the initial concentration profile obtained from the first run. Simulation results are then compared to experimental data. Such data consist of time-series of Cs-134 concentrations at various depths in soil. Cs-134 is exclusively present in soils affected by the Chernobyl accident. This in contrast to Cs-137, which may also originate from the nuclear weapon tests. In addition, exhaustive information about soil properties from samples and precipitation records need to be available. These factors are described in more detail in the next section.

7.2 *Review context of Cs migration in soils*

For predicting the migration of radionuclides in soil, the water flow and the solute transport have to be assessed. The soil pore water originates mainly from precipitation, while water flow is due to infiltration in soil and distribution along the soil matrix. The radionuclides are transported in soil because of dispersive and convective processes.

7.2.1 Relevant processes

Infiltration of radionuclides in soil depends on various transfer processes between the surface layer and deeper soil layers, which are not considered in this work. The translocation process of materials in the soil is very complex, affecting very different substances (minerals, organic matter and complex organic minerals, whether they are in solutions or suspensions) and for very different reasons (gravity, capillarity, evaporation, biotic activity, or because of the soil mass swelling and contracting). For example, retention on surface due to the presence of plants and vegetation next to the presence of earthworms in soil, which cause bioturbation transport and enhance diffusion processes, are not taken into account. Also for the two locations considered, no snow layer is taken into account. Packs of snow act as sinks of radioactive matter and soil saturation in spring as well as the existence of permafrost diminish the infiltration of radionuclides in soil (Hürkamp et al., 2012). It is also known that radionuclides stored in a snowpack become available for migration during the melting season (Monte et al., 2004) and this could enhance migration in soil sometime after the deposition event. In addition, when first snow falls, resuspension due to snowflakes may increase again the activity levels in air.

Sorption occurs on different time scales, ranging from milliseconds to months and even years. The type of soil component has a major effect on the sorption rate. For example, sorption reactions are often more rapid on clay minerals such as kaolinite and smectite than on vermiculites and micaceous minerals. This is mainly due to the availability of sites for sorption. For example, kaolinite has readily available planar external sites and smectites have predominantly internal sites that are not quite as available for retention of sorbates. Thus, sorption reactions on these soil constituents are often quite rapid, even occurring on time scales of seconds and milliseconds (Sparks, 1989, 2002). On the other hand, vermiculite and micas have multiple sites for retention of ions, including planar, edge, and interlayer sites, with some of the latter sites being partially up to totally collapsed. Therefore, sorption and desorption reactions on these sites can be slow, tortuous, and controlled by mass transfer. Often, an apparent equilibrium may not be attained even after several days or weeks. A number of studies have shown that heavy metal sorption on oxides (Ainsworth et al., 1994; Barrow, 1986; Bruemmer et al., 1988; Scheidegger et al., 1997, 1998) and clay minerals (Lövgren et al., 1990) increases with residence times (contact time between the metal and the sorbent). The

mechanisms for these lower reaction rates are not well understood, but have been ascribed to diffusion phenomena, sites of lower reactivity, and surface nucleation/precipitation (Scheidegger et al., 1997; Sparks, 2002). Sorption/desorption of metals, oxyanions, radionuclides, and organic chemicals on soils can be very slow. This type of retention may demonstrate a residence time effect, which has been ascribed to diffusion into micropores of inorganic minerals such as some metal oxides and into humic substances, retention on sites of varying reactivity, and to surface nucleation/precipitation (Alexander, 2000; Pignatello, 2000; Scheidegger et al., 1997; Sparks, 2002; Strawn and Sparks, 1999; Trivedi et al., 2002). In this work, the sorption is mathematically expressed by the partition coefficient (K_d), which indicates the distribution of Cs concentrations between the aqueous and the solid phase and hence, the overall retention of this contaminant within the soil matrix. Finally, it is well known that some fraction of Cs undergoes an irreversible fixation to soil, which is not included as a sink term in the applied CDE.

7.2.2 Water flow

For water flow, the dependent variable is generally expressed in terms of head, draw down, or pressure as a function of space and time. Boundary conditions are usually defined in terms of heads and flows and the parameters to be specified for one-dimensional vertical flow are the hydraulic parameters, namely the hydraulic conductivity K (cm d^{-1}), pressure head ψ (cm) or hydraulic head h (cm) and the volumetric water content θ [$\text{cm}^3 \text{cm}^{-3}$] along the vertical depth x (cm).

In a variably saturated porous medium, the water flow is described using the Richards' equation:

$$\frac{\partial \theta}{\partial t} = \frac{\partial}{\partial x} \left[K \left(\frac{\partial \psi}{\partial x} + 1 \right) \right] \quad (\text{Eq. 7.2})$$

It combines the equation of continuity for mass flow to the so-called Darcy flux q (cm d^{-1}):

$$q = -K(\psi) \frac{dh}{dx} \quad (\text{Eq. 7.3})$$

The pore water velocity \bar{v} can be obtained by dividing the Darcy flux by the effective porosity. In unsaturated porous media, the moisture content θ and K are related to ψ . Widely accepted empirical relationships (so called VGM parameters) were established by van Genuchten (1980). These relationships are:

$$\theta(\psi) = \theta_r + (\theta_s - \theta_r) \left(1 + |\alpha \psi|^n \right)^{-m} \quad \text{with } m = 1 - \frac{1}{n} \quad \text{and } S_e = \frac{\theta(\psi) - \theta_r}{\theta_s - \theta_r} \quad (\text{Eq. 7.4})$$

$$K(S_e) = K_s S_e^\tau \left[1 - (1 - S_e^{1/m})^m \right]^2 \quad (\text{Eq. 7.5})$$

where

θ_r and θ_s are the residual and saturated water content, respectively,
 S_e is the relative saturation,
 K_s is the hydraulic conductivity in saturation (cm d^{-1}), and
 n , α and τ are shape parameters, specific of a given material.

The physical meaning of the VGM parameters is limited. For a given soil texture type, the hydraulic properties are taken from tabulated data, using the soil catalogue of Carsel and Parrish (1988). VGM parameters depend on the type of material and need to be estimated for example by outflow measurements.

The upper boundary condition is defined as equal to the atmospheric condition (1 bar) in this study. This implies that water infiltration corresponds to daily rainfall rates. Surplus of water is assumed to be removed by run-off. Of course, this is depending on the type and degree of coverage, next to hillslope. In case of grassland or forest as vegetation unit and a nearly flat surface, no surface run-off can occur. The lower boundary condition is defined as a zero pressure gradient, meaning a free drainage.

7.2.3 Solute transport: the convection-dispersion equation (CDE)

In contrast to water flow, the dependent variable in solute-transport studies is the concentration of solute in water phase $C(x,t)$ as a function of space and time. The convection-dispersion equation (CDE) is a 2nd order partial differential equation, which describes the transport of radionuclides in soil at equilibrium and has the following form:

$$\frac{\partial(\theta C + \rho \bar{C})}{\partial t} + \frac{\partial v C}{\partial x} = \frac{\partial}{\partial x} \theta D \frac{\partial C}{\partial x} - \lambda \rho \bar{C} - \lambda \theta C \quad (\text{Eq. 7.6})$$

where C is the concentration in water phase (Bq cm^{-3}) or (Bq l^{-1}), \bar{C} is the concentration in solid phase (Bq g^{-1}), D is the dispersion coefficient ($\text{cm}^2 \text{d}^{-1}$), \bar{v} is the pore velocity (cm d^{-1}) and λ is the radioactive decay constant (d^{-1}). Hydrodynamic dispersion is calculated, neglecting diffusion effects, as $D = \alpha \bar{v}$, with α being the dispersivity (cm), which is an intrinsic property of soil. In HYDRUS, it is recommended for numerical stability to consider the dispersivity value to cover about 1/10 of the transport domain.

Sorption is described linearly as $\bar{C} = K_d C$, where K_d ($\text{cm}^3 \text{g}^{-1}$) is the distribution coefficient. The general initial condition is given by $C(x,0) = f(x)$. As boundary, we use the flux-type at the upper boundary and a zero concentration value at the lower boundary. Once sorption processes play a role, they are assumed kinetically faster than typical migration in soil and hence equilibrium conditions are considered valid. This allows the use of the distribution coefficient K_d .

The CDE is derived from the mathematical formulation of mass conservation assuming a steady-state flow, for which θ and the volumetric flux q are constant. Such a definition implies a uniform water flow, with no distinction between mobile and immobile water regions. Hence, no dual-porosity type description is needed. Additionally, vertical migration is assumed to dominate over the horizontal spread of contamination. The diffusion and dispersion in the top soil layer may be different from those in the bulk of the soil. In addition, sorption properties may vary along the soil profile. These aspects, though, are not considered here.

By applying the CDE model with the above-indicated assumptions, we assume that convective-dispersive processes dominate the transport neglecting effects of root uptake, biodegradation, retention on surface. In addition, evapotranspiration, snow hydrology and runoff are not considered in the model. In principle, however, these effects should be taken into account. In addition, the water content is probably dominated by the mobile part. The full set of equations

(solute transport equation and initial boundary conditions) represents a coupled system. However, for simplified models, analytical solutions exist (Van Genuchten and Alves, 1982).

Bossew and Kirchner (2004), for instance, carried out studies applying the convection-dispersion equation to the migration of radionuclides by solving analytically the CDE and assuming a pulse-like input function and an initial condition of $C(x,0) = 0$. They fitted the CDE to 500 experimental profiles of undisturbed Austrian soils and collected samples (18 · 18 cm² cubes at 10 – 20 cm depths). The authors started from 1987 with undisturbed soils from six sampling locations and measured bulk soil density and water content but no detailed chemical and physical analysis of the soils was carried out. Gamma spectroscopy was used to analyse the samples. By fitting the CDE to those profiles, they obtained v and D and were able to group them in relation to the geography, e.g. roughly regarding soil-type and geology and hence could interpret the fitted parameters as physical quantities.

They could demonstrate radionuclide specific behaviour, i.e. Sb-125 and Ru-106 being significantly more mobile than Cs-134 and Cs-137. These last two radionuclides also showed marked differences. This suggests that non-equilibrium condition may be valid at this stage of migration in soil, and assuming equilibrium conditions would be an oversimplification. Despite concluding that the CDE with its parameters could be a sound approach for predictive modelling, the authors nevertheless observed that a small fraction of the deposited radionuclide activities was at greater depths than predicted by the CDE.

7.3 *Geo-hydrological code HYDRUS-1D*

Hydrological codes have been developed to simulate water flow and contaminant transport. One of the state-of-the-art codes is HYDRUS-1D (Simunek et al., 2008), which is used in this work. Other examples are the combined soil-water-plant (SWP) hydrological model and solute transport model (SLT), developed at the London Imperial College (Tompkins and Butler, 1996a; 1996b) and the 2-D code VS2DT (Lappala et al., 1993). The SWP code is based on a block-centred finite differences solution of the one-dimensional unsaturated flow (Richards' equation). Various parametric relationships are included in the model for characterising soil water content and hydraulic conductivity. The outputs of SWP are then used in SLT, which employs a similar solution scheme for the CDE and considers sorption, root uptake and radioactive decay. Alternatively, HYDRUS-1D can cope with different kind of complexities, e.g. uniform/non-uniform water flow, transient/steady-state flow as well as saturated/non-saturated water flow. It can solve the CDE in parallel with the Richards' equation for water flow, starting from given soil parameters and initial boundary conditions. HYDRUS-1D can handle evapotranspiration processes, snow and vapour hydrology. The CDE in HYDRUS-1D is implemented for equilibrium conditions by considering first-order decay reactions, like for example, physical decay of radionuclides. HYDRUS-1D relies on hydraulic properties for a given soil texture, based on the soil catalogue of Carsel and Parrish (1998). VGM parameters (residual, saturated, volumetric water content θ_r , θ_s , K_s) are either tabulated or determined by outflow measurements. The dispersion coefficient D and the interstitial pore velocity are calculated in HYDRUS-1D using the equations presented above.

Solving the CDE analytically, the initial condition as an exponential profile is taken into account. The relaxation length of the exponential profile needs to be defined either empirically or with some physicochemical argument, based on information from the hydrological context. Then, D and v can be inversely determined. When solving the CDE numerically, a forward

calculation for quantifying the time-evolution of radionuclide concentration as a function of depth is necessary.

7.4 Available experimental data

After the Chernobyl accident in April 1986, a large part of European territory was affected by increased radioactivity levels following the radioactive plume passage. Especially North-European countries like Norway, Finland, Germany, and Austria were partially heavily contaminated. One of the radionuclides released was Cs-134, which is the only Cs isotope present in soil exclusively because of the Chernobyl accident. It undergoes a beta decay (β^-), producing Ba-134, which is stable. Cs-134 has a half-life of 2.06 years and therefore its contamination in soil could be detected for no longer than 20 years, because a detection limit of 0.05 Bq kg^{-1} is typically applied for environmental samples. The data required for the present analysis consists of time-series for Cs-134 concentrations at different depths in undisturbed soils in order to be able to compare the evolution of Cs-134 both in time and in space. Ideally, the time-series should start shortly after the Chernobyl accident and should be continued throughout the following years. Measurements of the following soil properties are required: textural analysis, bulk soil density, water content at various depths in soil. Climatic information, such as measurements of rainfall intensity, air temperature, heat transport (i.e. snow hydrology) and modelled evapotranspiration need to be taken into account. Information on the amount of deposited activity of Cs-134 on local surface is determinant. Data on pore water pH, organic matter content, amounts of oxides and carbonates are helpful for estimating K_d values more specifically. If not available, K_d values catalogued in IAEA (2010) are used and specifically for Cs-134, a K_d value of $530 \text{ cm}^3 \text{ g}^{-1}$ is chosen. This value is a compromise between the value of $1000 \text{ cm}^3 \text{ g}^{-1}$ valid for 'realistic' scenarios and the value of $270 \text{ cm}^3 \text{ g}^{-1}$ for the 'low probability model' considered in the IAEA (2005). The German radiation protection commission considers a conservative K_d value for Cs-134 of 10 L kg^{-1} (SSK, 1998).

Norwegian data considered were supplied by Rudjord and Haugen (1989) and Backe et al. (1987) and cover contamination information from the years 1986, 1987 and 1988. In Norway, the main fall-out period due to Chernobyl started at April 28, 1986 and lasted until May 15, 1986, i.e. the main deposition occurred within 18 days. The available data refer to two areas, Berset and Heimdalen, located in the southern part of Norway. Samples were taken in meadow (Berset) and natural pasture (Heimdalen). Berset soil was classified as sandy loam and Heimdalen as silt-loam. In the first mentioned region, the total deposition of Cs-134 and Cs-137 was about 19.5 kBq m^{-2} , whereas in the second it ranged from 53.3 to 482 kBq m^{-2} . Backe et al. (1987) estimate a value of 1.9 (corrected for decay of Cs-134 between May 15 and July 1, 1986) for the activity ratio Cs-137/Cs-134 during the Chernobyl deposition. Thus, the total Cs deposition may be described as Cs-134 and 1.9 Cs-134, rendering a factor of 2.9 by which the total deposition has to be divided to account for the Cs-134 contribution. Hence, a Cs-134 deposition of 6.72 kBq m^{-2} is assessed for Berset and 64.1 kBq m^{-2} for Heimdalen. This last value is obtained by averaging the 6 different depositions sampled. In Berset the deposition of Cs-134 is about double the average deposition of Cs-134 measured in Norway. For Heimdalen, it is 20 times higher. By the end of 1988 (2.6 years after the end of deposition, assumed to be on May 15, 1986) about 40% of Cs-134 has decayed. Then, the Cs-134 deposition in soil has decreased to 0.27 Bq cm^{-2} at Berset and to about 2.65 Bq cm^{-2} at Heimdalen.

Precipitation data (mm d^{-1}) from Norway is taken from the historical weather and climate data from the Norwegian meteorological institute (www.eklima.met.no). For Berset, data was taken from the meteorological station of Beito (~ 30 km away) and for Heimdalen, data from the meteorological station Bjornholen was considered (about 23 km away). Precipitation in Bjornholen summed up to 52.1 mm from 28 April 1986 to 15 May 1986 and to 1985.4 mm from 16 May 1986 to 31 December 1988. In Beito, precipitation summed up to 60.8 mm from 28 April 1986 to 15 May 1986 and to 2289.2 mm from May 1986 to 31 December 1988.

In figure 7.1, the experimentally determined distribution of Cs-134 in soil profiles from Berset are shown for three years. We assume that the activity fraction is given in Bq m^{-2} and that it is possible to recover the Bq g^{-1} dry weight (dw) by dividing this quantity by the weight of the surface layer (kg dw m^{-2}) and by the bulk soil density (g cm^{-3}). This becomes multiplied by the depth of the considered soil layer provided in Rudjord and Haugen (1989). From this analysis, the activity in dry soil ranges between 0 and 7 Bq g^{-1} dw. Figure 7.1 and figure 7.2 show that in the first years after the deposition, Cs-134 mainly stays within the surface layer (0 – 1.5 cm). In the 1988 profiles, an increased fraction of Cs-134 was found in the 0 – 1.5 cm layer. A few percent of the Cs-134 was found below 3.5 cm depth already in 1986, indicating that part of the Chernobyl caesium has been transported to deeper layers shortly after the accident.

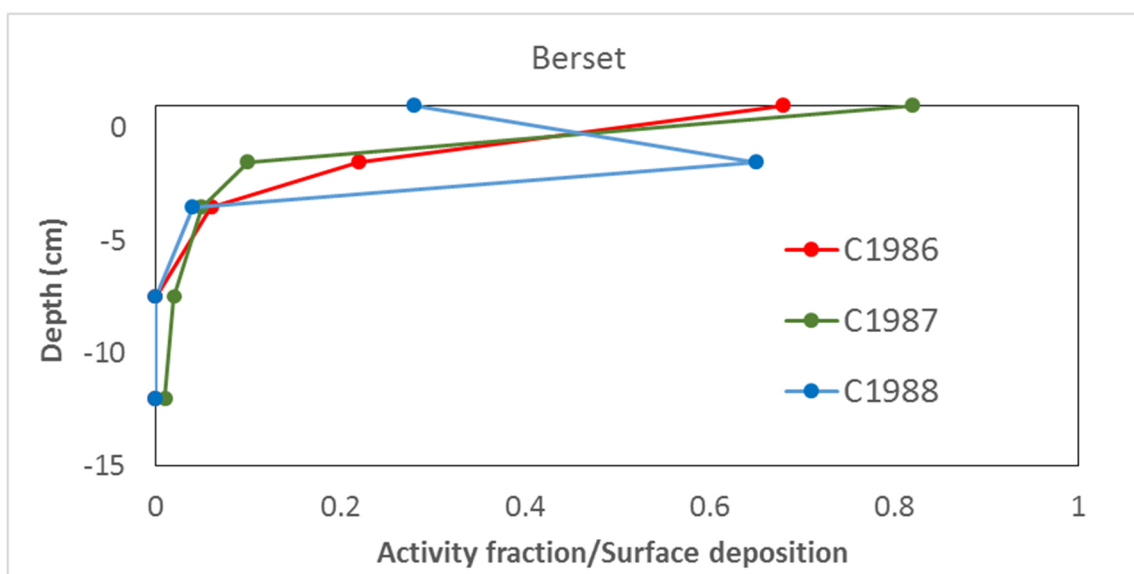


Figure 7.1: Distribution of Cs-134 normalised to surface deposition in soil profiles from Berset 1986-1988

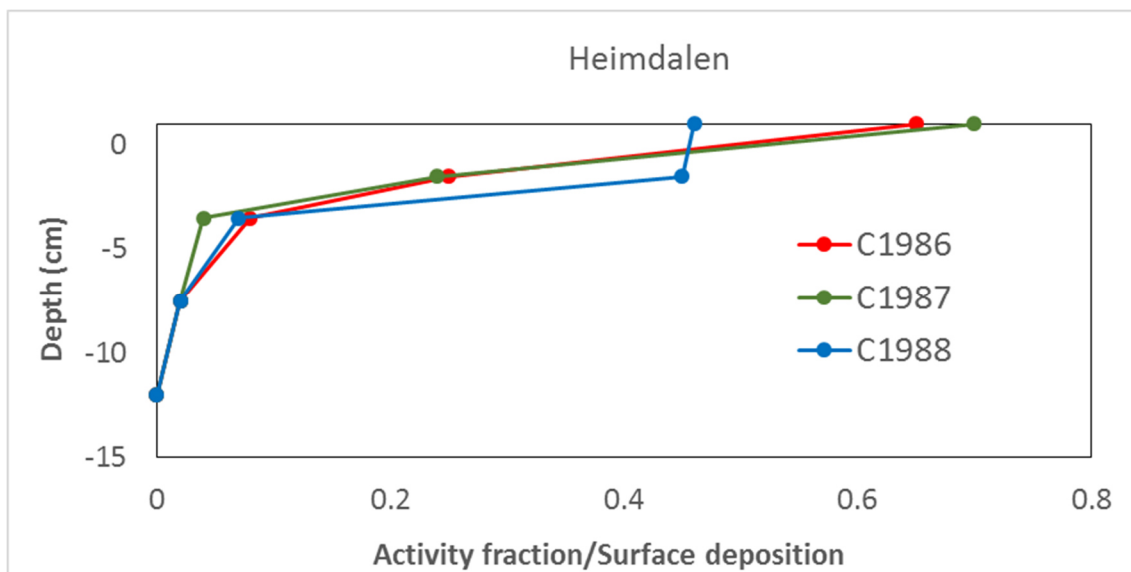


Figure 7.2: Distribution of Cs-134 normalised to surface deposition in soil profiles from Heimdalen 1986-1988

7.5 HYDRUS simulation with Norwegian data

As mentioned above, two simulations are run within HYDRUS: the first simulation for both water flow and solute transport is carried out by considering a contaminated precipitation between 28 April 1986 and 15 May 1986, $K_d = 0 \text{ cm}^3 \text{ g}^{-1}$ and no initial concentration $C(x,0) = 0$. The second simulation for both, water flow and solute transport is carried out by considering uncontaminated precipitation between 16 May 1986 and 31 December 1988, $K_d = 530 \text{ cm}^3 \text{ g}^{-1}$ and $C(x,0)$ being the output concentration profile of the first run.

Water flow calculation

The model is set up as a one-dimensional vertical 20 cm column, discretised with a 0.02 cm grid mesh with upper boundary condition being atmospheric boundary layer with surface layer and lower boundary condition being free drainage. The soil is divided into 4 layers, each characterised by specific soil density and water content, as indicated in table 7.1. For Berset, water flow is expected to be faster than for Heimdalen as the soil is classified as sandy loam and its water flow parameters are higher than for silt-loam (type of soil found in Heimdalen).

Table 7.1: Data available for soils, such as dry bulk density ρ (g cm^{-3}) and soil porosity at different soil depths for samples collected at Berset and Heimdalen

	Berset	Heimdalen
0 – 4 cm	$\theta = 0.12$	$\theta = 0.41$
4 - 15 cm	$\theta = 0.09$	$\theta = 0.12$

	Berset	Heimdalen
0 - 1.5 cm	$\rho = 0.6 \text{ g cm}^{-3}$	$\rho = 0.3 \text{ g cm}^{-3}$
1.5 - 3.5 cm	$\rho = 1.2 \text{ g cm}^{-3}$	$\rho = 0.6 \text{ g cm}^{-3}$
3.5 - 7.5 cm	$\rho = 0.9 \text{ g cm}^{-3}$	$\rho = 0.7 \text{ g cm}^{-3}$
7.5 - 12 cm	$\rho = 1.0 \text{ g cm}^{-3}$	$\rho = 1.1 \text{ g cm}^{-3}$

Solute transport calculation

In the following analysis, it has been assumed that wet deposition is the dominant mechanism for radiocaesium entering the soil and that the effect of dry deposition on the soil inventory can be ignored (Clark and Smith, 1988). The Cs-134 concentration in rainwater (Bq cm^{-3}) is then calculated as the ratio between the deposited activity (kBq m^{-2}) and the amount of rain that precipitated during the 18 days following Chernobyl accident. The contaminated rain water concentration is then obtained as follows:

$$\text{Berset} \quad \frac{6,72 \text{ kBq m}^{-2}}{60,8 \text{ l m}^{-2}} = 110.52 \frac{\text{Bq}}{\text{l}} = 0.11 \frac{\text{Bq}}{\text{cm}^3} \quad (\text{Eq. 7.7})$$

$$\text{Heimdalen} \quad \frac{64,1 \text{ kBq m}^{-2}}{52,1 \text{ l m}^{-2}} = 1230 \frac{\text{Bq}}{\text{l}} = 1.23 \frac{\text{Bq}}{\text{cm}^3} \quad (\text{Eq. 7.8})$$

The two-step approach to obtain the migration profile in soil until the end of 1988, requires two different inputs in HYDRUS; for step 1 no sorption occurs and therefore the initial concentration is specified as liquid phase concentration (shown in figure 7.3 for Heimdalen case).

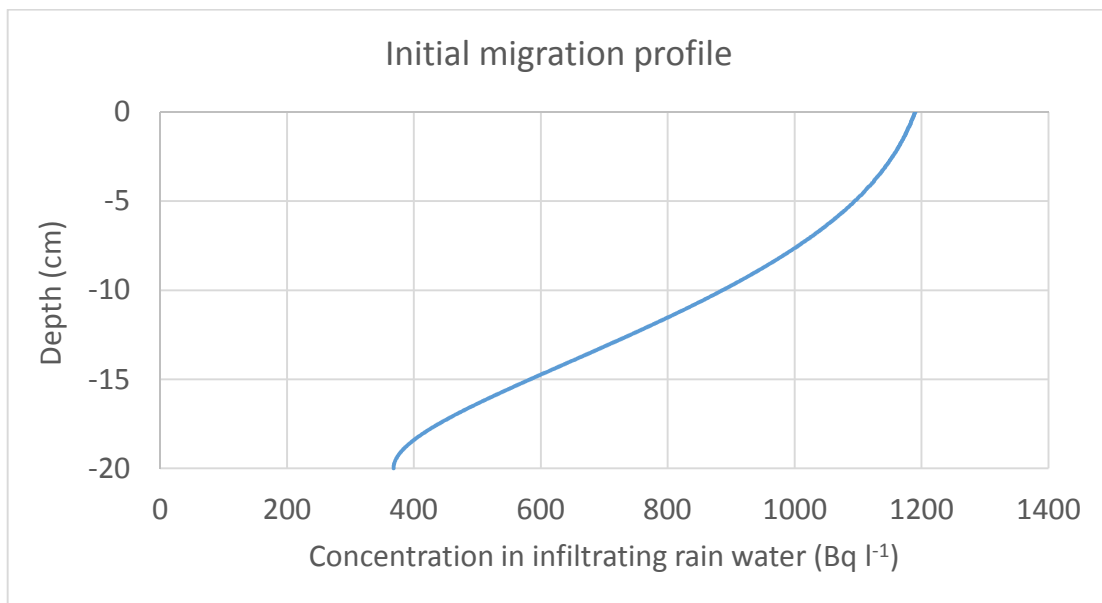


Figure 7.3: Initial migration profile of Cs-134 in Heimdalen soil for deposited activity during the 18 days deposition

On the opposite, it is necessary to consider the initial concentrations in the total solute mass in the next step, i.e. the code then redistributes this mass into both, liquid and solid phases, by using given K_d . Since no continuous profile over the soil column is available for soil density, the initial distribution of activity for both phases shows a stepwise form (figures 7.4 – 7.7). The same calculation was done for Heimdalen and Berset, by considering one single, average value of soil density and the result did not differ much from the presented one.

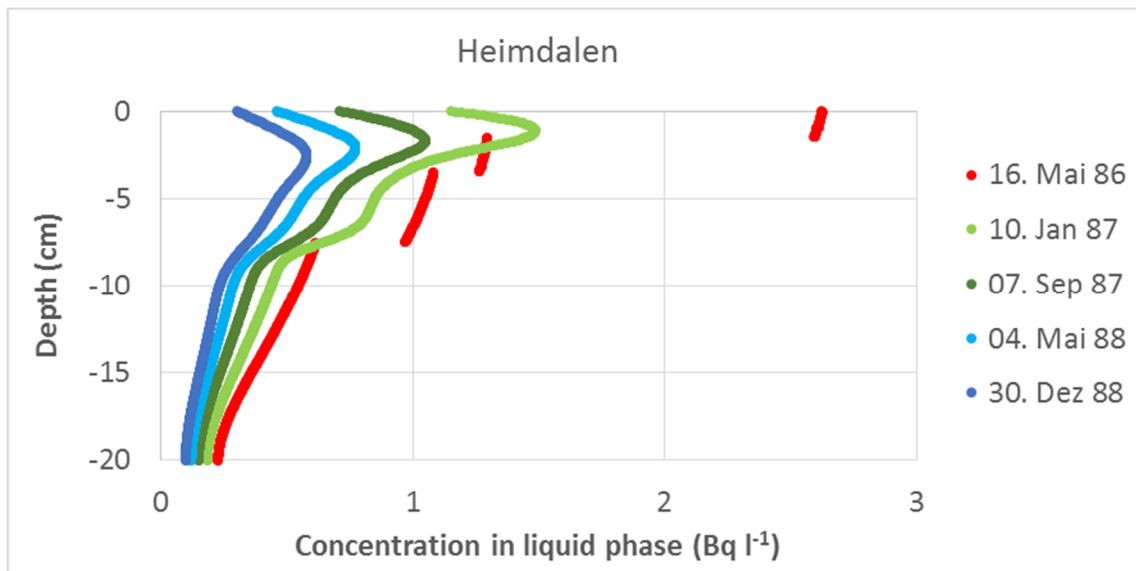


Figure 7.4: Migration profile of Cs-134 in Heimdalen soil for activity in liquid phase

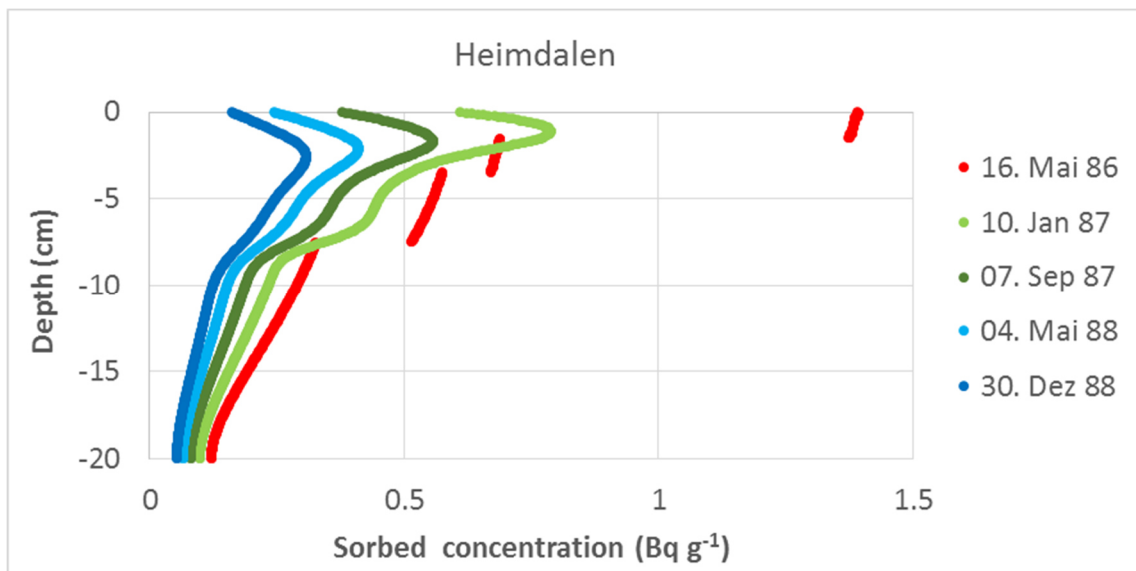


Figure 7.5: Migration profile of Cs-134 in Heimdalen soil for activity in sorbed phase

For Heimdalen, the following migration profiles are obtained for liquid and sorbed phase (figure 7.4 and 7.5). Initially, the total deposition in Heimdalen is 6.4 Bq cm^{-2} . After 18 days, about 0.1

Bq cm⁻² are lost, because of physical decay and 0.345 Bq cm⁻² are lost from the considered vertical soil profile. Hence, on the 16 May 1986, about 5.96 Bq cm⁻² remain in the soil column. After about 2.5 years (until end of 1988), 3.49 Bq cm⁻² are lost further due to physical decay and 0.03 Bq cm⁻² from the considered region. About 2.44 Bq cm⁻² stay in soil and distribute between liquid phase and sorbed phase. However, due to the relatively large K_d value assumed, almost all Cs-134 is sorbed to soil. By the end of deposition phase (from 28 April until 16 May 1986), the distribution of Cs-134 in soil is by far determined, since afterwards due to sorption mechanism, Cs-134 does not migrate as fast as in the initial phase. Furthermore, physical decay decreases considerably the amount of Cs-134 in soil.

For Berset, the following migration profiles are obtained for liquid and sorbed phase (figure 7.6 and 7.7). Initially, the total deposition in Berset is 0.67 Bq cm⁻². After 18 days, about 0.01 Bq cm⁻² are lost because of physical decay and 0.28 Bq cm⁻² flow deeper down in soil. Hence, at 16 May 1986, about 0.37 Bq cm⁻² remain in the soil column. After about 2.5 years, equal to the end of 1988, 0.22 Bq cm⁻² are lost further due to physical decay and 0.05 Bq cm⁻² flow deeper down in the soil. About 0.15 Bq cm⁻² stay in soil and distribute between liquid phase and sorbed phase. In addition, in this case, almost all Cs-134 is sorbed to soil. Berset case is characterised by much faster initial transport of activity in soil than Heimdalen: this is mainly explained by the fact that for Berset soil, classified as sandy loam, the set of hydraulic parameters imply a much faster percolation through soil than for Heimdalen case, which consists of silt loam.

The simulated profiles show some difference compared to the experimental results. The initial migration profile extends further than 20 cm, which is especially important in Berset case, where amount of precipitation and type of soil account for increased water transport through the soil depth. Next aspect is that after sorption, equilibrium establishes and the K_d is switched on in the CDE. The radionuclide migration profile modifies only slightly and most of the activity stays within the first 10 cm of soil for the whole observation period. Finally, the radioactive decay of Cs-134 and the amount of Cs-134 sorbed to soil significantly decrease the amount of Cs-134 in water phase.

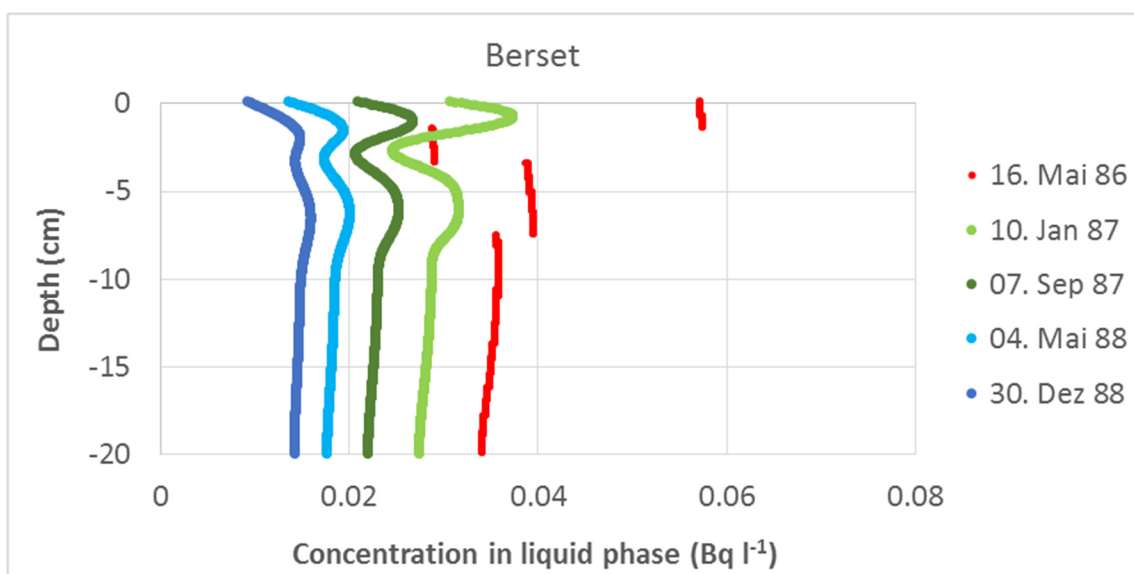


Figure 7.6: Migration profile of Cs-134 in Berset soil for activity in liquid phase

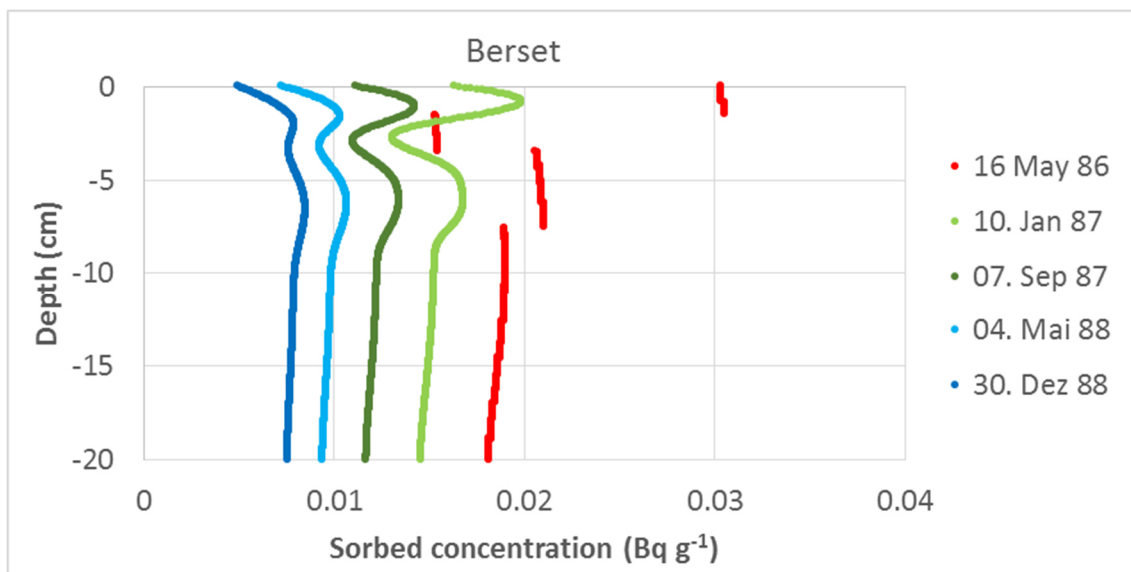


Figure 7.7: Migration profile of Cs-134 in Berset soil for activity in sorbed phase

7.6 Discussion

In this study, a new modelling approach is demonstrated for migration processes in soil for two observation sites. Measurements of contamination profiles from both sites show significant caesium concentrations at greater depths than it would be expected from dry deposition of the contaminant with subsequent migration due to long-term processes. This is because during the phase of wet deposition, the nuclides migrate through the surface layers of the soil to great depths before sorption processes start to play a significant role. The results from the model show unexpectedly large migration depths of caesium being caused by the initial infiltration phase.

The migration model has been tested for two locations and datasets available from Norway for Cs-134 following the Chernobyl plume passage. The division of the migration process into two phases is motivated by the fact that the deposition of the Chernobyl fallout was a wet deposition process enduring 18 days. During this period, sorption processes are neglected, because they occur mainly at much slower time scales. Infiltration with the contaminated rainwater is a very quick transport process with only low retention due to geochemical processes and leads to quicker migration compared to long-term migration.

The comparison between experimental and calculated data show that the predictions suggest a quicker process than observed. Possible explanations for this are the presence of snow layer during deposition, mechanical attenuation processes due to presence of vegetation on the surface layers or effects of evapotranspiration. Furthermore, changes in the migration processes from snow and effects of permafrost are not considered in the migration model. Both factors can reduce the infiltration speed and thus delay migration. Hence, further comparisons with experimental findings are needed to test the quality of this new model approach. It is worth noting that the data for precipitation values stems from meteorological stations in a distance of about 20 – 30 km from the sampling area. The meteorological stations considered are at altitudes similar to the sampling sites: 1000 m (for Bjornholen) and 700 m (for Beito) height above sea level. Precipitation values have significant impact on the results, so this imposes

considerable uncertainty. Finally important to mention, the uncertainty of the K_d value assumed for Cs-134 in this work has a large impact on the calculation. A smaller K_d value would reduce the amount of activity present within the 20 cm layer and increase the amount of activity that flow in deeper soil layers. A larger K_d , instead, would lead to an increase of the sorbed contribution and less Cs-134 activity flowing into the deeper layers of soil.

The presented study for process-oriented modelling serves as an example for addressing non-equilibrium states of a dynamic process. A prolonged wet deposition phase leads to a quick, initial infiltration of the soil without relevant retention by sorption processes. During the initial infiltration period, the equilibrium assumption for geochemical processes is not valid. Hence, the calculation of the system has to be solved by using different assumptions than in the subsequent equilibrium period. Non-equilibrium states are a very common and a fundamental challenge in radioecological modelling. By considering phases of transition and phases of equilibrium individually, simple and well-established models can be used for the description of dynamic processes.

7.7 Bibliography

Ainsworth, C. C., Pilou, J. L., Gassman, P. L. and Van Der Sluys, W. G. (1994): Cobalt, cadmium, and lead sorption to hydrous iron oxide: Residence time effect. *Soil Science Society of American Journal* 58: 1615-1623.

Alexander, M., (2000): Aging, bioavailability, and overestimate on of risk from environmental pollutants. *Environmental Science and Technology* 34: 4259-4265.

Backe, S., Bjerke, H., Rudjord, A. L. and Ugletveit, F. (1987): Fall-out pattern in Norway after the Chernobyl accident estimated from soil samples. *Radiation protection Dosimetry* 18: 105-107.

Barrow, N.J. (1986): Testing a mechanistic model: II. The effects of time and temperature on the reaction of zinc with a soil. *Journal of Soil Science* 37: 277-286.

Bossew, P. and Kirchner, G. (2004): Modelling the vertical distribution of radionuclides in soil. Part 1: the convection-dispersion equation revisited. *Journal of Environmental Radioactivity* 73: 127-150.

Bossew, P. (2013): Private Communication. 2013.

Bruemmer, G. W., Gerth, J. and Tiller, K. G. (1988): Reaction kinetics of the adsorption and desorption of nickel, zinc and cadmium by goethite: I. Adsorption and diffusion of metals. *Journal of Soil Science* 39: 37-52.

Bunzl, K. (1978): Transport and accumulation of radionuclides in the soil. A kinetic Model. 74 p. GSF-Bericht 527.

Carsel, R. F. and Parrish, R. S. (1988): Developing joint probability distributions of soil water retention characteristics. *Water Resources Research* 24: 755-769.

Clark, M. J. and Smith, F. B. (1988): Wet and dry deposition of Chernobyl releases. *Nature* 332: 245-249.

Elshamy, M. E., Mathias, S. A. and Butler, A. P. (2007): Demonstration of radionuclide transport modelling under field conditions: 50-year simulation of caesium migration in soil. *Research Report Number: Imperial/NRP_016*. Department of Civil and Environmental Engineering – Imperial College London.

Hürkamp, K., Bernauer, F., Tafelmeier, S. and Tschiersch, J. (2012): Radioökologie bei Schnee. Umweltforschungsstation Schneefernerhaus auf der Zugspitze: Wissenschaftliche Resultate 2011/2012, 33-34. Retrieved June 12, 2015, from http://www.schneefernerhaus.de/fileadmin/web_data/bilder/pdf/UFS-Broschuere_2012.pdf

IAEA (2010): Handbook of parameter values for the prediction of Radionuclide Transferradionuclide transfer in Terrestrial and freshwater environments. Technical Reports Series No. 472. International Atomic Energy Agency, Vienna, Austria.

IAEA (2005): Derivation of activity concentration values for exclusion, exemption and clearance. Safety Reports Series 44. Vienna, Austria.

Isaksson, M., and Erlandsson, B. (1995): Experimental determination of the vertical and horizontal distribution of Cs-137 in the ground. *Journal of Environmental Radioactivity* 27: 141-160.

- Kirchner, G. and Steiner, M. (2008): Uncertainties in radioecological assessment models – Their nature and approaches to reduce them. *Applied Radiation and Isotopes* 66: 1750-1753.
- Kirchner, G., Strebl, F., Bossew, P., Ehlken, S. and Gerzabek, M. H. (2009): Vertical migration of radionuclides in undisturbed grassland soils. *Journal of Environmental Radioactivity* 100: 716-720.
- Lappala, E. G., Healy, R. W. and Weeks E. P. (1993): Documentation of computer program VS2D to solve the equations of fluid flow in variably saturated porous media. USGS Open File Reports. Water Resources Investigation Report 83-4099: 1-193.
- Lövgren, L., Sjöberg, S. and Schindler, P. W. (1990): Acid/base reactions and Al(III) complexation at the surface of goethite. *Geochimica Cosmochimica Acta* 54: 1301-1306.
- Monte, L., Brittain, J. E., Hakanson, L., Smith, J. T. and van der Perk, M. (2004): Review and assessment of models for predicting the migration of radionuclides from catchments. *Journal of Environmental Radioactivity* 75: 83-103.
- Pignatello, J. J. (2000): The measurement and interpretation of sorption and desorption rates for organic compounds in soil media. In: *Advances in Agronomy*. Sparks, D. L. (Ed.), Academic Press, San Diego, 1-73.
- Poiarkov, V. A., Nazarov, A. N. and Kaletnik, N. N. (1995): Post-Chernobyl monitoring of Ukrainian forest ecosystems. *Journal of Environmental Radioactivity* 26: 259-271.
- Rudjord, A. and Haugen, L. (1989): Distribution of radiocesium in soil profiles 1986-1988, NJF-seminar 158. Deposition and transfer of radionuclides in nordic terrestrial environment 21-23 August, Beilostoelen, Norway.
- Scheidegger, A. M., Lamble, G. M. and Sparks, D. L. (1997): The kinetics of nickel sorption on pyrophyllite as monitored by x-ray absorption fine structure (XAFS) spectroscopy. *Journal Physique IV* 4. C2: 773-775.
- Scheidegger, A. M., Strawn, D. G., Lamble, G. M. and Sparks, D. L. (1998): The kinetics of mixed Ni-Al hydroxide formation on clay and aluminum oxide minerals: A time-resolved XAFS study. *Geochimica Cosmochimica Acta* 62: 2233-2245.
- Simunek, J., Sejna, M. and Van Genuchten, M. T. (1998): The HYDRUS-1D Software package for simulating the one-dimensional movement of water, heat, and multiple solutes in variably-saturated media, version 4.0, Hydrus Series 3. Department of Environmental Sciences, University of California, Riverside, CA, USA.
- SSK (1998): Freigabe von Materialien, Gebäuden und Bodenflächen mit geringfügiger Radioaktivität aus anzeige- oder genehmigungspflichtigem Umgang. Empfehlung der Strahlenschutzkommission. SSK, Heft 16. 1. Auflage, 124 pp. ISBN 3-437-21306-X.
- Sparks, D. L. (1989): Kinetics of Soil Chemical Processes. 1. Volume, 210 p. Academic Press, San Diego.
- Sparks, D. L. (2002): Environmental Soil Chemistry. 2. Volume, 352 p. Academic Press, New York.
- Strawn, D. G. and Sparks, D. L. (1999): The use of XAFS to distinguish between inner- and outer-sphere lead adsorption complexes on montmorillonite. *Journal of Colloids and Interface Science* 216, 257-269.

Tompkins, J. A. and Butler, A. P. (1996a): Documentation for the Imperial College Coupled Soil-Plant-Water Model (SPW1v5). Imperial College Internal Report.

Tompkins, J. A. and Butler, A. P. (1996b): Documentation for the Imperial College 1-D finite difference unsaturated soil solute transport model (SLT1v3). Imperial College Internal Report.

Trivedi, P., Axe, L. and Tyson, T. A. (2002): Understanding diffusion mechanisms in microporous iron oxides with x-ray absorption spectroscopy. *Abstracts of Papers of the American Chemical Society* 223: U604.

Van Genuchten, M. T. (1980): A closed-form equation for predicting the hydraulic conductivity of unsaturated soils. *Soil Science Society of American Journal* 44: 892-898.

8 A process-oriented model for C-14 uptake of C3 crops near nuclear power plants

Most modelling approaches in radioecology are based on the assumption that the entire system or specific subsystems are in an equilibrium state. This simplifies the structure of the mathematical description and reduces the number of parameters. In many cases, an equilibrium is considered even though the system is continuously transitioning between different states. Especially changes in meteorological parameters, which vary in diurnal and seasonal rhythm, cause ecological systems to never rest in an equilibrium state. In such cases, it is mandatory to investigate temporal correlations between the model variables and assess if these correlations can have an increasing effect on the contamination.

In the following section, the effects of diurnal changes in solar irradiation, temperature and light intensity on the uptake of C-14 from nuclear power plants (NPPs) by field crops are investigated. The presented approach tests the hypothesis that correlations between mixing effects in the atmosphere and photosynthetic activity due to daily changes in the intensity of solar irradiation and temperature lead to a systematic underestimation of the contamination by equilibrium approaches.

8.1 Introduction

Authorized emissions of radionuclides play an important role for licensing procedures and policymaking. One notable example is the emission of carbon 14 (C-14) by NPPs. C-14 a by-product in NPPs and is emitted in form of oxidized carbon $^{14}\text{CO}_2$ and reduced carbon, mainly as $^{14}\text{CH}_4$. $^{14}\text{CO}_2$ is taken up by crops and thus enters the food cycle. Contrarily, microorganisms in the environment eventually oxidize $^{14}\text{CH}_4$. This is a slow process and the resulting $^{14}\text{CO}_2$ is distributed in a large area in the environment and appears in very low concentrations. Therefore, the contribution of the $^{14}\text{CH}_4$ emission to the area in the proximity of the NPP is negligible.

Photosynthetic uptake of CO_2 is limited by light, carbon concentration in the close atmosphere, nutrient uptake from the soil, water supply, temperature and relative humidity. Some of these growth factors vary on an hourly to daily basis; sunlight intensity being the most obvious one. The air concentration of the contaminant changes due to different operation modes of the NPP (Aquilonius, 2004) and varying meteorological conditions. NPPs emit $^{14}\text{CO}_2$ in a height of 150 – 200 m. Prior to its assimilation by plants, the plume has to be transported to the bottom atmosphere by mixing processes. The intensity of these mixing processes determines the degree of contamination in the lower atmosphere with $^{14}\text{CO}_2$. Furthermore, the intensity of atmospheric mixing is correlated with the intensity of solar irradiation. In summary, the peak values for the contamination of the atmosphere near field crops are expected at times of the day with highest photosynthesis rates. For licensing procedures, C-14 concentrations in the crops are considered equal to the average values of $^{14}\text{CO}_2$ concentrations in the low atmospheric layers throughout the growth season. This ‘equilibrium approach’ implicitly disregards the effects of variations in photosynthetic activity of the plants and mixing processes in the atmosphere.

There exist several studies on the behaviour of C-14 in the biosphere and especially $^{14}\text{CO}_2$ uptake by field crops. Translocation of $^{14}\text{CO}_2$ within the plant to its different parts has received special attention in this context (Tani, 2011). Comparison of such a model with experimental data (Limer, 2013) shows little difference in the C-14 content for different parts of the plants. Le Dizès (2005) applies the TOCATTA model for the scenario of accidental releases of $^{14}\text{CO}_2$.

All presented models use generic growth models, which are not accounting for growth-limiting factors such as light or nutrients. Aquilonius and Hallberg (2004) present the dynamical model POM¹⁴C, implying site-specific parameters such as temperature or the length of the growing season, in order to account for the specific conditions of the crop site. For the calculation of the plant uptake, they consider varying ¹⁴CO₂ concentrations due to the operation of the NPP. However, daily variations of the concentration of the contaminant are not considered in their studies.

The influence of diurnal variations of the ¹⁴CO₂ concentrations in the ground atmosphere on the contamination of field crops is an open research question. It is the aim of this study to investigate the impact of daily variations in carbon fixation rate and C-14 concentration in the surrounding atmosphere on the resulting activity of the crop biomass. For this purpose, a photosynthesis model accounting for multiple growth-limiting factors in combination with a particle dispersion model (ARTM) is used to estimate the uptake from ¹⁴CO₂ due to photosynthesis by field crops in the proximity of a NPP. Real weather and emission data for a NPP in northern Germany of 2005 has been used in order to compare the prediction of contamination by the proposed model with the one estimated by a static equilibrium approach.

8.2 *Material and Methods*

Regarding crop plants in Germany, two basic types using different photosynthetic mechanisms can be found: C3 plants and C4 plants. Wheat, oat, rye and sugar beets are C3 plants. Corn and millet are C4 plants. Thus, C3 Plants play the most important role in German agricultural production. C3 plants assimilate CO₂ synchronously to electron transfer, which is triggered by sunlight. Therefore, the effects of the considered correlations between environmental factors should be expressed more strongly than for C4 plants.

Common wheat (*Triticum aestivum*) is one of the most important agricultural crop plants for food production in Germany and has been chosen as an example for this study. We use a C3 plant growth model, which has been presented by Farquhar et al. (1980), accounting for limitation by light, atmospheric CO₂ and phosphorus. We further choose a parameterization for *Triticum aestivum* as it has been presented by Alonso et al. (2009). The proposed model has a mechanistic structure; all equations mathematically describe physiological processes. In the following paragraphs, these physiological processes and the corresponding equations are presented.

8.2.1 Model formulation

In the model for carbon uptake by plants, we consider that environmental influence changes at an hourly to daily time scale due to changes in sunlight intensity and air temperature. The chosen biological model to describe the influence of these factors on the photosynthetic activity, has a relatively complex structure and depends on many parameters, which describe various physiological processes. The model seemingly has a high complexity for describing a static relationship between carbon uptake and two environmental parameters. However, its specific structure, the fact that the physiological parameters can be estimated in lab experiments and the requirement of providing a generic approach for all C3 plants, justifies this choice.

Carbon fixation is limited by light irradiation, disposable CO₂ or inorganic phosphate. Wullschleger (1993) proposed a modified version of the model by Farquhar et al. (1980, 1979) for carbon fixation in variously limiting conditions. For the assimilation of CO₂ they suggest:

$$A = \left(1 - \frac{\Gamma}{C_i}\right) \cdot \min\{W_c, W_j, W_p\} - R_d \quad (\text{Eq. 8.1})$$

Where A (μmol/(m²s)) is CO₂ assimilation, C_i (μmol/mol) the intercellular partial pressure of CO₂, Γ (μmol/mol) is the CO₂ compensation point in the absence of dark respiration and R_d (μmol CO₂ m⁻²s⁻¹) the dark respiration rate. The first factor in this term describes the losses through photorespiration. The factor increases with available CO₂ and is bound within the interval [0 ... 1]. This corresponds well with the understanding of oxygenation and carboxylation as concurrent processes. W_c, W_j and W_p are the maximum rate functions for the limiting factors C_i, electron transport *j* and phosphor p. As Wullschleger (1993) has reported, no phosphor limitation for wheat plants, only W_c and W_j are considered. The W- functions are increasing functions with the respective growth factors. In coherence to Liebig's law of the minimum, the function with the smallest value is considered as the limiting growth factor. According to Farquhar et al. (1980), W_c can be formulated as:

$$W_c = \left(\frac{V_{cmax}C_i}{C_i + K_c \left(1 + \frac{O}{K_o}\right)}\right) \quad (\text{Eq. 8.2})$$

V_{cmax} (μmol CO₂/(m²s)) is the maximum carbon assimilation rate, while K_c (μmol/mol) and K_o(mmol/mol) are Michaelis-Menten constants for carboxylation and oxygenation. This function describes limitation of growth by available intercellular CO₂. It is formulated as a Michaelis-Menten function that saturates at the value V_{cmax}. It describes the condition, where carbon fixation is limited by the maximum carboxylation rate of the RuBisCo, which implies abundance of ADP and NADPH. Consequently, this function is only limiting, if the light irradiation provides more electrons than necessary for the fixation of available CO₂. Oxygenation of RuBisCo reduces the possible carboxylation rate. This function is therefore decreasing with the atmospheric partial pressure of oxygen *O*. The function W_j describing the limitation by light can be formulated as (Alonso et al. 2009):

$$W_j = \frac{J \cdot C_i}{4.5C_i + 10.5\Gamma} \quad (\text{Eq. 8.3})$$

J (μmol/(m²s)) is the electron transport rate that can be modelled as a function of light intensity I (μmol/(m²s)), according to von Caemmerer (2009) and Alonso et al. (2009):

$$J = \frac{(Q_2 + J_{max}) - \sqrt{(Q_2 + J_{max})^2 - 4\theta Q_2 J_{max}}}{2\theta} \quad (\text{Eq. 8.4})$$

Where θ (-) is the curvature of the light response curve and J_{max} (μmol/(m²s)) the maximum rate of electron transport. Q₂ (μmol/(m²s)) is “photosynthetically effective light”, which is calculated as:

$$Q_2 = \frac{I \cdot abs \cdot (1-f)}{2} \quad (\text{Eq. 8.5})$$

abs (-) is the absorbance of the leaves and *f* (-) a correction factor for the spectral quality of light.

Temperature dependency

For the temperature dependency of the model parameters, we use a special form of the Arrhenius function describing chemical reaction kinetics:

$$k(T) = k_{25} \cdot \exp\left(\frac{E(T-298K)}{R \cdot 298K \cdot T}\right) \quad (\text{Eq. 8.6})$$

Whereas k_{25} is the parameter value at 25°C, E (J/mol) the activation energy and R the molar gas constant (8.314 J/ (mol K)).

Stomatal conductance

A relation for the intercellular CO₂ partial pressure was proposed by Ball et al. (1987). This is a simple formulation for the dependency of stomatal conductance to photosynthetic productivity, relative humidity of the atmosphere and CO₂ content of the surrounding atmosphere. It has been used extensively in many studies. Even though this formulation is simple and empirical, Damour et al. (2010) denominate it a ‘Very practical and accurate prediction of g_s under variable environment’ in their very extensive review of models for stomatal conductance.

$$C_i = C_a - \left(\frac{A \cdot 1.6}{g_s(A, RH, C_a)}\right) \quad (\text{Eq. 8.7})$$

Apart from the external CO₂ partial pressure C_a ($\mu\text{mol}/(\text{m}^2\text{s})$), this expression is dependent on the carbon assimilation A ($\mu\text{mol}/(\text{m}^2\text{s})$) and the stomatal conductance g_s ($\text{mmol}/(\text{m}^2\text{s})$). The stomatal conductance is a measure for the permeability of the openings, connecting the intercellular space with the outer atmosphere. This formulation accounts for the differences in intercellular partial pressure of CO₂ due to carbon fixation or respiration (A). The kinetics of the exchange of CO₂ from outside the leaf is dependent on the stomatal conductance g_s , defined by the expression:

$$g_s = g_0 + g_l \cdot A \cdot \left(\frac{RH}{C_a}\right) \quad (\text{Eq. 8.8})$$

g_0 ($\text{mmol m}^{-2} \text{s}^{-1}$) is the parameter for the minimal conductance and g_l (-) is an empirical coefficient, representing the composite sensitivity of conductance to assimilation. RH ($\in[0 \dots 1]$) represents the relative humidity of the air outside the leaf. According to this function, the stomatal conductance is adapted by the plant in order to control CO₂ influx and water loss due to transpiration from the intercellular space. The stoma permeability is physiologically adapted to the carbon demand due to fixation (A), relative humidity (RH) and available atmospheric CO₂.

C_i and A are not independent. Accordingly, both of the values have to be determined in a numerical way. C_i can be obtained by finding the root of the function

$$f(C_i) = C_a - \left(\frac{A(C_i) \cdot 1.6}{g_s(A(C_i), RH, C_a)}\right) - C_i \quad (\text{Eq. 8.9})$$

numerically within the domain [1e-12 ... 1000].

8.2.2 Environmental conditions

In order to assess ^{14}C assimilation by crop plants at the NPP site, time series for different environmental conditions have been utilized:

- Solar irradiation intensity
- Air temperature
- Relative humidity of the atmosphere

Data for the solar irradiation intensity has been taken from satellite image estimations from the SOLEMI (WDC-RSAT) service. In the data, the solar irradiation power is given in Ws . For the determination of the rate of available physiologically active photons from the total power of radiation, it must be considered that only about 43 % of the irradiation power is in the physiologically active interval of wavelengths [400 nm ... 700 nm] (Liou, 2002). Further, the conversion factor for sunlight to photosynthetically active radiation of $4.6 \mu\text{mol} / \text{Ws}$ (LICOR) is applied. From these considerations, the following conversion from sun light irradiation power to photosynthetically relevant photon flux is derived:

$$I_{sun} = P_{sun} \cdot 1.978 \frac{\mu\text{mol}}{\text{Ws}} \quad (\text{Eq. 8.10})$$

For air temperature and relative humidity, we take data from the German Meteorological Service (Deutscher Wetterdienst, DWD). We use data from the nearest meteorological station, which is located in Muenster. The time series of all meteorological data has a resolution of one measurement per hour.

Table 8.1: Parameters for the model of Harley (1992) for *Triticum aestivum*. In accordance with Alonso et al. (2009), the data comprise the absolute value for 25°C (k_{25}) and the activation energy E

Parameter	k_{25}	E	Unit	Reference
J_{max}	240.4	23.1	$\frac{\mu \text{ mol}}{\text{m}^2 \text{ s}}$	Alonso et al. (2009)
Γ	31.8	22.1	$\mu\text{mol}/\text{mol}$	Alonso et al. (2009)
θ	0.88		–	Alonso et al. (2009)
V_{cmax}	88.3	55.3	$\frac{\mu \text{ mol}}{\text{m}^2 \text{ s}}$	Alonso et al. (2009)
K_c	272.38	80.99	$\mu\text{mol}/\text{mol}$	Alonso et al. (2009)
K_o	165.82	23.72	mmol/mol	Alonso et al. (2009)
R_d	0.40	108	$\frac{\mu \text{ mol}}{\text{m}^2 \text{ s}}$	Alonso et al. (2009)
g_o	30.0		$\text{mmol}/(\text{m}^2 \text{ s})$	Müller et al. (2005)
g_l	9.585			Müller et al. (2005)
abs	0.8		–	Alonso et al. (2009)

Parameter	k25	E	Unit	Reference
f	0.25		–	Alonso et al. (2009)
C_a	370		$\mu\text{mol}/\text{mol}$	
O	209.6		mmol/mol	

8.2.3 Parameterisation

In this study, we use a parameter set for flag leaves of *Triticum aestivum* provided by Alonso et al. (2009). The authors measured gas exchange of such leaves in varying temperature, carbon dioxide concentration in the atmosphere and light irradiation. From the experimental data, they fit the model of Harley and chose the Arrhenius function as sub-model for the temperature dependence of the parameters $R_d, K_c, K_o, J_{max}, V_{c_{max}}, \Gamma$. For K_c and K_o , they fixed the parameters E and k_{25} for the Arrhenius equation, as proposed by Bernacchi et al. (2002). The Arrhenius parameters for $R_d, J_{max}, V_{c_{max}}$ were estimated by fitting the experimental data in the temperature range [15°C ... 35°C] with an ambient CO₂ concentration of 370 $\mu\text{mol}/\text{mol}$. Temporary changes in the atmospheric CO₂ concentration are accounted by the variable C_a in the model. Long-term changes of the CO₂ concentration can trigger acclimation processes, which can lead to a changed physiological behavior (Alonso et al., 2009). For this study, C_a is fixed to 370 $\mu\text{mol}/\text{mol}$. Thus, such acclimation processes are neglected. The parameters for the Arrhenius functions of $R_d, K_c, K_o, J_{max}, V_{c_{max}}, \Gamma$, as they are proposed by Alonso et al. (2009), are presented in table 8.1. Parameters g_0 and g_1 for the stomatal conductance model are taken from Müller et al. (2005).

8.2.4 Atmospheric dispersion model

For the estimation of the time dependent contamination of the atmosphere with ¹⁴CO₂ close to the plants, a Lagrangian particle dispersion model (ARTM) is used. In the model, time dependent meteorological parameters such as wind speed, direction and stability class are considered in order to predict dispersion of the radionuclides. The orographic features of the terrain in the proximity of the emission site and the time dependent emission are site-specific characteristics necessary for the calculation. From the result of the calculation, the air contamination in Bq/m^3 at the plant, the isotope ratio of the atmosphere $R = {}^{14}\text{C}_{atm}/{}^{12}\text{C}_{atm}$ is calculated.

8.2.5 Modelling of C-14 uptake

Based on the presented carbon uptake model, a model for the temporal evolution of C-14 in the plant biomass in dependency of the concentration of C-14 in the surrounding atmosphere can be derived. For this model, we are following these assumptions:

- There are no discrimination effects between the isotopes by the plant.
- There are two compartments (S_{nat}, S_{em}) with infinite size, one for natural carbon isotopes and one for C-14 from the NPP emission. The plant itself is considered homogeneous, translocation effects are neglected.
- All the fixed carbon is stored in the respective compartment. There is no temporal evolution of the plant physiology and plant age has no impact on carbon uptake.
- The partial pressure of CO₂ and O₂ in the surrounding atmosphere is constant.

These assumptions motivate the formulation of the C-14 model as a two variable system of differential equations.

$$S_{nat} \cdot = \begin{cases} A(I(t), T(t), \dots) \cdot (1 - R) & \text{if } A(I(t)) > 0 \\ A(I(t), T(t), \dots) \cdot (1 - R_p) & \text{if } A(I(t)) \leq 0 \end{cases} \quad (\text{Eq. 8.11})$$

$$S_{em} \cdot = \begin{cases} A(I(t), T(t), \dots) \cdot R & \text{if } A(I(t)) > 0 \\ A(I(t), T(t), \dots) \cdot R_p & \text{if } A(I(t)) \leq 0 \end{cases} \quad (\text{Eq. 8.12})$$

In this formulation S_{nat} ($\mu\text{mol}/\text{m}^2$) represents the pool of natural Carbon taken up by the plants, and S_{em} ($\mu\text{mol}/\text{m}^2$) represents the amount of C-14 stemming from the emissions from the NPP which has been taken up. The piecewise definition is necessary, because we assume that the carbon taken up in growth phases has the isotope distribution in the atmosphere of $(1 - R) : R$, while the respired carbon has the isotope distribution in the plant compartment $(1 - R_p) : R_p$ with $R_p = S_{em}/(S_{nat} + S_{em})$.

8.3 Results

In the proposed model, biomass growth is represented by the carbon uptake, and thus by the model variable S_{nat} . For the calculation of the concentration of emitted S_{em} incorporated into the plant biomass, the isotope ratio of R_p is used. In figure 8.1, the time-dependent variations of the local ¹⁴C concentration within the plant and the carbon uptake according to the dynamical photosynthesis model for a sunny day in summer are presented. In this example, the dynamics of atmospheric mixing make the plume pass the location of the plant in the timeframe between 08:00 and 20:00. Carbon uptake due to photosynthetic activity occurs between 05:00 and 19:00. The observations are in accordance with the hypothesis that there is a correlation between photosynthetic activity and C-14 concentration.

Figure 8.3 shows the evolution of the predicted value by the dynamic and the equilibrium approach throughout the growth season of 2005. It can be observed that both approaches differ in their prediction from the summer months onwards by a significant factor. For comparison, the final values of the prediction should be considered. While the equilibrium approach predicts a value of $8.1 \cdot 10^{-16}$ for the final isotope ratio, the dynamic approach predicts $1.5 \cdot 10^{-15}$. Throughout the growth season of the year 2005, the equilibrium approach underestimates the contamination from the emission of C-14 by 85 %.

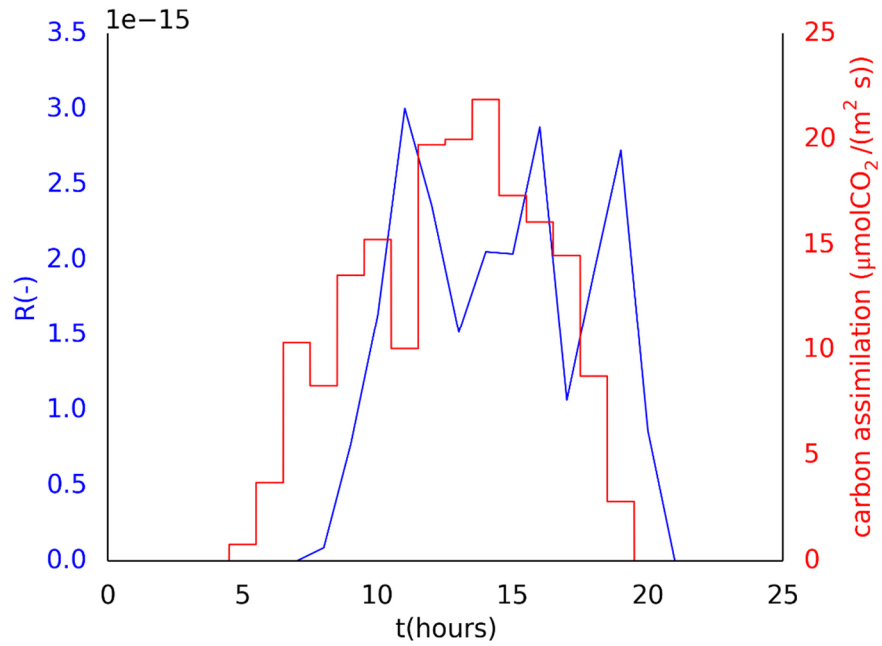


Figure 8.1: Evolution of the carbon isotope ratio in the bottom atmosphere according to ARTM (blue) and the carbon assimilation of the plant (red) throughout one day in summer (10th August 2005)

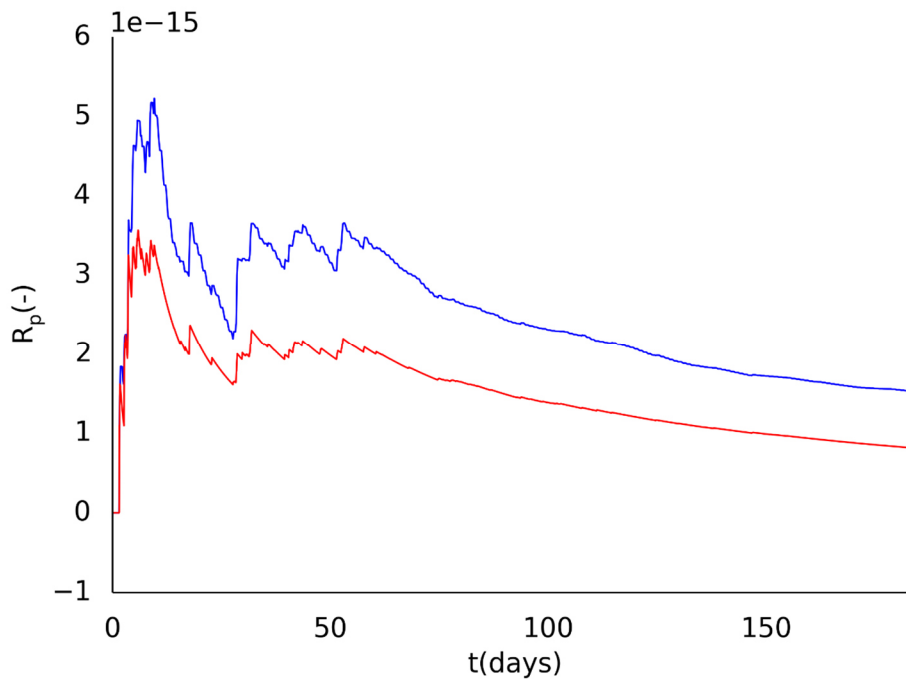


Figure 8.3: Evolution of the carbon isotope ratio in the plant, according to the proposed approach considering a varying uptake rate and contamination (blue) and the equilibrium approach (red) throughout the growth season of 2005

8.4 Parameters influencing the content of C-14 in *Triticum aestivum*

For the sensitivity analysis, the ratio $R_p = S_{em}/(S_{nat} + S_{em})$, resulting from integration of the dynamical model over the full year 2005, was taken as a measure. The calculation has been executed for variations of 10 % and 50 % of the original parameter values from their standard value (cf. Table 1). From the partial derivative, in respect to the parameter x , the relative sensitivity for this parameter has been calculated:

$$Sens(x) = \left. \frac{\partial R_p}{\partial x} \right|_{x=x_0} \cdot \frac{x_0}{R_p(x_0)} \quad (\text{Eq. 8.13})$$

Where x_0 is the default value for the respective parameter x . The results of the sensitivity analysis are presented in Table 8.2. No parameter has an absolute relative sensitivity exceeding 0.1. This means that variation of any parameter in the model by 10 %, changes the prediction value by less than 1 %. This proves that for the conditions of the exemplary data set, the model is very robust against parameter uncertainties. It could be argued, if parameters with very low sensitivity can be removed by simplifications of the model.

The estimated sensitivities are strictly linked to the time series for meteorological data and $^{14}\text{CO}_2$ emission. While the presented values indicate a possible over parameterisation of the model, it is not guaranteed that the sensitivities are equally low for other data sets. In Table 8.2, also the standard deviations for the model parameters are presented, as they are given by Alonso et al. (2009). These error values reflect the parameter uncertainty resulting from the data set and the fitting procedure. For some of the parameters this uncertainty is not defined, as they were used as a fixed literature value in the fitting procedure. The parameter uncertainty of the fit is thus represented in the error values for the remaining parameters.

Table 8.2: Relative sensitivities for all model parameters calculated by variation of 10 % and 50 %

Parameter	Value	Error	10%	50%
$J_{\max}(25)$	240.4	5	-0.031	0.030
$J_{\max}(E)$	23.1	9	0.0056	-0.0011
$V_{c\max}(25)$	88.3	1.1	0.093	0.073
$V_{c\max}(E)$	55.3	2.5	-0.023	-0.084
$R_d(25)$	0.4	0.11	0.020	7.7E-4
$R_d(E)$	108	23	-0.020	0.016
$K_c(25)$	272.38	n.d.	-0.085	-0.029
$K_c(E)$	80.99	n.d.	0.071	0.051
$K_o(25)$	165.82	n.d.	0.051	0.046
$K_o(E)$	23.72	n.d.	0.0019	0.0011
$\Gamma(25)$	31.8	0.5	-0.013	0.022

Parameter	Value	Error	10%	50%
$\Gamma(E)$	22.1	1.7	0.0018	0.0048
C_a	370	n.d.	0.097	0.042
O_a	209.602	n.d.	-0.057	-0.036
g_0	30.0	n.d.	0.037	0.0093
g_I	9.59	n.d.	0.033	0.027

8.5 Discussion

In the presented study, we could show that the correlation between the $^{14}\text{CO}_2$ contamination in the bottom atmosphere and the photosynthetic activity leads to an elevated amount of C-14 in the plants. The dynamic model predicts an assimilation rate of $^{14}\text{CO}_2$ that is 85% higher than the prediction of the equilibrium model. This result is based on real meteorological and emission data for a NPP in Northern Germany from the year 2005. Based on this data, a sensitivity analysis for all parameters of the plant model has been carried out. The parameters for the plant model proved to be highly insensitive. It can be concluded that the model is very robust and that uncertainties in the biological parameters increase the uncertainty of the prediction only marginally. However, among different species of C3 plants, these parameters may vary considerably and different site-specific conditions may lead to different results of the calculations. Therefore, the quantitative effect from daily variations in contaminant concentrations near the plant and photosynthetic activity may vary from site to site.

An important conclusion can be drawn: The average $^{14}\text{CO}_2$ content of the surrounding air is not a realistic or conservative estimation of the C-14 concentration in the plants. Depending on the changes in C-14 in the atmosphere and the variation in carbon uptake rate, the concentration in plants can differ dramatically from the long-term average in the atmosphere. For licensing procedures, the location in the surrounding with the highest contamination resulting from the emission source is selected and the concentration is determined. With the proposed approach, it is possible that not only the predicted degree of contamination is higher but also that the area with the highest contamination is located differently.

In the presented approach, variations in the growth rate of plants and atmospheric mixing have been considered, underlying a daily periodicity. However, there are some effects, which are difficult to quantify and which have not been taken into account. In different meteorological conditions, the spectral distribution and the angle of incidence from sunlight changes significantly. From a mechanistic perspective, this necessarily has an effect on photosynthesis: The spectral distribution directly changes the amount of photosynthetically effective photons, while the absorption characteristics of the plant pigments and therefore the physiological effects of photons with different wavelength vary. However, neither the level of detail of the dynamic biological models, nor the information in the meteorological data allows for accounting such effects.

Another effect, which might play a role but is difficult to assess, are variations in partial pressure of natural CO_2 due to degradation of organic compounds in the soil, the photosynthetic uptake due to the plants and varying exchange between the atmosphere close to the plant and the surrounding. Varying CO_2 partial pressure affects not only the carbon fixation rate but also the

isotopic composition in the atmosphere close to the soil. Modelling the influence of this important environmental parameter on the C-14 content in plant biomass is an important step towards a better understanding of the process.

The presented approach shows that C-14 contamination of field crops from NPP emission is an example for a process which cannot be described conservatively by an equilibrium approach. The influence of the dynamical processes following a diurnal cycle can be quantified to be 85% of the equilibrium value. With further research using data for different locations and contamination situations, it seems possible to estimate an upper limit for this effect and therefore improve the equilibrium approach by a correction factor accounting this. The result would be a model as simple as the equilibrium approach guaranteeing a conservative estimate.

From this example, a more general conclusion can be drawn: Whenever an equilibrium approach is applied, special care should be taken regarding neglected dynamic processes in the system. Correlations in dynamic model properties can lead to underestimation by the equilibrium approach and should therefore be considered by suitable methods.

8.6 Bibliography

- Alonso, A., Pérez, P., & Martínez-Carrasco, R. (2009). Growth in elevated CO₂ enhances temperature response of photosynthesis in wheat. *Physiologia plantarum*, 135(2): 109-120.
- Aquilonius, K., & Hallberg, B. (2005). Process-oriented dose assessment model for ¹⁴C due to releases during normal operation of a nuclear power plant. *Journal of environmental radioactivity*, 82(3): 267-283.
- Ball, J. T., Woodrow, I. E., & Berry, J. A. (1987). A model predicting stomatal conductance and its contribution to the control of photosynthesis under different environmental conditions. *Progress in photosynthesis research*: 221-224.
- Damour, G., Simonneau, T., Cochard, H., & Urban, L. (2010). An overview of models of stomatal conductance at the leaf level. *Plant, Cell & Environment*, 33(9): 1419-1438.
- Le Dizès (2005). Modelling chronic and accidental releases of carbon 14 to the environment. *Radioprotection*, 40(S1): 771-777.
- Farquhar, G. D., von Caemmerer, S. V., & Berry, J. A. (1980). A biochemical model of photosynthetic CO₂ assimilation in leaves of C₃ species. *Planta*, 149(1): 78-90.
- Gross, L. J., Kirschbaum, M. U. F., & Pearcy, R. W. (1991). A dynamic model of photosynthesis in varying light taking account of stomatal conductance, C₃-cycle intermediates, photorespiration and Rubisco activation. *Plant, Cell & Environment*, 14(9): 881-893.
- WDC-RSAT. ICSU World Data Center for Remote Sensing of the Atmosphere, URL: <https://wdc.dlr.de/>
- Limer, L., Klos, R., Walke, R., Shaw, G., Nordén, M., & Xu, S. (2013). Soil-Plant-Atmosphere Modeling in the Context of Releases of ¹⁴C as a Consequence of Nuclear Activities. *Radiocarbon*, 55(2-3): 804-813.
- Müller, J., Wernecke, P., & Diepenbrock, W. (2005). LEAFC3-N: a nitrogen-sensitive extension of the CO₂ and H₂O gas exchange model LEAFC3 parameterised and tested for winter wheat (*Triticum aestivum* L.). *Ecological Modelling*, 183(2): 183-210.
- LI-COR, Principles of radiation measurement, URL: http://www.licor.com/env/pdf/light/Rad_Meas.pdf, Accessed at: 29.7.2015
- Liou, K. N. (2002). *An introduction to atmospheric radiation* (Vol. 84). Academic press.
- Tani, T., Arai, R., Susumu Nozoe, Yasuhiro Tako, Tomoyuki Takahashi, Yuji Nakamura, Development of a dynamic transfer model of ¹⁴C from the atmosphere to rice plants, *Journal of Environmental Radioactivity*, 102(4): 340-347
- Wullschleger, S. D. (1993). Biochemical limitations to carbon assimilation in C₃ plants—a retrospective analysis of the A/Ci curves from 109 species. *Journal of Experimental Botany*, 44(5): 907-920.

9 Contamination of wild boar meat

9.1 Introduction

Even three decades after the Chernobyl accident, radiocaesium contamination of wild boar (*Sus scrofa*) still achieves more than 10,000 Bq kg⁻¹ fresh weight (fw) in some parts of Europe, concurrently exhibiting an extraordinary variability. Whereas radiocaesium levels of roe deer (*Capreolus capreolus*) and red deer (*Cervus elaphus*), apart from seasonal variations, are continuously decreasing, those of wild boar are either remaining fairly constant or even increasing. The reasons for the peculiar contamination pattern of wild boar have intensively been investigated (e.g. Hohmann and Huckschlag, 2005; Steiner and Fielitz, 2009). The authors conclude that the irregular uptake of highly contaminated deer truffles (*Elaphomyces granulatus*), a ‘treat’ for these animals, in conjunction with the short biological half-life of Cs-137 in wild boar is the dominant factor for the observed contamination pattern.

The Cs-137 contamination of wild boar is often quantified by using an aggregated transfer factor that relates the activity levels in these animals (Bq kg⁻¹ fw) to the total inventory in soil (Bq m⁻²). Aggregated transfer factors are empirical parameters to describe the transfer from soil to animal in a simplified way (see section 4.1.5). They are inappropriate to describe time-dependent processes, such as the varying composition of the food spectrum and the irregular uptake of specific food items. In addition, they do not provide information about the variability of the contamination levels of wild boar.

Within a research project initiated by the German Federal Office for Radiation Protection, Fielitz (2005) developed a radioecological model to predict the time-dependent Cs-137 contamination of wild boar and its variability. The variability of the model parameters were accounted for by attributing probability density functions to each model parameter. This model was used to predict the time-dependent Cs-137 contamination of wild boar in Germany based on factors that have been identified to determine the contamination levels of wild boar, e.g. the occurrence of deer truffles, the size and structure of forests (Fielitz and Richter, 2012). The model requires an empirical transfer factor from food to meat. The transfer factor was derived by fitting the model predictions to the measured activity levels of wild boars (Fielitz, 2005).

Barthel and Thierfeldt (2012) stress that the application of a probabilistic approach to model a process that is intrinsically of stochastic nature can be misleading. The following section presents a radioecological model that aims at predicting the Cs-137 contamination of wild boar from first principles. It provides an adequate stochastic description of the irregular uptake of deer truffles by modelling it as a time-discrete stochastic process.

9.2 Basic information about wild boars

Wild boars (figure 9.1) take up radiocaesium via their food. They are omnivores with a high potential to adapt to locally and seasonally varying food supplies. The reproductive period is usually October/November. In this period, wild boars are capable of fasting for several weeks. In Middle Europe, the body mass ranges typically between 50 and 90 kg for female and between 60 and 180 kg for male adult animals.



Figure 9.1: Wild boar (*Sus scrofa*). Photo credit: Ulrich Fielitz

9.2.1 Contamination levels of wild boar

In Germany, several studies on the Cs-137 contamination of wild boar meat were carried out in the past (Fielitz, 2005; Hohmann and Huckschlag, 2005; Semizhon et al., 2009). The authors analysed the activity levels of wild boar meat in Rhineland-Palatinate, Bavaria and Baden-Württemberg, respectively. Strebl and Tataruch (2007) measured the concentration of Cs-137 in wild boar meat in Austria. The results from the mentioned authors are summarized in Table 9.1. Data sets often reveal a large variability of Cs-137 concentrations in wild boar meat. Data from the Bavarian Forest are shown in figure 9.2 (Fielitz, 2005). The activity levels ranged from 80 Bq kg⁻¹ fw to 40,000 Bq kg⁻¹ fw. The data sets have a comparable average value and can be well described by a lognormal distribution.

Table 9.1: Cs-137 concentration in wild boar meat in Germany and Austria

Location and sampling date	Inventory (Bq m ⁻²)	Cs-137 contamination of meat (Bq kg ⁻¹ fw)
Rhineland-Palatinate 2001-2003 (2433 wild boars; 45,400 ha)	Min-max: 10,500-39,000	Median values in the range 200-600
Bavaria (Bavarian Forest) 1987-2004 (232 wild boars; 40,000 ha)	Average: 54,000	Min-max: 80-40,000
Baden-Württemberg 1998-2008 (656 wild boars; 7 ha)	Min-max: 10,000-50,000	Min-max: 1-10,000
Austria 1986-2003 Weinsberger Forest (218 wild boars; 6500 ha) Kobernausser Forest (20 wild boars; 15,000 ha)	Min-max: 17,900-103,900 Min-max: 8000-105,500	Min-max: 200-3000 Min-max: 1000-6000

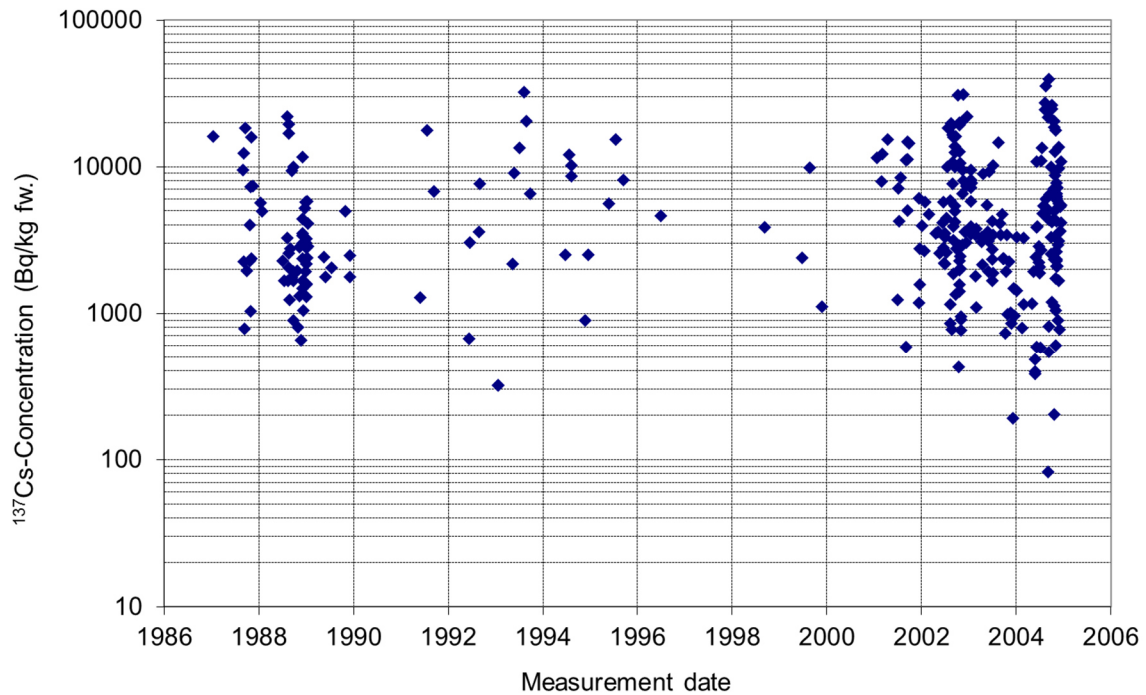


Figure 9.2: Cs-137 concentration (Bq kg⁻¹ fw) in wild boar meat in the Bavarian Forest between 1987 and 2005 (Fielitz, 2005)

9.2.2 Food of wild boar

Wild boars are omnivores with a broad food spectrum. Fielitz (2005) collected 102 stomachs between May 2002 and August 2004 and analysed their content. In about one third (32 stomachs), agricultural products originating from supplementary feed and bait, such as maize and fodder beet, accounted for more than 95% of the stomach content. Obviously, these animals were fed just before being shot and were excluded from further consideration being unrepresentative. The diet composition as deduced from the analyses of the remaining 70 stomachs is depicted in figure 9.3. The total quantity of food taken up per day was estimated to be 1.8 kg d⁻¹ (Fielitz, 2005).

Deer truffles (*Elaphomyces granulatus*; figure 9.4) have turned out to play a key role for the Cs-137 uptake because of their exceptionally high contamination levels ranging between 25,000 and 122,000 Bq kg⁻¹ fw. Despite their low weight proportion of an average of only about 6 % of the stomach content, more than three quarters of the radiocaesium intake could be ascribed to this fungus. Soil contributed about 13 % and all other food items together less than 12 % to the ¹³⁷Cs intake of wild boar (average values).

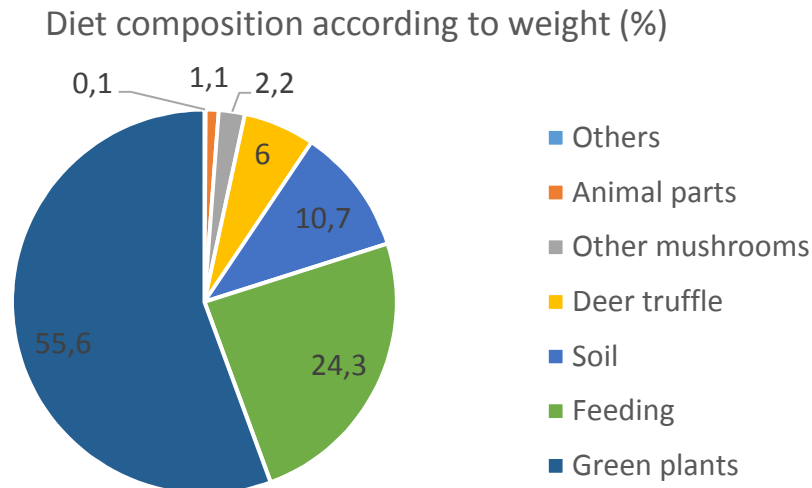


Figure 9.3: Diet composition of wild boars according to weight as deduced from the analyses of the stomach contents (Fielitz, 2005)



Figure 9.4: Deer truffle (*Elaphomyces granulatus*). Photo credit: Ulrich Fielitz

The diet composition changed completely in the second half of 2003 owing to a beech mast event. From September 2003 until February 2004, beechnuts dominated the food spectrum. Since the Cs-137 concentration in beechnuts was rather low, about 20 Bq kg⁻¹ fw on average, the activity levels in wild boar meat dropped significantly.

9.3 Stochastic modelling of Cs-137 contamination of wild boar

9.3.1 Mathematical framework

For modelling purposes, wild boars are represented by individual, homogeneously contaminated compartments with identical properties. The characteristic parameters of these identical compartments are the body mass m of the animal and the biological half-life T_{bio} of Cs-137. The activity A of Cs-137 in wild boar is given by:

$$\frac{d}{dt}A(t) = fI(t) - (\lambda_{bio} + \lambda_{phys}) \cdot A(t) \quad (\text{Eq. 9.1})$$

where $A(t)$ is the activity of Cs-137 in wild boar (Bq), $I(t)$ is the intake rate of Cs-137 (Bq d⁻¹), f is the fraction of Cs-137 absorbed in the gastro-intestinal tract, $\lambda_{bio} = \ln 2 / T_{bio}$ is the rate constant for the excretion of Cs-137 (d⁻¹) and $\lambda_{phys} = \ln 2 / T_{phys}$ is the rate constant for the physical decay of Cs-137 (d⁻¹).

Hence, the concentration C of Cs-137 in wild boar can be expressed by:

$$\frac{d}{dt}C(t) = \frac{1}{m}fI(t) - \lambda \cdot C(t) \quad (\text{Eq. 9.2})$$

with $\lambda = \lambda_{bio} + \lambda_{phys}$ and C given in Bq kg⁻¹ fw.

The solution of equation 9.2 is:

$$C(t) = e^{-\lambda t} \cdot \left(C(t_0) + \frac{1}{m}f \int_0^t I(s) \cdot e^{\lambda s} ds \right) \quad (\text{Eq. 9.3})$$

Deer truffles are the dominant contribution to radiocaesium uptake by wild boars. Since they are taken up irregularly, they represent a stochastic contribution to the intake rate. The total intake rate of Cs-137 can reasonably be approximated by a stochastic term I_{tr} (tr = truffles) representing the intake of Cs-137 via deer truffles and a smooth function I_{of} (of = other food) representing the contribution of all other food items:

$$I(t) = I_{tr}(t) + I_{of}(t) \quad (\text{Eq. 9.4})$$

For simplicity it is assumed that wild boars take up their food once per day at points in time $t_k = k \cdot \Delta t$:

$$I(t) = \sum_k (I_{tr,k} + I_{of,k}) \cdot \delta(t - t_k) \quad (\text{Eq. 9.5})$$

Here, $\delta(\cdot)$ denotes the Dirac delta distribution. The index k identifies a specific day and $\Delta t = 1$ d.

Stomach analyses reveal the frequency distribution $Z_{mass,tr}$ of the mass of deer truffles taken up per day. It is derived from the mass abundance of deer truffles in the analysed stomachs and the average total mass of food consumed per day. It is assumed that the intake of deer truffles by one wild boar at different points in time is equivalent to the intake by all animals of a group at one point in time, i.e. the group of identical animals is considered ergodic. The stochastic contribution to the daily intake can be written as:

$$I_{tr}(t) = Z_{mass,tr} \cdot Z_{act,tr} \quad (\text{Eq. 9.6})$$

where $Z_{mass,tr}$ is a random variable describing the frequency distribution of the mass of deer truffles (kg) taken up per day, and $Z_{act,tr}$ is a random variable describing the frequency distribution of the activity concentration of deer truffles (Bq kg⁻¹ fw).

For simplicity, it is assumed that the composition of the food spectrum and the activity levels of the food items stay constant, i.e. $I_{of}(t) = I_{of}$. The activity concentration at time $t_j = j \cdot \Delta t$ is:

$$\begin{aligned}
C(t_j) &= e^{-\lambda t} \cdot \left(C_0 + \frac{f}{m} \cdot \int_0^{t_j} \sum_{k=1}^j (I_{tr,k} + I_{of}) \cdot \delta(t_j - t_k) \cdot e^{\lambda s} ds \right) \\
&= C_0 e^{-\lambda t_j} + \frac{f}{m} \cdot \sum_{k=1}^j (I_{tr,k} + I_{of}) \cdot e^{-\lambda(t_j - t_k)} \\
&= C_0 e^{-\lambda t_j} + \frac{f}{m} \cdot \sum_{k=1}^j (Z_{mass,tr,k} \cdot Z_{act,tr,k} + I_{of}) \cdot e^{-\lambda(t_j - t_k)} \tag{Eq. 9.7}
\end{aligned}$$

Since the quantity of deer truffles consumed and the contamination levels of deer truffles are not related, they are independent random variables. Hence, the expected value $E[C(t_j)]$ is:

$$\begin{aligned}
E[C(t_j)] &= C_0 e^{-\lambda t_j} + \frac{f}{m} \cdot (E[Z_{mass,tr,k}] \cdot E[Z_{act,tr,k}] + I_{of}) \cdot \sum_{k=1}^j e^{-\lambda(t_j - t_k)} \\
&= C_0 e^{-\lambda t_j} + \frac{f}{m} \cdot (E[Z_{mass,tr,k}] \cdot E[Z_{act,tr,k}] + I_{of}) \cdot \frac{1 - e^{-\lambda t_j}}{1 - e^{-\lambda \Delta t}} \tag{Eq. 9.8}
\end{aligned}$$

The asymptotic expected value is:

$$E[C(t_j \rightarrow \infty)] = \frac{f}{m} \cdot (E[Z_{mass,tr,k}] \cdot E[Z_{act,tr,k}] + I_{of}) \cdot \frac{1}{1 - e^{-\lambda \Delta t}} \tag{Eq. 9.9}$$

9.3.2 Model parameters

Data for the model parameters were taken from Fielitz (2005), except the biological half-life.

Activity concentration of deer truffles:

The frequency distribution of the activity concentration of deer truffles $Z_{act,tr}$ was derived from the original data set. Activity levels in deer truffles (Bq kg⁻¹ fw) collected between August 2000 and August 2004 are approximately lognormally distributed: $Z_{act,tr} \sim LN(\mu, \sigma)$ with $\mu = 10.1$ and $\sigma = 0.417$.

Mass of deer truffles taken up per day:

The frequency distribution of the mass of deer truffles taken up per day, $Z_{mass,tr}$, was calculated from the average relative abundance of deer truffles in 70 analysed stomachs (see table 9.2). A discrete probability density function according to these values was assumed for $Z_{mass,tr}$ and the average total quantity of food taken up per day is considered to be constant at 1.8 kg d⁻¹.

Table 9.2: Average relative abundance of deer truffles in 70 analysed stomachs (Fielitz, 2005)

Relative abundance (%)	Number of stomachs
0%	13
0 – 10%	45
10 – 20%	5
20 – 30%	5
30 – 40%	2
> 40%	0

Body mass of wild boar:

The stochastic calculations assume identical animals. An average body mass of 100 kg was taken.

Biological half-life of Cs-137:

The biological half-life of 55 d was calculated for an animal with a body mass of 100 kg using the allometric relationship

$$T_{bio} = a \cdot m^b \quad (\text{Eq. 9.10})$$

with $a = 3.5$ and $b = 0.24$ for Cs-137 and m expressed in g (U.S. Department of Energy, 2002).

Cs-137 intake due to other food items, except deer truffles:

The Cs-137 intake due to other food items, except deer truffles, was calculated from their relative contribution to food intake (expected value) and their measured activity levels (mean values).

Fraction absorbed in the gastro-intestinal tract:

The fraction of Cs-137 absorbed in the gastro-intestinal tract was assumed to be 1.

9.3.3 Results

The results of the stochastic modelling approach are summarized in table 9.3, together with the statistical parameters derived from the measured activity levels in wild boar in the period 2002-2004. The predicted and the measured median agree well. However, the stochastic modelling approach underestimates the mean (expected value) and the 95th percentile by a factor of 2 and 6, respectively. At the same time, the approach overestimates the 5th percentile by almost a factor of 5. The predicted frequency distribution is depicted in figure 9.5.

Table 9.3: Statistical parameters as derived from the stochastic modelling approach described in section 9.3.2, together with the statistical parameters of the experimental data set

Statistical parameter	Predicted activity levels (Bq kg⁻¹)	Measured activity levels¹⁾ (Bq kg⁻¹)
Median	3164	3424
Mean (expected value)	3180	6217
5th percentile	2767	582
95th percentile	3649	21,886

¹⁾ Data from 2002-2004

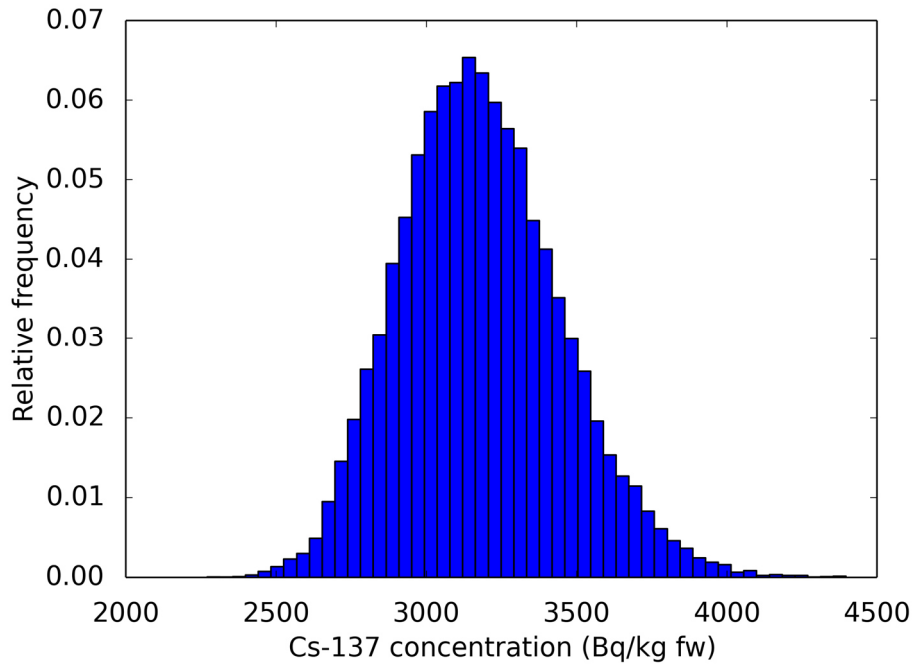


Figure 9.5: Predicted frequency distribution of the Cs-137 contamination of wild boar

9.4 Discussion

Biological half-life of Cs-137 in wild boar

The biological half-life of Cs-137 is a sensitive parameter for predicting activity levels in wild boar. The body mass m of an animal and its biological half-life T_{bio} are interdependent model parameters. From an allometric relationship (equation 9.10) a biological half-life of 55 d was calculated for an animal with a body mass of 100 kg (U.S. Department of Energy, 2002). Fielitz (2005) assumed a biological half-life of only 20 d, and Hohmann und Huckschlag (2005) report biological half-lives of only 20 – 40 d.

The consistency of the value for the biological half-life was checked using the published data for the transfer factor from food to meat. Using the notation of equation 9.2 and assuming equilibrium conditions, the transfer factor from food to meat can be written as:

$$T_f = \frac{C_i}{I_i} = \frac{f_i}{m \lambda_i} = \frac{f_i T_{bio}}{m \ln 2} \quad (\text{Eq. 9.11})$$

From transfer factors between 0.17 and 0.33 d kg⁻¹ for domestic pigs (Voigt et al., 1988) and $f_i = 1$, biological half-lives between 12 and 23 d were calculated for animals with a body mass of 100 kg. Following the arguments in Hohmann and Huckschlag (2005), the transfer factor for wild boars is expected to be higher by a factor of 2 to 3 (lower average body weight at harvest, higher proportions of oxidative muscle fibres, low potassium content in the natural forage). Accordingly, the biological half-life of a wild boar with a body mass of 100 kg is expected to range between 24 and 69 d, which is in good agreement with the result derived from the allometric relationship (55 d).

Variation with body mass

The stochastic modelling approach is based on the simplifying assumption that all animals are identical and have the same body mass. It is straightforward to show that the expected value of Cs-137 concentration in wild boar varies with body mass.

Since the biological half-life is of the order of several 10 days, it follows:

$$\lambda \Delta t \ll 1 \text{ and } 1 - e^{-\lambda \Delta t} \approx \lambda \Delta t \approx \frac{\ln 2}{T_{bio}} \Delta t$$

Using this approximation and the allometric relationship between body mass m and biological half-life T_{bio} (equation 9.10), the asymptotic expected value $E[C(t_j \rightarrow \infty)]$ (equation 9.9) can be rewritten as:

$$E[C(t_j \rightarrow \infty)] = f \cdot (E[Z_{mass,tr,k}] \cdot E[Z_{act,tr,k}] + I_{of}) \cdot \frac{a}{\ln 2 \Delta t} \cdot m^{b-1} \quad (\text{Eq. 9.12})$$

Since $b = 0.24$ for Cs-137 (U.S. Department of Energy, 2002), the asymptotic expected value $E[C(t_j \rightarrow \infty)]$ varies with body mass m according to:

$$E[C(t_j \rightarrow \infty)] \sim m^{-0.76} \quad (\text{Eq. 9.13})$$

A comparison with experimental data, however, is not possible, since data on the body mass of the wild boars have not been published in Fielitz (2005).

Robustness of model predictions

The predicted and the measured median agree well. However, the stochastic modelling approach underestimates the mean (expected value) and the 95th percentile by a factor of 2 and 6, respectively, and overestimates the 5th percentile by almost a factor of 5. The smaller variability of the model predictions might be caused by several reasons:

- The stochastic model is based on the simplifying assumption that all animals have the same body mass of 100 kg. A lower body mass would give rise to higher contamination levels and vice versa (see equation 9.13). Moreover, considering a variability in the body mass of the animals would possibly lead to an increased variability in the contamination levels.
- Fielitz (2005) reports a mean food composition, averaged over the period from May 2002 until August 2004. From September 2003 until February 2004, beechnuts dominated the food spectrum (beech mast event), leading to a significantly smaller intake of Cs-137.
- Wild boars could have migrated from neighbouring areas, where the food spectrum of wild boars and the activity levels in specific food items are different.

The stochastic modelling approach presented here allows robust predictions of the median of the activity levels in wild boar from first principles, i.e. without calibrating empirical parameter against measured values. The reasons for the smaller predicted variability are qualitatively understood. The stochastic modelling approach demonstrates that rather simple model structure might be sufficient for robust predictions, provided that the key processes are properly taken into account.

9.5 Bibliography

- Barthel, R. & Thierfeldt, S. (2012): Vergleichende Betrachtung der probabilistischen/stochastischen und deterministischen Modellierung von Expositionen im Hinblick auf die Belastbarkeit des Modellergebnisses und die Anforderungen an die Qualität der Eingangsdaten. Final report of the project 3609S50002 (in German).
- Fielitz, U. (2005): Untersuchungen zum Verhalten von Radiocäsium in Wildschweinen und anderen Biomedien des Waldes. Abschlussbericht Forschungsvorhaben StSch 4324 im Auftrag des BMU.
- Fielitz, U. & Richter, K. (2012): Bundesweiter Überblick über die Radiocäsiumkontamination von Wildschweinen. Final Report Project 3607S04561.
- Hohmann, U. & Huckschlag, D. (2005): Investigations on the radiocaesium contamination of wild boar (*Sus scrofa*) meat in Rhineland-Palatinate: a stomach content analysis. *European Journal of Wildlife Research* 51: 263-270.
- Semizhon, T., Putyrskaya, V., Zibold, G. & Klemm, E. (2009): Time-dependency of the Cs-137 contamination of wild boar from a region in Southern Germany in the years 1998 to 2008. *Journal of Environmental Radioactivity* 100: 988-992.
- Steiner, M. & Fielitz, U. (2009): Deer truffles – the dominant source of radioactive contamination of wild boar. *Radioprotection* 44(5): 585-588.
- Strebl, F. & Tataruch, F. (2007): Time trends (1986-2003) of radiocesium transfer to roe deer and wild boar in two Austrian forest regions. *Journal of Environmental Radioactivity* 98: 137-152.
- U.S. Department of Energy (2002): A Graded Approach for Evaluating Radiation Doses to Aquatic and Terrestrial Biota, Module 3: Methods Derivation, DOE-STD-1153-2002.
- Voigt, G., Henrichs, K., Pröhl, G. & Paretzke, H. G. (1988): The transfer of Cs-137 and Co-60 from feed to pork. *Journal of Environmental Radioactivity* 8: 195-207.

10 Conclusion

The overall intention of the presented case studies was to demonstrate that the quality of radioecological model predictions can benefit from integrating a process-oriented approach. Four different examples were selected where common modelling approaches are based on simplistic concepts, albeit better knowledge of the processes involved is available:

- The first example showed that highly uncertain empirical parameters can successfully be replaced by submodels. The hydrogeochemical speciation model PHREEQC was used to predict the distribution coefficient K_d for radium. Experimentally determined values vary up to seven orders of magnitude. Although several thermodynamic constants for radium were lacking and had to be replaced by the corresponding values for the chemically similar elements barium and strontium, the predictive uncertainty could be reduced to only one or two orders of magnitude.
- The second example investigated the consequences of simplistic assumptions for the migration of radionuclides in soil. During heavy rain showers radionuclide infiltrate with water in soil and lead to an 'initial' depth profile. This first phase was modelled neglecting sorption processes. After the deposition event, the long-term migration of radionuclides accounts for sorption processes in a simplified way by using K_d values. This approach realistically describes the key processes infiltration and sorption.
- The third example demonstrates that equilibrium approaches are not necessarily conservative. It deals with the assimilation of C-14 originating from nuclear power plants by C3 plants. Model calculations confirm the correlation of the diurnal variations of turbulent atmospheric mixing and photosynthetic activity. Since elevated activity levels in the lower atmospheric layer coincide with high photosynthetic activity, established equilibrium approaches underestimate the C-14 contamination of plants.
- The last example is a stochastic modelling approach to describe the Cs-137 contamination of wild boars due to the irregular uptake of highly contaminated deer truffles. The stochastic modelling approach successfully predicted the median of the activity levels in wild boars from first principles. The predicted and experimental values for the 5th and 95th percentiles were within one order of magnitude. The differences between measured data and model prediction can partially be explained by a lack of knowledge regarding the mass of the wild boars. This example shows that stochastic modelling allows to predict the variability of radioecological parameters.

The examples demonstrate that process-oriented modelling might help to reduce the uncertainty of empirical parameters and/or remove conceptual deficiencies. Process-oriented approaches provide the opportunity

- To reduce the uncertainties of empirical parameters by replacing them with robust submodels,
- To adequately describe non-equilibrium processes and avoid the systematic underestimation of doses to humans and the environment, and
- To explain and quantify the variability due to the stochastic nature of the processes involved.

Apart from improved predictive capabilities and a broader range of applicability, process-oriented models are the key for paving the way towards a better understanding of the process itself. They might, for example, provide guidance for planning and carrying out field investigations of dynamic, non-equilibrated systems.